Examensarbete

TVVR 11/5010

Evaluating a hydrological flood routing function for implementation into a hydrological energy model

2012-03-16

Victor Pelin
Alexander Påhlsson

Division of Water Resources Engineering

Department of Building and Environmental Technology

Lund University

Abstract

In 2011 the Bonneville Power Administration (BPA) released new data for the streamflow in the Columbia River. This extends the previous database record (1928-1999) to include the last nine years (1999-2008). Thomson Reuters Point Carbon are using this database to apply their proprietary hydrological HBV-type energy model in the Columbia River and therefore need a complete understanding of the data and the methods behind them.

This master thesis aims at understanding the different aspects of hydrological routing in general and more specifically in the Columbia River and to develop a hydrological routing function. The routing function should be simple yet robust and applicable in areas where data is scarce.

A routing routine based on the ”cascade of reservoir” routing technique, similar to the one used in the SSARR model, is developed. The routine is verified by using the parameter values and the average daily unregulated routed flow (ARF) data provided by the BPA. A methodology for parameter estimation, in Columbia River and in the general case, is developed. For the general case where the parameters are unknown, two alternative parameters estimation methods are presented, one method that can be used with a scarce amount of data and a second one for when additional data is available.

The overall effects of routing in the Columbia River catchment are relatively small. There are apparent lag times of around 2-3 days and noticeable flow attenuation between the dams Mica (headwaters) and The Dalles (distance 1300 km). Most of the water in the Columbia River enters as tributaries or local inflows along the flow path; this reduces the effects of routing at The Dalles. The reasonableness of the routing routine is evaluated with the Muskingum method. The Muskingum parameter values are calibrated to fit the effects of routing between Mica and The Dalles, produced by the routing routine. The calibrated Muskingum parameters are evaluated and considered to be reasonable.

Keywords: Hydrological routing, cascade of reservoirs, Columbia River, Muskingum

Sammanfattning

2011 släppte Bonneville Power Administration (BPA) uppdaterade flödesdata för Columbia River. Den nya databasen förlänger den tidigare (1928-1999) så att den nu även inkluderar de senaste nio åren (1999-2008). Thomson Reuters Point Carbon använder denna databas för att applicera sin HBV-baserade energimodell i Columbia River och behöver därför en full förståelse för data och bakomliggande metoder.

Målet med detta examensarbete är att få förståelse för de olika aspekterna av hydrologisk routing i allmänhet och mer specifikt i Columbia River och att utveckla en hydrologisk routing-funktion. Routing-funktionen ska vara enkel och robust samt tillämpningsbar i områden där tillgången till data är begränsad.

En routing-rutin baserad på ”cascade of reservoirs” routing-metoden, liknande den som används i SSARR-modellen, utvecklas. Rutinen verifieras med hjälp av parametervärdena och de dagliga oreglerade routade medelflödena från BPA. En metod för att uppskatta parametrarna, i Columbia River och i det allmänna fallet, utvecklas. För det generella fallet då parametrarna är okända, presenteras två alternativa metoder, en metod som kan användas vid begränsad datamängd och en som kan användas när mer data finns tillgänglig.

De övergripande effekterna av routing i Columbia Rivers avrinningsområde är förhållandevis små. Det finns tydliga tidsfördröjningar på 2-3 dagar och en märkbar utjämning av flödet mellan Mica (källflöde) och The Dalles (avstånd 1300 km). Det mesta av vattnet i Columbia River rinner till som biflöden eller lokala tillflöden längs med flodsträckan, vilket reducerar effekterna av routing vid The Dalles. Rimligheten i routing-rutinen utvärderas med hjälp av Muskingum –metoden. Värdena på Muskingum-parametrarna kalibreras för att passa effekterna av routing, genererade av routing-rutinen, mellan Mica och The Dalles. De kalibrerade Muskingum-parametrarna utvärderas och anses rimliga.

Nyckelord: Hydrologisk routing, cascade of reservoirs, Columbia River, Muskingum

Acknowledgements

We would like to thank our supervisors Dr. Rolf Larsson at Water Resource Engineering (Lund University) and Stefan Söderberg at Thomson Reuters Point Carbon for valuable comments and guidance throughout this thesis project. Thank you Rolf for always taking the time to answer and discuss our questions and sorry for always showing up five minutes early to our meetings. Thank you Stefan for our interesting meetings and for giving us the opportunity to make this thesis.

To our friends and families, we are thankful for your support and encouragement through rain and shine. Lastly, we would also like to express our gratitude to Prof. Magnus Larson at Water Resource Engineering (Lund University) for helping us with contact information.

Acronyms and unit converter

Station acronym	Full station name
ALF	Albeni Falls
ARD	Hugh Keenleyside
BDY	Boundary
BOX	Box Canyon
CHJ	Chief Joseph
CIB	Columbia River at international border
CP	Control Point used for routing, at Pasco, WA
GCL	Grand Coulee
IHR	Ice Harbor
JDA	John Day
MCD	Mica
MCN	McNary
MUC	Murphy Creek
PRD	Priest Rapids
RIS	Rock Island
RRH	Rocky Reach
RVC	Revelstoke
SEV	Seven Mile
TDA	The Dalles
WAN	Wanapum
WAT	Waneta
WEL	Wells
YAK	Yakima River

Data ID	Explanation	Unit
A	Average daily project inflow	cfs
ARF	Average daily unregulated routed flow	cfs
H	Average daily observed streamflow or project outflow	cfs
L	Average daily local flow (between two adjacent stations or projects)	cfs
S	Average daily observed storage change at project site	cfs

Acronym	Full name
BPA	Bonneville Power Administration
HBV	Hydrologiska Byråns Vattenbalansavdelning
SMHI	Swedish Meteorological Hydrological Institute
SSARR	The Stream-flow Synthesis and Reservoir Regulation Model
USACE	U.S. Army Corps of Engineers
USBR	U.S. Bureau of Reclamation
USGS	U.S. Geological Survey

US units	Metric units
1 ft	0.305 m
1 ft^3/s (cfs)	0.0283 m^3/s
3.28 ft	1 m
35.3 ft^3/s (cfs)	1 m^3/s
1 mile	1.61 km
0.621 mile	1 km

Table of Contents

Statement of contribution

Alexander has written most of chapter 2.2 and Victor has written the main part of chapter 2.1.3. The rest has been written by both authors. It is the authors' opinion that both of authors have contributed equally to this master thesis.

1. Introduction

1.1 The importance of rivers in the hydrological cycle

The ever ongoing circulation of water in different forms between the atmosphere and the land surfaces or oceans, a concept called the hydrologic cycle, was the starting point for the science of hydrology (Chow, et al., 1988). Dating as far back as hundreds of year B.C. the Greek philosopher Theophrastus (c. 372-287 B.C.) managed to correctly describe the hydrological cycle in the atmosphere, with a sound explanation of how precipitation was formed by condensation and freezing (ibid.). His theory was later extended by the Roman architect and engineer Vitruvius, around the time of Christ, to include the explanation that groundwater was mainly derived from precipitation that infiltrated the ground surface (ibid.). Their work can be seen as a predecessor to the modern version of the hydrological cycle (ibid.).

The hydrological cycle (see Figure 1) describes the continuous cycling and interdependence of all phases of water, i.e. gaseous, liquid and solid (Ward and Robinson, 2000). The precipitation that falls out of the atmosphere can have many different fates, e.g. it can be intercepted by the canopy before it reaches the ground and then evaporated or it can hit the ground and form surface runoff that eventually ends up in a nearby stream. The stream then runs out into the ocean or a lake, where water is evaporated into the atmosphere and forms clouds by condensation, until it finally goes back to being precipitation again and the circle is complete.

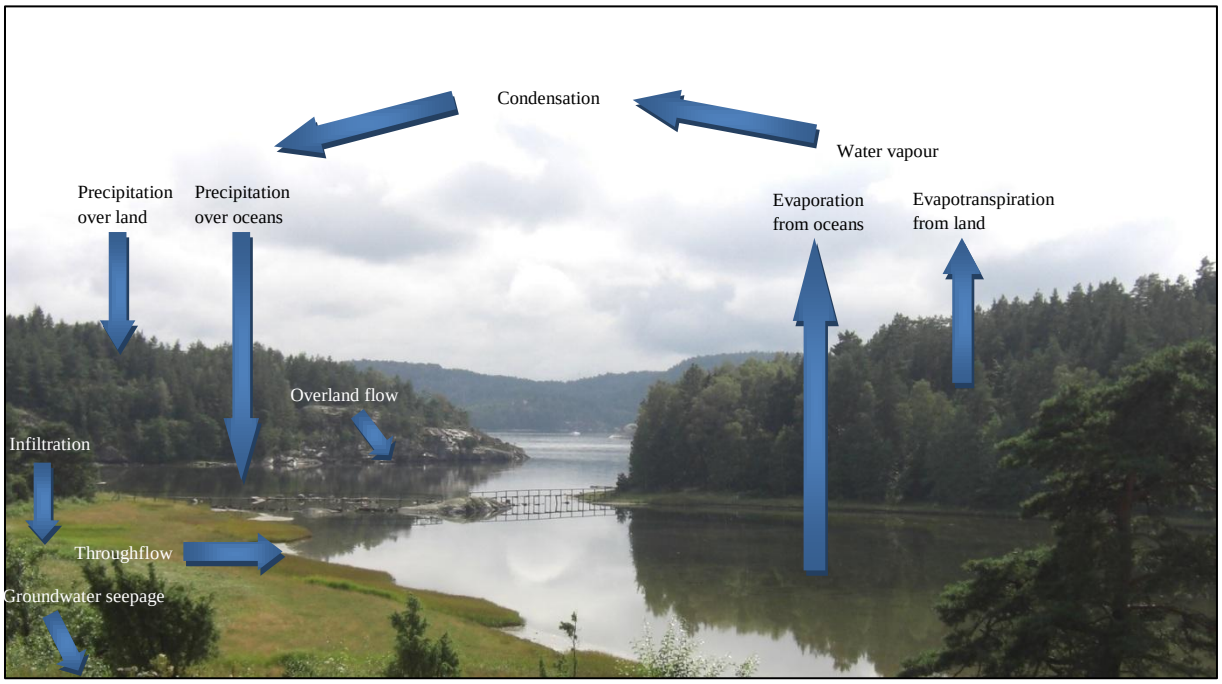

Figure 1: Schematic picture illustrating the hydrological cycle.

In other words, rivers play an important role in the hydrological cycle, receiving water that originates from overland flow (Q_o), throughflow (Q_t), groundwater flow (Q_g) and direct precipitation (Q_p), see Figure 2; and subsequently transporting it to the sea (Ward and Robinson, 2000).

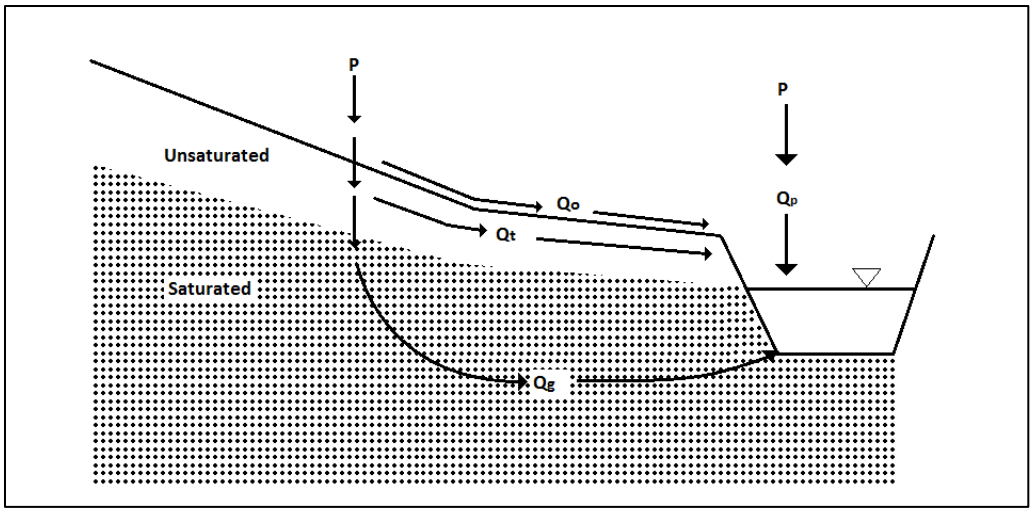

Figure 2: Illustration of a cross-section near a river with different flowpaths.

1.2 Rivers in hydrological rainfall-runoff models

Hydrological rainfall-runoff models can be divided, according to how physical processes within the watershed are modeled, into two categories: conceptual and physically based models. Conceptual models are based on limited representation of the physical processes that produce the model outputs, e.g. the drainage basin is represented by a number of different storages. Physically based models are founded on a more solid understanding of the physical processes (Ward and Robinson, 2000). Examples of conceptual and physically based models are presented below.

The HBV model is a conceptual rainfall-runoff model that was originally developed by SMHI in 1972 (SMHI, n.d.a). River routing, which is a way of modeling the change in the appearance of the hydrograph as water moves from an upstream to a downstream location, can be described by the Muskingum method or simple time lags in the HBV model. The Muskingum method is described more in detail later and is built upon a simple relationship between storage and the inflow and outflow hydrograph. Although it is popular and easy to use, Henderson (1966) argues that it is based on a relationship that is not logically complete.

The Système Hydrologique Européen (SHE) model is a physically based rainfall-runoff model that was developed collaboratively by the UK Institute of Hydrology (IH), the Danish Hydraulic Institute (DHI) and the Société Grenoblois d'Étude et d'Applications Hydrauliques (SOGREAH) (Ward and Robinson, 2000). In MIKE SHE there is a program called MIKE 11 that computes the streamflow in rivers by using an implicit, 1D, finite-difference formulation. There are many options available for how river routing can be modeled in this program. The options range from the most advanced case where the complete non-linear Saint-Venant equations (described more in detail later) are used, to the most simple case where the Muskingum method is used (no routing is also an option) (Singh & Frevert, 2005). A disadvantage with the Saint-Venant equations is the demand of a lot of site specific data to be able to model the watershed.

1.3 Developing a simple streamflow routing routine – incentives for this thesis

The main incentive of this thesis is the potential improvement of an existing conceptual rainfall-runoff model – the HBV-type energy model used by Thomson Reuters Point Carbon – that can comes from implementing streamflow routing into the model. In 2011 the Bonneville Power Administration released new data for the streamflow in Columbia River. Thomson Reuters Point Carbon are using this

database to apply their proprietary hydrological HBV-type energy model in Columbia River and therefore need a complete understanding of this data and the methods behind them. Since the model is currently being run without specifically accounting for streamflow routing, it is vital to understand if and how streamflow routing affects the model performance and moreover if and how streamflow routing should be accounted for.

1.4 Objectives, scope and limitations

This thesis includes four major parts:

- ✓ The first part is to unravel and investigate the data set from the Columbia River (US) produced by the Bonneville Power Administration in 2010 (BPA, 2011).
- ✓ The second part is to develop a routing routine which can be implemented into an existing HBV-type model.
- ✓ The third part is to create a simple methodology for estimating the model parameters, both in the Columbia River basin, but also in the general case where the available data is limited.
- ✓ The fourth part is to investigate when it is favorable to include streamflow routing in a hydrologic rainfall runoff model.

The routing routine will be evaluated on different geographical scales using the Columbia River data set from BPA.

The aim of this thesis is not to develop a new routing technique; instead it will be based on existing knowledge in the subject.

This thesis does not include testing the developed routing routine with the Thomson Reuter Point Carbons HBV-type energy model.

2. Background

2.1 Streamflow modeling

2.1.1 Basic concepts and principles

Hydrograph

A hydrograph is explained by Chow et al. (1988) as "a graph or table showing the flow rate as a function of time at a given location on the stream". Any specific hydrograph is a result of a complex array of factors summarized by Chow (1959) as "an integral expression of the physiographic and climatic characteristics that govern the relations between rainfall and runoff of a particular drainage basin". Common time scales of hydrographs are for example storm hydrographs where the catchment response during a single storm is shown and annual hydrographs where effects of the long term water balance in the catchment are shown (Chow, et al., 1988).

Flow classification

A common way of classifying flow in open-channel hydraulics is by classifying the flow as steady or non-steady and uniform or non-uniform (Chadwick, et al., 2004). Steady or non-steady refers to if or if not the channel flow changes over time, and uniform or non-uniform refers to if or if not the channel flow changes in space along the channel length (Chadwick, et al., 2004). Non-uniform flow can in turn be classified as gradually or rapidly varied flow depending on how much it changes along the channel length (Chaudhry, 2007).

Manning's and Chezy´s formula

The Manning and Chezy formulas are resistance equations for steady, uniform, open channel flow (Henderson, 1966; French, 1994). They describe how flow velocity depends on channel friction and slope.

The Chezy formula was developed in 1769 by Antoine Chezy and was originally used for the purpose of designing a canal in the Paris water supply (Henderson, 1966; French, 1994). The formula can be derived by combining the force balance of any water element in the channel with dimensional analysis of the bottom shear stress (Henderson, 1966). It is given by French (1994) as:

$$u = C\sqrt{RS} \tag{1}$$

where u is the mean flow velocity (m/s), C $(\sqrt{m}/s)$ is a resistant coefficient, R (m) is the hydraulic radius and S (m/m) is the bottom slope.

The Manning formula was developed by Robert Manning in 1889 and was based on empirical curve fitting (French, 1994; Chow, et al., 1988). The formula can be written as (French, 1994):

$$u = \frac{1}{n} R^{\frac{2}{3}} S^{\frac{1}{2}} \tag{2}$$

where n $(s/m^{\frac{1}{3}})$ is the Manning roughness coefficient. The Manning formula is widely used, because of its simplicity and reliability, and the Chezy formula is still used in some European countries (Henderson, 1966; Gordon, et al., 2004).

Continuity equation

The conservation of mass principle is simple and is regarded as the most useful physical principal in hydrologic analysis. Equations expressing this conservation principle, so called "continuity

equations", can be developed for a fluid volume, flow cross-section, and a point within a flow (Chow, et al., 1988).

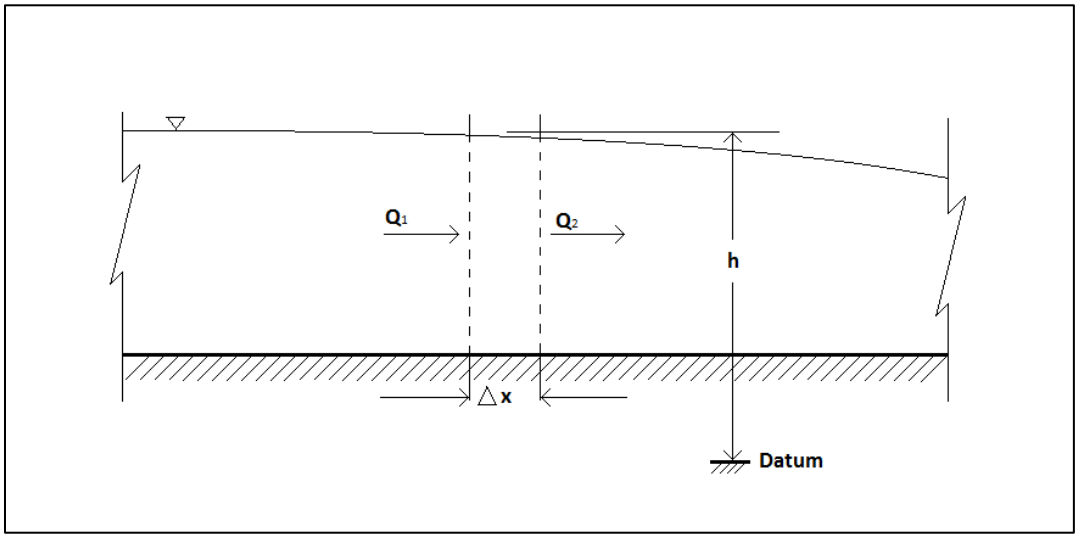

Figure 3: Definition sketch for the continuity equation.

An example of where the continuity principle can be applied is that of a river stretch with a changing water-surface level (Henderson, 1966). Consider the river section shown in Figure 3 with a section of a very short length, Δx. The discharges at the two ends (Q_1, Q_2) do not have to be the same and will differ according to equation 3:

$$Q_2 - Q_1 = \frac{\partial Q}{\partial x}\Delta x \qquad (3)$$

The term on the right-hand side of equation 3 gives the rate at which the volume within this region is decreasing. If h is the height of the water surface above a certain datum level, then the volume of water in the section with length Δx is increasing with a rate according to (Henderson, 1966):

$$B\frac{\partial h}{\partial t}\Delta x$$

where *B* is the water surface width. The two terms that were presented in the expression above and equation 3 must be equal in magnitude but with opposite signs, which together result in the equation of continuity for unsteady open channel flow (Henderson, 1966):

$$\frac{\partial Q}{\partial x} + B\frac{\partial h}{\partial t} = 0 \qquad (4)$$

This equation is later used in the chapter about hydraulic routing where it has been rewritten by expanding the term $\partial Q/\partial x = \partial(Av)/\partial x$, which results in (Henderson, 1966):

$$A\frac{\partial v}{\partial x} + v\frac{\partial A}{\partial x} + B\frac{\partial y}{\partial t} = 0 \qquad (5)$$

where *v* is the flow velocity of the water, *y* is the water depth and *A* is the cross-sectional area.

Momentum equation

The momentum equation describes the unsteady non-uniform open channel flow and is not as easily derived as the continuity equation described above. The derivation starts with the equation (equation 6) describing the gradient of the total energy line (Henderson, 1966):

$$\frac{\partial H}{\partial x} = \frac{\partial}{\partial x}\left(h + \frac{v^2}{2g}\right) \quad (6)$$

where *H* is the height of the total energy line above a certain datum level, *h* is the height of the water surface above the same datum level and *v* is the velocity of the water. From there it is further rewritten until it finally becomes:

$$S_f = S_0 - \frac{\partial y}{\partial x} - \frac{v}{g}\frac{\partial v}{\partial x} - \frac{1}{g}\frac{\partial v}{\partial t} \quad (7)$$

The interested reader can find the complete derivation of the momentum equation (equation 7) in the book "Open Channel Flow" by Henderson (1966).

2.1.2 Rainfall-runoff modeling

HBV

The Hydrologiska Byråns Vattenbalansavdelning (HBV) model is a rainfall runoff model developed by Bergström for the Swedish Meteorological and Hydrological Institute (SMHI) in the early 1970s (Bergström, 1976; SMHI, n.d.b; Lindström, et al., 1997; Hasan & Elshamy, 2011). The model was originally developed for runoff simulation and hydrological forecasting in Scandinavian countries, but has had an increasing range of applications (Lindström, et al., 1997). It has been applied in more than 40 countries all over the world with varying climatic conditions and on scales ranging from small lysimeter plots to the entire Baltic Sea drainage basin (SMHI, n.d.b).

Many versions of the HBV model have been produced around the world since it was first developed in the 1970s (Lindström, et al., 1997). The HBV model used by the SMHI is a semi-distributed model, where the modeled catchment can be divided into several sub basins (SMHI, n.d.b). Each sub basin is then described according to land use, lake area percentage and elevation (ibid.). The HBV model is based on conceptual descriptions of a few main features of the hydrological cycle. In its standard form, it comprises of three major parts: A snow routine, a soil moisture routine and a runoff response routine (Amenu & Killingtveit, 2001). The snow routine handles snow melt and snow accumulation, the soil moisture routine handles precipitation and evapotranspiration and computes the storage of water in the soil, and the runoff routine transforms the percolation from the soil moisture routine into different levels of runoff (Amenu & Killingtveit, 2001; SMHI, n.d.b). The model is usually run on a daily or monthly time scale (SMHI, n.d.b; Hasan & Elshamy, 2011).

The HBV model is used for a wide range of applications, from flood forecasting in Nordic countries, to evaluating climate change scenarios and nutrient load estimates (SMHI, n.d.b).

SSARR

The Stream-flow Synthesis and Reservoir Regulation Model (SSARR) was initially developed for the North Pacific Division of the U.S. Army Corps of Engineers (USACE) to aid them in their planning, design, and operation of water control works (USACE, 1991). It has been in the process of development and application since 1956 and has been applied to numerous river systems in the United States and elsewhere (ibid.).

It is a numeric model that describes the hydrology of a river catchment system and consists of two "models"; a watershed model and a streamflow and reservoir regulation model (USACE, 1991). The watershed model simulates rainfall-runoff, snow accumulation and snowmelt-runoff (ibid.). The streamflow and reservoir regulation model – which uses a routing technique called the "cascade of linear reservoirs"– routes the water in the river from an upstream location to a downstream location

through channel and lake storage, and is also able to simulate flow through man-made reservoirs (ibid.). In addition, there is also an option to include effects of backwater, diversion and overbank flows (ibid.). The SSARR MODEL is able to simulate with time increments that are between 0.1 and 24 hours long (ibid.).

The SSARR model is used by the BPA, the USACE, and the U.S. Bureau of Reclamation (USBR) to perform a number of studies, e.g. hydro-regulation studies of the Columbia River basin (BPA, 2011).

The SSARR model, in which the cascade routing routine is included, is used as a tool for both forecasting and long term hydrology studies. Examples of applications are (USACE, 1991):

- Simulation of design storms
- Daily streamflow forecasting at many points throughout a river system
- Seasonal streamflow forecasting.

The model has been developed to be used in relatively large drainage basins with limited amounts of available observed data, but has been applied to a wide variety of large and small catchments around the world (USACE, 1991). One specific case where the SSARR model should not be used is for studies of small drainage areas in urban hydrology since it is a conceptual model rather than a hydraulic model (ibid.). Also, the minimum computation step is one tenth of an hour, which can be too long to be able to accurately simulate runoff peaks from very small areas (ibid.).

2.1.3 Streamflow routing

Hydrologic routing

As the flow through a water body changes due to any kind of disturbance, so does the water level and thereby the water storage in the water body. The change in flow over time can be visualized in a hydrograph and seen as a flood wave that propagates in the direction of the flow. The hydrograph will, depending on the properties of the reservoir or channel, change as it propagates. Describing this change of the hydrograph along the water course is referred to as routing the flow along its course. The routing is often divided into two effects, time lag and flow attenuation. The time lag refers to the time lag between two hydrographs caused by the fact that it takes time for a water volume to travel from an upstream location to a downstream location. The attenuation refers to the change in the shape of the hydrograph as it propagates caused by the storage capacity of the reservoir or friction and irregularities of a channel reach (Henderson, 1966; Subramanya, 2008). Hydrologic routing is based on the simple concept of continuity, which means that the change in storage S over time t in a water body equals the difference between the inflow I and the outflow O (Chow, et al., 1988):

$$\frac{dS}{dt} = I - O \tag{8}$$

If the inflow hydrograph to a water body is known, two unknowns in the equation above remain. This means that in order to solve the continuity equation, a second equation is required. For this reason a storage function that relates storage to outflow and inflow is introduced (Chow, et al., 1988).

Hydrologic reservoir or lake routing

In order to solve the continuity equation (equation 8) a second relation between storage and flow is required. One type of routing is when a flood wave passes through an unregulated lake or reservoir. For a reservoir with an uncontrolled outflow and a level water surface, there is, depending on the properties of the discharge point, a fixed relation between lake elevation (h) and the outflow from the lake (Chow, et al., 1988). Thus:

$$O = f_1(h) \quad (9)$$

As the lake elevation changes, so does, depending on the topographical properties of the lake, the volumetric storage in the lake (Chow, et al., 1988). Thus:

$$S = f_2(h) \quad (10)$$

Since both storage and outflow are functions of the lake stage, there is an indirect relation between outflow and storage (Chow, et al., 1988):

$$S = f(O) \quad (11)$$

The relation between stage and outflow can sometimes be determined using hydraulic equations. For example, flow over several types of weirs can be described as (French, 1994):

$$O = C * h^m \quad (12)$$

where *m* and *C* depend on the physical properties of the weir. The relation between stage and storage can be estimated using topographical maps. For any lake, the storage can be calculated as:

$$S = \int_0^h A_{lake}\, dh \quad (13)$$

where the lake area A_{lake} is a function of the lake elevation *h*. As an example, consider a case where the lake area doesn't change as the lake elevation changes, then equation 13 becomes:

$$S = A_{lake} * h \quad (14)$$

Combining equation 12 and equation 14 yields a relation between storage and outflow as:

$$S = A_{lake} * \left(\frac{O}{C}\right)^{\frac{1}{m}} = B * O^C \quad (15)$$

where both *B* and *C* depend on the properties at the outflow point, and shape of the lake. The simplest reservoir routing is the linear reservoir routing where the storage varies linearly with outflow as (Chow, et al., 1988):

$$S = k * O \quad (16)$$

where *k* (s) is a constant parameter that can be determined by calibration. A physical interpretation of the *k* parameter is the lake residence time, a definition of residence time can be found in Chow, et al. (1988).

Hydrologic channel or river routing

In river routing the continuity equation is still valid. However, the storage is no longer solely a function of reach discharge. As can be seen in Figure 4, two different storages are possible for the same reach discharge (Q_{ref}), one where the flood wave is rising, and one where the flood wave is falling. Hence the storage in the reach is no longer a unique function of discharge; instead there is a looped relationship (USACE, 1994).

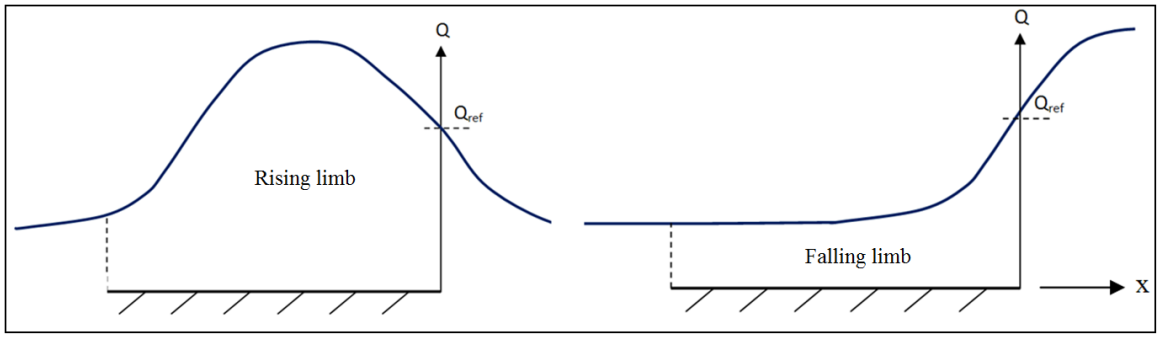

Figure 4: Rising and falling floodwave giving rise to a looped discharge-storage relationship.

A way of describing the routing through a river is by dividing the river into a discrete number of identical cascading reservoirs (see Figure 5), with level pools, where the storage in each sub reservoir is assumed to be a function of discharge. The storage is still different depending on whether the flood wave is rising or falling, but the looped storage-outflow relationship of the total reach is improvingly mimicked as compared to having a single reservoir (see Figure 5) (USACE, 1994). An example of the cascading reservoir approach is the ”cascade of linear reservoirs” developed by Nash (1957), where storage in each sub reservoir is assumed to be linearly proportional to the discharge in each sub reservoir. The ”cascading reservoir” routing technique will be the approach used in this report, however not with the linear relationship described above, but where the constant term in the linear relationship is flow dependent.

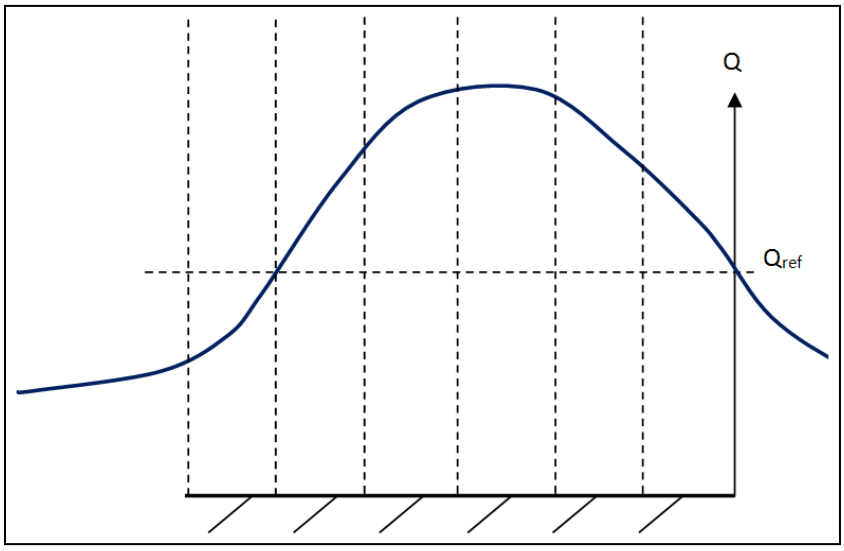

Figure 5: The channel reach is approximated as a number of equal reservoirs. The storages in two of the reservoirs with equal discharge are still different, but the error is reduced with increasing number of reservoirs.

Another popular way of better describing the flow through a river reach is by defining the concepts of prism and wedge storage as seen in Figure 6 below.

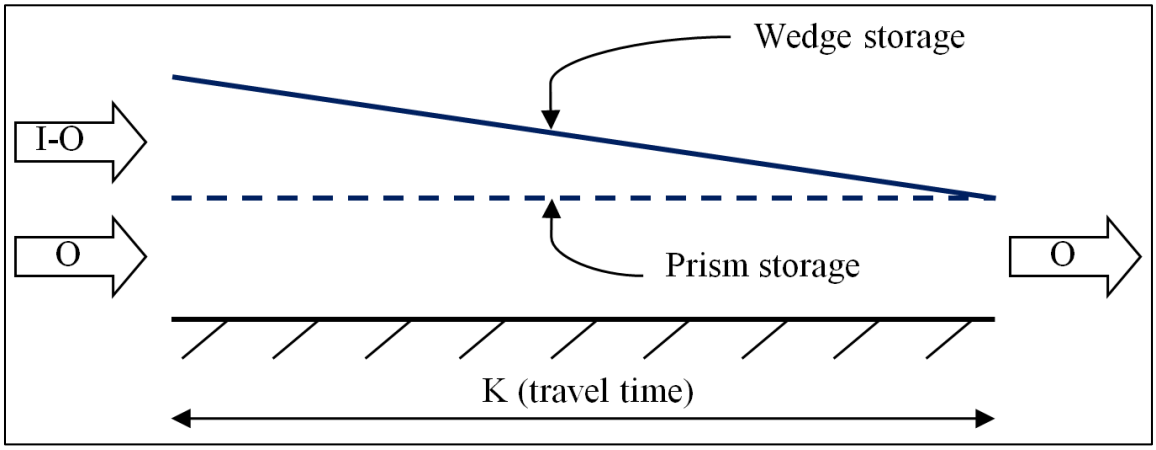

Figure 6: The concepts of wedge and prism storage.

The total storage in the reach is then:

$$S = Wedge\ storage + Prism\ storage = K * O + K * (I - O) * \frac{1}{2} \quad (17)$$

This can be rewritten in the form known as the Muskingum method (Henderson, 1966):

$$S = K[XI + (1 - X)O] \quad (18)$$

where *K* is a model parameter often associated to travel time, *X* is a model parameter that depends on the wedge properties of the flood wave (Chow, et al., 1988). Hence the storage does now not only depend on the reach discharge, but on the inflow as well.

2.1.4 Alternative routing methods

Hydraulic routing

Despite the popularity and ease of use of the hydrologic Muskingum routing method, it is as mentioned previously not logically complete. The equations of motion do not justify the belief that storage is strictly determined by inflow and outflow alone (Henderson, 1966). A more physical approach to river routing is to use hydraulic routing techniques, which utilize some form of the momentum equation to solve the continuity equation. In many cases some terms in the momentum equation can be neglected, because of their insignificance in comparison to other terms. Below follows a discussion of three special cases where it is valid to make certain approximations.

Dynamic routing

The equations of motion or the St Venant equations – the continuity and the momentum equation (equation 5 and equation 7) – solved together with proper boundary conditions are called the complete dynamic wave equations (USACE, 1994). These equations are considered to be the most accurate solution to 1-D unsteady flow problems in open channels (ibid.). However, they are based on assumptions that give rise to limitations of use. The assumptions used to derive the dynamic wave equations are (ibid.):

i. Velocity is constant and the water surface is horizontal across any channel section.

ii. All flows are gradually varied with hydrostatic pressure prevailing at all points in the flow, such that vertical accelerations can be neglected.
iii. No lateral secondary circulation occurs.
iv. Channel boundaries are treated as fixed; therefore, no erosion or deposition occurs.
v. Water is of uniform density, and resistance to flow can be described by empirical formulas, such as Manning's and Chezy's equation.

$$A\frac{\partial v}{\partial x} + vB\frac{\partial y}{\partial x} + B\frac{\partial y}{\partial t} = q \quad (19)$$

$$S_f = S_0 - \frac{\partial y}{\partial x} - \frac{v}{g}\frac{\partial v}{\partial x} - \frac{1}{g}\frac{\partial v}{\partial t} \quad (20)$$

where A is the cross-sectional area, v is the water velocity, B is the width of the river, y is the water depth, q is the discharge per width of river, S_f is the friction slope (which is the slope of the total energy line) and S_0 is the bottom slope (ibid.). Figure 7 shows a planar and cross-section of a section of a river where the notations described above are illustrated.

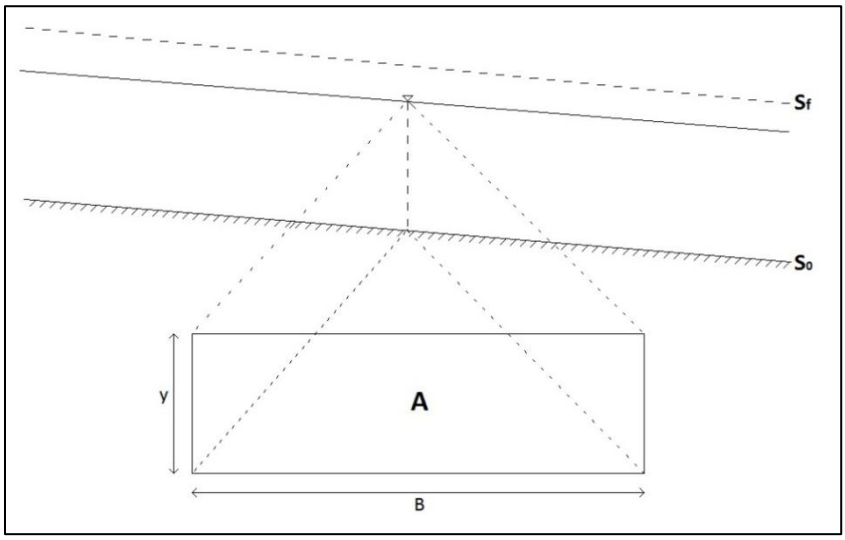

Figure 7: Planar and cross-sectional sketch of river section, with the total energy line (S_f), bottom slope (S_0), water depth (y), river width (B) and cross-sectional area (A).

Kinematic routing

For some flow situations the gravitational and frictional forces approach equilibrium. In such cases, changes in depth and velocity with respect to time and space are small compared to the bed slope of the channel (USACE, 1994). This justifies a deletion of the acceleration terms – both local and convective – from the full dynamic wave equations (equation 19 and equation 20), which then reduces to (ibid.): $S_f = S_0$.

This equality between the friction slope and the bottom slope can be utilized in river routing. By combining Manning's or Chezy's equation with the continuity equation, the governing kinematic wave equation becomes (USACE, 1994):

$$\frac{\partial A}{\partial t} + \alpha m A^{(m-1)}\frac{\partial A}{\partial x} = q \quad (21)$$

where α and m are terms related to flow geometry and surface roughness. Since the kinematic wave equation lacks all acceleration terms it assumes steady uniform flow and therefore it does not allow

hydrograph diffusion (USACE, 1994). In other words, the kinematic wave equation only translates the hydrograph in time without any attenuation of the peak flow (ibid.).

Diffusion routing

Another approximation of the dynamic wave equations, but one which allows for diffusion of the hydrograph (unlike the kinematic approximation), is the diffusion wave model. It adds a term for the pressure differential to the kinematic wave equation (equation 23), which then becomes the diffusion wave equation (USACE, 1994):

$$S_f = S_0 - \frac{\partial y}{\partial x} \quad (22)$$

The pressure differential term allows the diffusion model to describe the attenuation of a flood wave and also provides a possibility of specifying the boundary condition at the downstream end, to account for backwater effects (USACE, 1994). Although it does not include the last two inertial terms of the dynamic wave equation (equation 23), which limits the application to slow and moderately rising flood waves, it can still describe most natural flood waves (ibid.).

$$\frac{\partial V}{\partial t} + V\frac{\partial V}{\partial x} + g\frac{\partial y}{\partial x} - g(S_0 - S_f) = 0 \quad (23)$$

Kinematic wave

Diffusion wave

Dynamic wave

2.1.5 Routing in the HBV model

An additional part of the HBV model is to include routing. SMHI (n.d.b) mentions the possibility of describing routing between sub basins by using the Muskingum method or by using simple time lags. Another option is to entirely skip routing by simply adding the contributions of the different sub basins (ibid.). As mentioned previously, lake area percentage is determined for all modeled sub basins. This is because the model also includes level pool lake routing (SMHI, n.d.b; Lindström, et al., 1997).

2.1.6 Routing in the SSARR model

The SSARR model is divided into several sub-models, one of which is the "River and Reservoir model". This sub-model routes the streamflow from an upstream point to a downstream point and uses a routing method referred to as a "cascade of reservoirs" technique (USACE, 1991). The cascade of reservoirs technique simulates the lag and peak attenuation – the effects of routing – by dividing the river into successive increments (ibid.). Thus, the river channel can be thought of as a series of small "lakes" representing the natural delay and attenuation of runoff (ibid.).

2.1.7 Advantages and disadvantages of hydrologic modeling

The major advantage of conceptual hydrologic models as opposed to physical or hydraulic models is the low demand on the amount of available data. The model parameters have little or no physical meaning and cannot be measured; instead they are calibrated and validated using measured historic streamflow. Adapting the model to historic conditions of course brings problems if future conditions change, as for example if the climate would change. Furthermore streamflow data is often measured or modeled as daily or monthly average whilst the effects of routing in small catchments, as the reader will see later in this report, sometimes occur on a much smaller time scale.

2.2 Site description – Columbia River

This thesis is focused on developing a streamflow routing routine, by studying BPA's "Level Modified Streamflow" report on the Columbia River Basin. Below follows a short description of the area and some of the data types produced by BPA.

2.2.1 Description of the catchment

The Columbia River Basin (see Figure 8) stretches over 670,000 km^2, including parts of seven U.S. states and the Canadian Province of British Columbia (USEPA, 2012). Because it covers such a vast area the climate across the region is variable. Annual precipitation is highest in the mountain areas (e.g. Coast Mountains and Cascade Ranges) and lowest in the plateau areas (e.g. Columbia and Snake River Plateau) (BPA, 2011). Temperatures are milder along the coast than inland, and temperature variations are much more pronounced inland than along the coast (ibid.).

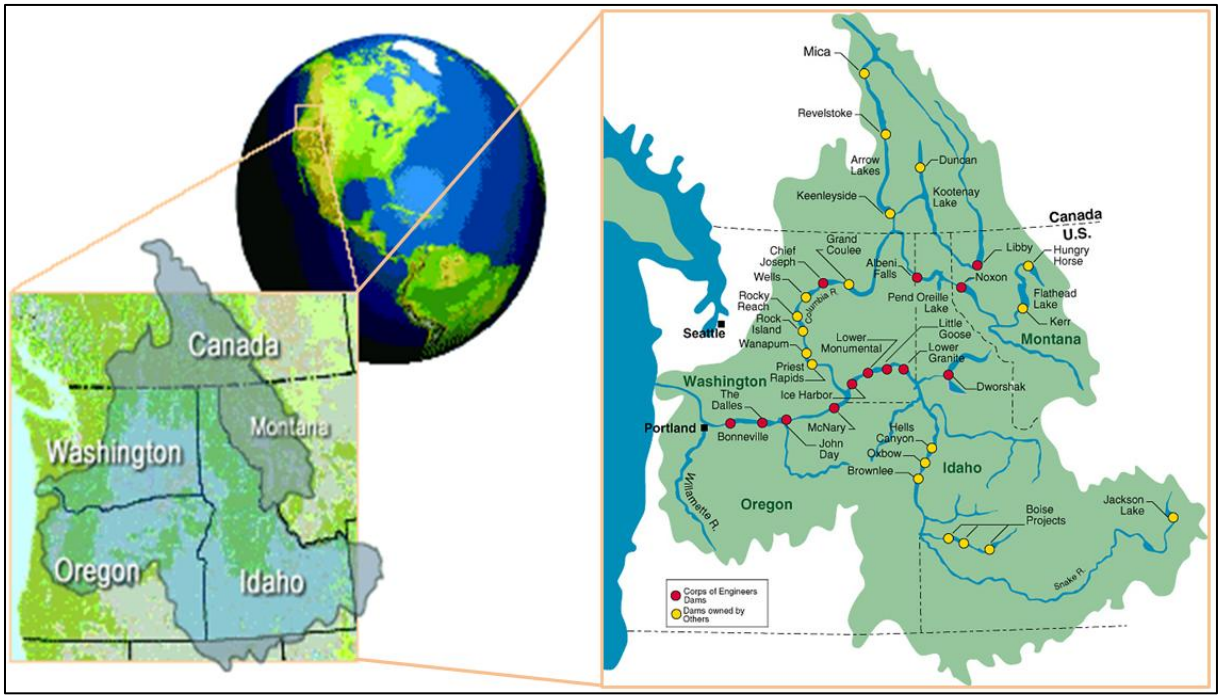

Figure 8: Map of the Columbia River Basin (USACE, n.d.).

The region is situated in a zone of prevailing westerly winds, which brings fronts that are associated with extensive precipitation (BPA, 2011). The dominating type of runoff divides the region in two: (1) one snowmelt-dominated regime east of the Cascade Range, and (2) one rainfall-dominated regime along the coast west of the Cascade Range (ibid.). East of the Cascades the snow melts in May through July, giving rise to peak streamflow discharges around early June (ibid.). West of the Cascades most rain falls during the winter months and most of the runoff occurs in the winter period that stretches from October to March (ibid.).

2.2.2 Bonneville Power Administration (BPA) data

The BPA in conjunction with the U.S. Army Corps (USACE) and the U.S. Bureau of Reclamation (USBR) releases a "Level Modified Streamflow" report once every ten years. According to BPA (2011) the definition of modified flows is: "…the historical streamflow that would have been observed if current irrigation depletions (as of 2008) existed in the past and if the effects of river regulation were removed (except at Snake, Deschutes, and Yakima basins where current upstream reservoir regulation practices are included)".

This streamflow dataset is, among other things, used for analysis of environmental impacts, power revenue forecasts, and flood control studies (BPA, 2011). Below follows an explanatory part of the data types that are of relevance for this thesis.

H

This data type is the average daily observed streamflow or project outflow, which are dams used for hydropower production (BPA, 2011). For some periods streamflow gaging data was missing, but this was corrected by using linear regression of the streamflow from nearby gaging stations (ibid.). At some places the gaging station was not placed at the project, which was corrected by taking the streamflow from an upstream station and then adding a portion of the incremental flow based on a drainage area ratio (based on the ungaged portion of the drainage area) (ibid.). Where obvious errors occur in the data set, linear interpolation between good data points were used instead (ibid.). However, if large amounts of data were missing, alternative sources had to be used (e.g. stream gage data from U.S. Geological Survey, USGS) (ibid.).

S

This data type is the average daily observed storage change at project sites, which includes the storage change that occurs during the initial filling of the project in question (BPA, 2011). As opposed to H values, S values can have both positive and negative values. The S data was taken from various sources, e.g. USGS, the USACE, Environmental Canada, and project owners. Missing and erroneous data was corrected using the same methods described in the section above (ibid.).

A

A is the average daily project inflow and was either calculated by using H and S values for the project (see equation 24) or given by the project owners (BPA, 2011).

$$A = H + S \tag{24}$$

However, when calculating the project inflow from equation 24, values were sometimes negative (which in most cases is incorrect). The probable cause of such errors is the S data and this is because reservoir storage is often determined by storage/elevation tables (BPA, 2011). Due to the large area that projects usually occupies, small errors in the elevation readings (e.g. caused by wind setup) can result in large errors in the corresponding storage and change in storage values. These errors were corrected by increasing the storage change values until a reasonable positive inflow was obtained (ibid.). In order to preserve the original overall monthly storage change volumes, the same amount of water that was added to correct the project inflow for one day was subtracted from another day that month (ibid.).

L

L is the average daily local flow that comes into the river system between two data points, e.g. between two projects or between a project and a gaging station (BPA, 2011). To retrieve the local flows it is necessary to route the upstream outflow to the downstream project or gaging station, by using the Streamflow Synthesis and Reservoir Regulation model (SSARR) (ibid.). An example that shows how the local flow is calculated between an upstream dam and a downstream gaging station is shown in equation 25 below (ibid.).

$$Local\ flow\ (L) = Downstream\ point\ gaged\ flow\ (H) - Upstream\ point\ Outflow\ (H)\ routed\ down \tag{25}$$

To check for errors calculated local flows are plotted and studied, in order to determine whether it has a logical hydrological shape or not. Most of the time, unfortunately, the local flow had erratic spikes or

negative values (BPA, 2011). Negative values of local flows can be caused by any of the following reasons: surface water – groundwater interconnections, evaporation, diversionary water uses or inaccurate project data (ibid.). These negative values were corrected by using a method called indexing, which is described in the "2010 Level Modified Streamflow" report (ibid.).

ARF

ARF is the average daily unregulated routed flow, which denotes the flow, in a point along the river, as it would have been if no upstream dams existed (BPA, 2011). ARF is calculated by adding the local flow between two locations (two dams or a dam and a gaging station) to the inflow (A) into the upstream dam, routed (by SSARR) down to the downstream location (ibid.). An example of the calculation procedure, when calculating the ARF value at Revelstoke Dam (which is the first downstream station from Mica Dam), is shown in equation 26 below. Revelstoke is denoted RVC, Mica is denoted MCD and the number after the name denotation (in this case 5) shows which revision of the "Level Modified Streamflow" report that the data originates from (ibid.).

$$RVC5ARF = (MCD5A\ routed\ to\ RVC) + RVC5L \quad (26)$$

ARF is the data type that will be used throughout this report, when for example model performance is evaluated. This is because ARF data is only influenced by routing and therefore was decided to be the most suitable for this routing study.

Alternative data method

In the mid-Columbia River reach, between the Chief Joseph and the Priest Rapids projects, all project inflows (A), outflows (H) and local inflows (L) have been recalculated due to problems with negative locals and odd runoff shapes (BPA, 2011). Since almost all the side streams coming into the river are gaged, the local inflows have instead been replaced by gaged data from these tributaries (ibid.). The observed outflow at Chief Joseph and the inflow at Priest rapids have been assumed to be correct (ibid.). All in-between project inflows have been recalculated by routing the upstream outflow to the next station and adding the new local inflows (ibid.). Storage data was also assumed to be correct in order to recalculate the project outflows according to equation 24 above (ibid.).

3. Method

3.1 Cascade Reservoir

3.1.1 Derivation of one reservoir

A routing equation, for one reservoir, similar to the one used in the SSARR model will be derived below.

The continuity equation for a river reach can be written as:

$$\frac{dS}{dt} = I - O \tag{27}$$

where *S* is storage, *t* is time, *I* and *O* are inflow and outflow respectively from the river reach. The above equation is discretized for a finite time increment, Δt:

$$\frac{S_{t+\Delta t} - S_t}{\Delta t} = I_{\Delta t} - O_{\Delta t} \tag{28}$$

If the inflow and outflow during the time period Δt are approximated as the mean over the period, the above equation becomes:

$$\frac{S_{t+\Delta t} - S_t}{\Delta t} = \frac{(I_{t+\Delta t} + I_t)}{2} - \frac{(O_{t+\Delta t} + O_t)}{2} \tag{29}$$

The storage is assumed to depend on the discharge as (USACE, 1991):

$$S = T_s * O, where\ T_s = f(O) \tag{30}$$

T_S is a proportionality factor between storage and outflow and could be interpreted as the time of storage (USACE, 1991) i.e. retention time. Inserting equation 30 into equation 29 yields:

$$(O * T_s)_{t+\Delta t} - (O * T_s)_t = \Delta t \left(\frac{(I_{t+\Delta t} + I_t)}{2} - \frac{(O_{t+\Delta t} + O_t)}{2} \right) \tag{31}$$

Rearranging and separating all terms related to outflow at $t+\Delta t$ to one side gives:

$$O_{t+\Delta t} * \left(T_{s(t+\Delta t)} + \frac{\Delta t}{2} \right) = I_m * \Delta t + O_t * \left(T_{s(t)} - \frac{\Delta t}{2} \right) \tag{32}$$

where $I_m = \frac{(I_{t+\Delta t} + I_t)}{2}$. Assuming that $T_{s(t+\Delta t)} \approx T_{s(t)} \approx T_{sm}$ and rearranging equation 32 gives:

$$O_{t+\Delta t} = \frac{\left(I_m * \Delta t + O_t * \left(T_{sm} - \frac{\Delta t}{2} \right) \right)}{\left(T_{sm} + \frac{\Delta t}{2} \right)} = \frac{\left(I_m * \Delta t + O_t * \left(T_{sm} + \frac{\Delta t}{2} - \Delta t \right) \right)}{\left(T_{sm} + \frac{\Delta t}{2} \right)} \tag{33}$$

The above equation can be rewritten as the final reservoir routing equation (USACE, 1991):

$$O_{t+\Delta t} = O_t + \frac{\Delta t (I_m - O_t)}{\left(T_{sm} + \frac{\Delta t}{2} \right)} \tag{34}$$

The time of storage T_s is assumed to vary with discharge as (Rice & Larson, 1972) (USACE, 1991):

$$T_s = \frac{KTS}{O^n} \tag{35}$$

where *KTS* and *n* are parameters obtained by calibration (USACE, 1991). The mean time of storage over a time increment Δt can based on equation 35 be written as:

$$T_{sm} = \frac{KTS}{\left(\frac{(O_{t+\Delta t}+O_t)}{2}\right)^n} \quad (36)$$

3.1.2 Model parameters and computational time step

The model parameters will be introduced below, in the subsequent parts of this chapter. The parameter units are user specified and are therefore only suggestions. Note that in equation 34, the time of storage and the computational time step have to be of the same unit, e.g. (hours). Also, the inflows and outflows have to be of the same units, e.g. (m^3/s). More physical interpretations and methods of estimating the parameters will be reviewed later in this chapter. Finally, the computational time step will be commented on.

The number of sub reservoirs

The number of sub reservoirs affects the attenuation of the discharge, where one single reservoir yields the greatest level of attenuation and an infinite number of reservoirs cause no flow attenuation, only translation of the hydrograph (Heatherman, 2008). The optimal number of sub reservoirs is reach specific and should ultimately be obtained by calibration (USACE, 1994). A rule of thumb presented by the U.S. Army Corps (USACE) (1994) is that time of storage in each sub reservoir should be less than 1/5 of the time of rise of the inflow hydrograph (ibid.). Another way of estimating the number of phases is to introduce the concept of "characteristic reach length" – first developed by Kalinin and Milyukov in 1958 – which is the conceptual channel length for which there is "a one-to-one relationship between the depth in the midpoint and the discharge at the downstream end" (Heatherman, 2008). This relationship also means that there exists a one-to one relationship between storage in the sub reach and the discharge at the downstream end (ibid.). The SSARR manual suggests that a crude approximation of the number of sub reservoirs can be obtained by assuming a characteristic reach length of 5-10 miles (USACE, 1991). The USACE (2000) suggests that the number of steps can be estimated using the following equation, based on empirical work done by Strelkoff in 1980:

$$nbrPhases = 2 * L * \frac{S_0}{y_0} \quad (37)$$

where *N* is the number of steps, *L* is the total reach length, S_0 is the bottom slope and y_0 is the normal flow depth at base flow (Heatherman, 2008). A similar equation can be formulated based on the derivation of the characteristic reach length derived by Perumal (1992) (Heatherman, 2008):

$$L_u = \frac{Q_0}{S_0 * T * C_0} \quad (38)$$

where L_u is the characteristic reach length, Q_0 is discharge, T is the top width, C_0 is the wave celerity at the reference discharge Q_0. Dividing the total reach length by the characteristic reach length gives the number of required sub reservoirs:

$$nbrPhases = \frac{L * C_0 * T * S_0}{Q_0} \quad (39)$$

The parameter value of the number of sub reservoirs is an integer value exceeding or equal to1.

The KTS parameter

The *KTS* parameter (h*(m^3/s)^n) linearly affects the time of storage in the sub reservoirs (see equation 35). A large *KTS* thus results in a large time of storage and vice versa. Since a negative time of storage is unrealistic, the *KTS* parameter has to be positive. *KTS* includes several physical properties of the river reach such as friction, geometry, length and slope (Tingsanchali, 1986).

The n parameter

The time of storage changes with different discharge according to equation 35. Hence T_s in equation 34 includes a dependence of the discharge. Whether the time of storage increases or decreases with discharge depends on the flow situation and is regulated by the exponential coefficient *n*. The range of the *n* parameter is according to USACE (1991) between -1 and 1.

Time of storage varies with discharge according to equation 35, where the *n* coefficient controls the impact that a change in discharge has on the time of storage. In other words, it is a coefficient which controls the linearity/non-linearity of time of storage, where the linearity increases as *n* decreases and vice versa when *n* increases.

Normally when streamflow is restricted to the channel, the time of storage varies inversely with discharge, in which case *n* becomes a positive number (USACE, 1991). This is intuitive since with a higher discharge the water stays within a particular stream reach for a shorter amount of time than compared to a case with lower discharge. Figure 9 shows how the time of storage varies for different discharge values when *n*=-0.2, *n*=0, *n*=0.2 and *n*=0.4 respectively. The *n* coefficient, as mentioned before, usually has a value that is between -1 and 1 (ibid.).

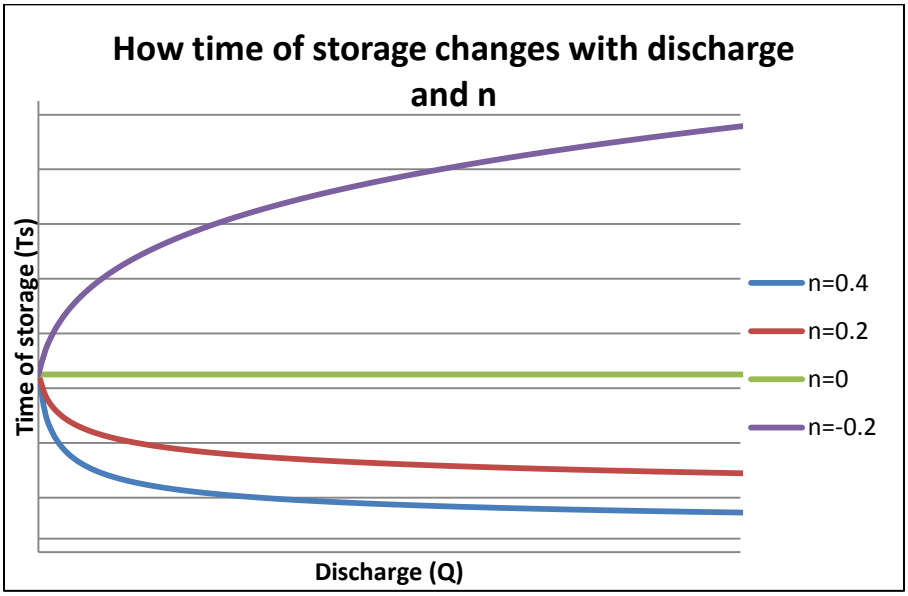

Figure 9: Time of storage plotted against *Q* for different values of *n*.

Sometimes it may be necessary to use negative values for *n*, which means that time of storage instead varies directly with the discharge. In this case an increase in discharge means an increase in time of storage (USACE, 1991). In order to explain such a relationship between discharge and time of storage consider a stream reach where overbank flow is dominant, when discharge increases the stream expands laterally onto its floodplains and the flow slows down markedly, thus increasing the time of storage of the water. Figure 9 shows how the time of storage varies for different discharge values when *n*=-0.2.

Time of storage is affected to a relatively large extent by the value of *n*. Smaller values of n yields a greater time of storage, assuming *KTS* to be constant for changes in *n*, and vice versa (USACE, 1991).

The total time of storage

All the above parameters combine into the flow dependent time of storage per phase (see equation 35). Depending on the *n* parameter, the time of storage will either increase or decrease with flow. The total time of storage in the reach will affect both attenuation and the lag time, where a large time of storage will cause more attenuation and a larger time lag, and vice versa.

The computational time

It is intuitive that a too large computational time step as compared to the time of storage, will affect the routing results negatively. In fact, as the computational time approaches two times the time of storage in equation 34, the outflow is less and less affected by the outflow at the previous time step. If the computational time step equals two times the time of storage, then the outflow (at $t+\Delta t$) is simply just the average of the inflow (at t and $t+\Delta t$) as equation 34 becomes:

$$O_{t+\Delta t} = O_t + \frac{\Delta t(I_m - O_t)}{\left(T_{sm} + \frac{\Delta t}{2}\right)} \xrightarrow{\Delta t \to 2*T_s} I_m$$

If the computational time step increases even further, the equation above will produce a negative effect of the outflow at the previous time step. In the limit where the computational time step approaches infinity, equation 34 becomes:

$$O_{t+\Delta t} = O_t + \frac{\Delta t(I_m - O_t)}{\left(T_{sm} + \frac{\Delta t}{2}\right)} \xrightarrow{\Delta t \to \infty} 2 * I_m - O_t$$

It is reasonable that as the computational time step increases, what happened at the previous time step has less and less effect on what is happening on the current time step. It is however not reasonable that what happened at the previous time step can affect the current time step negatively. Furthermore, the above equation could potentially produce negative outflows if $O_t > 2*I_m$. Therefore, the value of the computational time step should never exceed two times the minimum value of time of storage.

3.1.3 Interpolation

If the input data is of a cruder time resolution than the computational time step, the program has to interpolate the data between known data values. In the BPA data set, the input data is daily average at the finest. If the computational time step is set to for example 1 hour, the daily averages have to be interpolated to give data over all of the 24 hours of the day. In the cascade3 routing routine – which is the name of the routing routine that is developed in this thesis – daily average values are set to represent all the sub time steps of the day, giving rise to a step-wise appearance of the hydrograph, as can be seen in Figure 10.

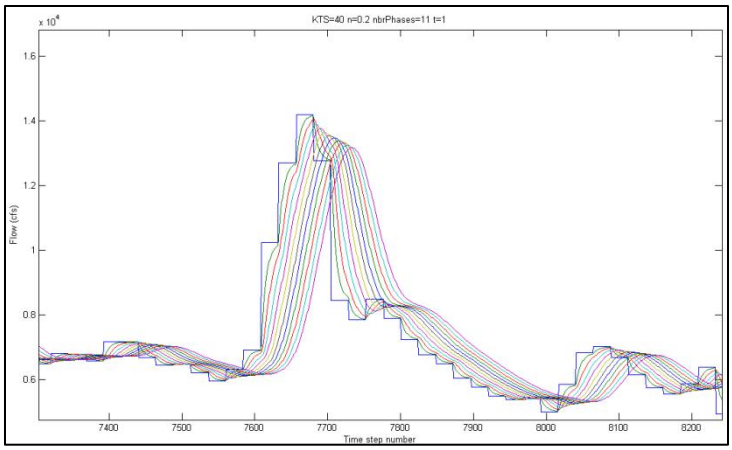

Figure 10: A solution matrix from the cascade3 routing routine. The blue line shows the "constant" interpolation.

3.2 Applying the model in the general case

3.2.1 Approximation of model parameters

If no model parameters are available, a general method of estimating the parameters is needed. The simplest method is to use parameters from similar areas, if available. Otherwise, the following methods can be used.

The n parameter

The residence time of a water body is by definition the volume of the water body divided by the throughflow (Chow, et al., 1988):

$$T_s = \frac{V}{Q} \tag{40}$$

If the water body is a channel reach of a certain length *L* and a cross sectional area *A*, the above equation can be rewritten as:

$$T_s = \frac{V}{Q} = \frac{L*A}{Q} \tag{41}$$

It is obvious that the cross sectional area will vary with the flow. For uniform steady flow, this can be described using the Manning formula (French, 1994):

$$Q = \frac{1}{m} * A * R_h^{\frac{2}{3}} * S^{\frac{1}{2}} = \frac{1}{m} * A * \left(\frac{A}{P}\right)^{\frac{2}{3}} * S^{\frac{1}{2}} \tag{42}$$

Assuming a wide channel ($B>>y$), and rearranging the above equation, the cross sectional area can be expressed as a function of the flow:

$$A = \left(\frac{B^{\frac{2}{3}}*m}{S^{\frac{1}{2}}}\right)^{\frac{3}{5}} Q^{\frac{3}{5}} \tag{43}$$

Inserting equation 43 into equation 41 gives:

$$T_s = \frac{L*B^{\frac{2}{5}}*m^{\frac{3}{5}}}{S^{\frac{3}{10}}} * \frac{1}{Q^{\frac{2}{5}}} = \frac{KTS}{Q^n} \Rightarrow \boxed{n = 0.4} \tag{44}$$

The above equation confirms what is intuitive, that the time of storage increases with increasing friction, and decreases with increasing slope. Furthermore it provides an estimate of the n parameter of 0.4.

The nbrPhases parameter

The *nbrPhases* parameter represents the number of sub reservoirs, or phases, that the total river reach is divided into. The *nbrPhases* parameter can be estimated with different methods depending on the amount of data available. The simplest way of estimating the parameter is by using the rule of thumb from the SSARR manual, previously mentioned as (USACE, 1991):

$$nbrPhases = \frac{L_{reach}}{16} \quad (45)$$

where the unit of L_{reach} is expressed in km.

If more reach data is available, equation 37 or equation 39 can be used to estimate the parameter:

$$nbrPhases = 2 * L_{reach} * \frac{S_0}{y_0} \quad (37)$$

$$nbrPhases = \frac{L_{reach} * C_0 * T * S_0}{Q_0} \quad (39)$$

where L_{reach} is the total reach length, y_0 is the water depth at base flow, C_0 is the flood wave velocity at the reference flow, T is the top width, S_0 is the bottom slope and Q_0 is the reference flow. The characteristic reach length will be different for different discharges (Heatherman, 2008), which means that the number of phases will be optimized for the reference flow, Q_0. Therefore the mean flow is used as the reference flow.

It should be kept in mind that the nbrPhases parameter has to be a positive integer value.

The total time of storage T_s

As for the nbrPhases parameter, two different methods, with different level of required data, will be used to estimate the total time of storage in the river reach. Both methods assume that the time of storage is approximately the travel time (USACE, 1991) through the reach.

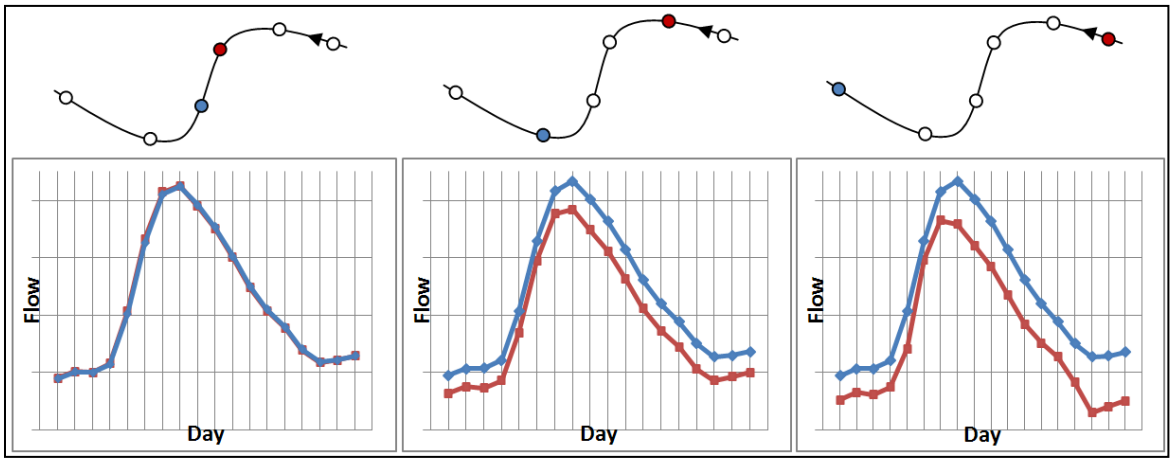

Figure 11: Estimating the travel time by studying inflow and outflow hydrographs at increasing intermediate distance. This specific peak is around the mean flow of the full hydrographs.

The first and most obvious method is to look at the streamflow data sets, study the inflow and outflow hydrographs from the river reach and estimate the time lag between the two hydrographs. Since high

and low flow will pass through the reach at different time of storage (see for example equation 35), it is suggested to study the hydrographs around the mean flow. A problem arises if the time lag between the inflow and outflow hydrographs is much less than the time resolution of the hydrograph data. The strategy to address this issue is then to compare outflow and inflow hydrographs at greater intermediate distance (see Figure 11) and to increase the intermediate distance until a clear time lag can be seen. This of course requires data at multiple gaging stations along the river. The time of storage for the different reaches is then simply determined by dividing the total time of storage according to the length of the sub reaches. Thus the time of storage for a reach is estimated as:

$$T_s = \frac{Total\ lag\ time}{total\ length} * length\ of\ reach \quad (46)$$

The second method for estimating the total time of storage is by estimating the flood wave velocity through the reach. The flood wave velocity can be estimated to be the mean velocity multiplied by 1.5 (USACE, 1991; USACE, 2000; Rantz, 1982):

$$U_{wave} = 1.5 * U_{mean} \quad (47)$$

where the mean velocity U_{mean} can be estimated using the Manning formula (see equation 2).

This means that the total time of storage can be approximated as:

$$T_s = \frac{L_{reach}}{1.5 * U_{mean}} \quad (48)$$

The KTS parameter

The only parameter that remains to be determined in equation 35 is the *KTS* parameter. This parameter can be calculated as (USACE, 1991):

$$KTS = \frac{T_s}{nbrPhases} * Q^n \quad (49)$$

where T_s is the time of storage for the reach and Q is the mean flow through the reach.

3.3 Applying the model in Columbia River

The cascade routing routine will be evaluated using the BPA (2011) data from the Columbia River. The evaluation partly involves verifying the performance of the model and also getting familiarized with the model and its parameters.

3.3.1 Model verification

To verify the performance of the cascade routing routine, the routing through Columbia River as performed by the BPA (2011) will be recreated and compared to the result from BPA. The data recreated is the ARF data, simply because they only consider the effects of routing and are unaffected of further refinements. This involves a stepwise routing procedure where the river is divided into a number of sub reaches separated by stations, either dams or gages. The flow at the headwater is routed to the next following station and simply added to the local inflow over the sub reach. This flow is in turn routed to the next station where the next local inflow is added, and so on (see appendix

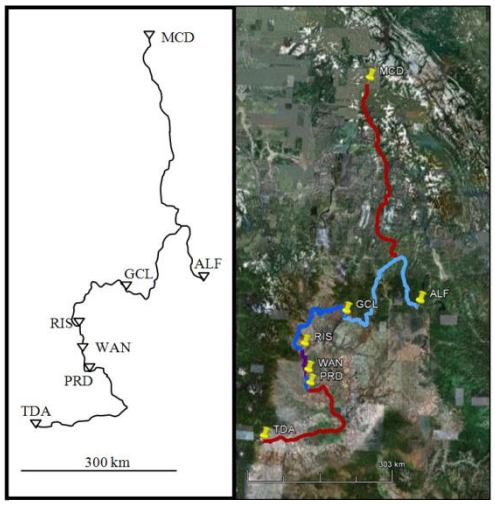

Figure 12: Maps showing the different geographic distances. The right hand map is taken from Google Earth (2011).

Table 20 and
Table 21 for the exact procedure). This process continues all the way down to a final station where the recreated ARF data is compared to the ARF data provided by the BPA (2011). The model verification is in this way a comparison between the recreated routing routine and the routing in the SSARR model, to confirm that the recreation is successful.

The model verification will be performed on three different geographical scales (Figure 12):

- ✓ Short distance: The river reach between Rock Island (RIS) and Wanapum (WAN), approximately 60 km. This particulate reach was chosen for the simplifying property of having negligible local inflow and thereby only shows the effects of routing.
- ✓ Intermediate distance: Two different river stretches of approximately the same length but with different routing parameters. The first one is the part of the river between Grand Coulee (GCL) and Priest Rapids (PRD), approximately 310 km. The second one is the part of the river between Albeni Falls (ALF) and Grand Coulee (GCL), approximately 360 km.
- ✓ Long distance: The part of the river between Mica (MCD) and The Dalles (TDA), approximately 1300 km.

3.3.2 Lumping channel sub-stretches

This section evaluates the possibility of adding, or lumping, together the parameters from several reaches into one set of "lumped" parameters for the entire reach. A procedure for how to lump known parameters is suggested and tested.

Lumping multiple known stream stretch parameters

If the parameter values of *nbrPhases*, *n* and *KTS* are known for a number of succeeding channel sub stretches, then the parameter values for the total channel stretch (including all sub reaches) can be estimated as follows.

The nbrPhases parameter

Since all of the sub reaches each has an optimal number of phases, the number of phases for the entire channel stretch is simply taken as the sum of the number of phases for all the sub reaches:

$$\boxed{nbrPhases_{tot} = \sum_{i=1}^{k} nbrPhases_i} \quad (50)$$

where *k* is the number of sub reaches.

The KTS parameter

The total time of storage for a lumped channel stretch of *k* number of channel reaches equals the sum of the time of storage for all the sub reaches:

$$T_{s,tot} = nbrPhases_{tot} * \frac{KTS_{tot}}{(Q_{tot})^{n_{tot}}} = nbrPhases_1 * \frac{KTS_1}{(Q_1)^{n_1}} + nbrPhases_2 * \frac{KTS_2}{(Q_2)^{n_2}} + \ \dots + nbrPhases_n * \frac{KTS_k}{(Q_n)^{n_k}} \quad (51)$$

If $(Q_{tot})^{n_{tot}} \approx (Q_1)^{n_1} \approx \ \dots \ \approx (Q_n)^{n_k}$ then the above equation can be rearranged and reduced to:

$$\boxed{KTS_{tot} = \frac{\sum_{i=1}^{k} KTS_i * nbrPhases_i}{nbrPhases_{tot}}} \quad (52)$$

This means that the *KTS* value for the entire reach can be estimated by weighing the *KTS* values from all the sub reaches based on their number of phases.

The n parameter

Taking the logarithm of both sides in equation 51 and rearranging gives:

$$n_{tot} = -\frac{\log\left(\frac{nbrPhases_1 * \frac{KTS_1}{(Q_1)^{n_1}} + nbrPhases_2 * \frac{KTS_2}{(Q_2)^{n_2}} + \ldots + nbrPhases_n * \frac{KTS_k}{(Q_n)^{n_k}}}{nbrPhases_{tot} * KTS_{tot}}\right)}{\log(Q_{tot})} \quad (53)$$

If $n_1 = \ldots = n_k$ and if $Q_{tot} \approx Q_1 \approx \ldots \approx Q_n$, then $\boxed{n_{tot} \approx n_1 = \ldots = n_k}$ (54)

Evaluating the performance of the lumped routing

In order to investigate if the lumped model produces the same routing effects as the stepwise routing, a stream reach that stretches from Mica (MCD) all the way down to The Dalles (TDA) (see Figure 12), will be used. The routing effects are first computed by routing the flow from the headwater MCD stepwise all the way down to TDA without adding the local inflows along the way. The lumped model is then run using the lumped parameters in one "lumped" step and then compared to the routing effects from the stepwise routing.

3.4 Optimizing model parameters

3.4.1 Sensitivity analysis

To make the calibration process more effective, it is important to know how the individual parameters affect the outcome of the model. In the sensitivity analysis all model parameters are modified individually to check how they affect the model output. One at a time, all of the parameter values are first reduced to half and then increased to twice their original values, while simultaneously checking the model output for these new values. This is done to get a better understanding of the model parameters, so that it is clear how one should modify the parameters in order to optimize the model performance during calibration.

3.4.2 Objective functions

The objective functions evaluate the model performance, which aids the user in deciding whether the model output is good or bad. Even if the objective functions give an exact number of the model performance it is still up to the user to decide if it is acceptable or not, in other words it is a subjective decision. Below follows a description of two objective functions, one which is used frequently to evaluate hydrological models and one that was created specifically to evaluate the cascade3 routing routine.

Nash-Sutcliffe efficiency – r²

Moriasi et al. (2007) describes the Nash-Sutcliffe efficiency (r^2) as: "a normalized statistic that determines the relative magnitude of the residual variance ("noise") compared to the measured data variance ("information")". The term residual is in this case referring to the "error" in the model result data as compared to the observed data.

$$r^2 = 1 - \frac{\sum_{t=1}^{T}(Q_o^t - Q_m^t)^2}{\sum_{t=1}^{T}(Q_o^t - \overline{Q_o})^2} \quad (55)$$

Q_o = observed discharge

Q_m = modeled discharge

Q_o^t / Q_m^t = observed/modeled discharge at time t

(Nash and Sutcliffe, 1970)

The r^2 value is commonly used to evaluate the performance of conceptual hydrological models. Acceptable levels of performance are when r^2 ranges between 0.0 and 1.0 (Moriasi, et al., 2007). When r^2 values are smaller than 0.0 it is an indication of that the mean observed value gives a better prediction than the simulated value, which means that the model performance is unacceptable (ibid.). An r^2 value of 1.0 on the other hand indicates optimal model performance (ibid.).

The Nash-Sutcliffe ratio was, as mentioned above, originally intended to evaluate the performance of conceptual hydrological models. Since streamflow routing only is a part of the hydrological cycle the use of r^2 is not optimal. Therefore, when evaluating the effects of routing, r^2 values will be near to 1.0. This means that to be able to compare the r^2 values from the different river reaches, a high number of significant digits is needed. In this report, the number of significant digits for r^2 will be kept high enough to show where it deviates from unity.

Mean of the absolute flow error – Q_{av}

The cascade3 routing routine strives to replicate U.S. Army Corps' (USACE) "cascade of reservoir" routing function as close as possible, which makes it interesting to compare simulated streamflow, from USACE's and the cascade3 routing routine, over time. To get a rough idea of how well the cascade3 routing routine depicts their model one can sum the difference in streamflow – between the two models – at each time step, and divide by the number of simulated time steps, which gives the average flow error of the cascade3 routing routine. However, to avoid the risk of negative flow errors cancelling out positive errors, it is necessary to take the absolute value of the flow error, before summing the errors and dividing by the number of time steps. As can be seen in equation 56, the objective function has the same unit as the discharge and is in other words not normalized. This is because the effects of routing are a small part in the hydrological cycle, as mentioned in the previous section, which would result in an insignificantly small value if it was normalized by for example the total discharge.

$$Q_{av} = \frac{\sum_{t=1}^{T} |Q_o^t - Q_m^t|}{T} \quad (56)$$

Q_o = observed discharge

Q_m = modeled discharge

Q_o^t / Q_m^t = observed/modeled discharge at time t

T = total number of time steps

3.4.3 Calibration

When all model parameters have been estimated, according to the methods described above, it will most likely be necessary to calibrate them. Calibration of hydrological models is done by changing the values of the model parameters, in order to get the modeled discharge to better fit the observed discharge, within the area that is being modeled.

The cascade3 routing routine is not a complete hydrological model – it is a routing function that is to be included into a hydrological rainfall runoff model – which can be calibrated with the use of stream

gage data. To calibrate a river routing function, stream gage data in two points are needed; one upstream and one downstream. Then one needs to find the model parameters that best translate the upstream hydrograph into the downstream hydrograph.

However, because the cascade3 routing routine is going to be a part of a hydrological rainfall runoff model, both the routing function and the hydrological model need to be calibrated simultaneously. This is because, as the water in the river is routed downstream, local inflows are generated by the hydrological model and added to the water that is currently being routed. For the effects of routing not to be completely "drenched" by local inflows it is important to find the "optimal" scale at which calibration is done. Finding this "optimal" scale for calibration is a balance between not dividing the catchment/-s into too small a scale at which the effects of routing are negligible but at the same time not increasing too much in scale at which the effects of routing are drenched by local inflows. Ultimately, this will be a balance between model precision and model simplicity. Once the optimal scale for calibration is decided upon, both the routed upstream hydrograph and the local inflows within the sub-area can be calibrated simultaneously against the downstream hydrograph (see Figure 13).

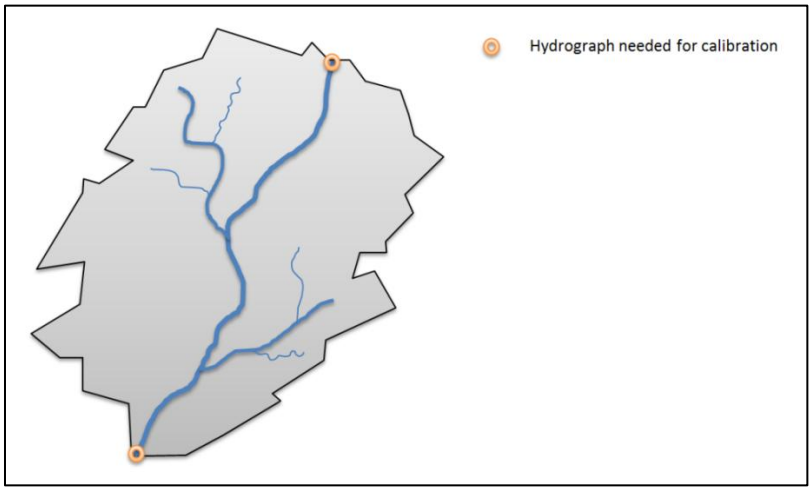

Figure 13: Example of how a sub-area used for calibration can look like, with points indicating where data is needed.

There are three model parameters that can be calibrated in order to optimize model performance: *KTS*, *n* and *nbrPhases*. *KTS* and *n* can be used to increase or decrease the time of storage within the reach (Eq.9). The *nbrPhases* parameter governs how much the upstream hydrograph is attenuated as it moves downstream. A more detailed description of the model parameters is presented in chapter 3.1.2.

3.5 The importance of routing

To evaluate the importance of routing in the Columbia River basin, three different routing procedures with different degrees of routing will be compared over the part of the river between Mica (MCD) and The Dalles (TDA).

- ✓ The first and most crude routing procedure is by routing the headwater flow at MCD all the way down to TDA and adding it to the sum of all the local inflows along the way. This will show how the final result is affected if there is no routing of the local inflows.

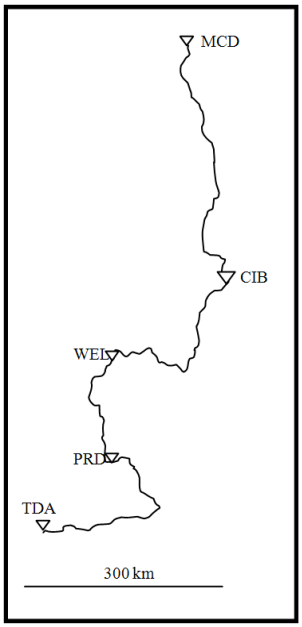

Figure 14: The stations where local inflows were added.

- ✓ The second less crude routing procedure is to divide the entire catchment in two, and to route the headwater flow to a station halfway down to The Dalles (WEL in Figure 14) where the summed local inflows along the first half of the river are added. This summed flow is then in turn routed the second half down to The Dalles where it is added to the summed local inflows along the second half of the river.
- ✓ The third routing procedure is the same as above, but with four divisions instead of two (as presented in Figure 14).

3.6 Comparison with Muskingum routing

A common way of modeling streamflow routing in HBV-type models is to use the Muskingum routing method. Routing over the stretch Mica to The Dalles will therefore also be modeled using the Muskingum method. The Muskingum parameters will be calibrated against the effects of routing (see chapter 3.3.1) from the cascade3 routing routine. Thus, the reasonableness of the calibrated Muskingum parameters can further verify the reasonableness of the cascade3 routing routine.

3.6.1 Derivation of Muskingum routing equation

The continuity equation for a river reach, discretized over the time step Δt can be written as equation 28:

$$\frac{S_{t+\Delta t}-S_t}{\Delta t} = I_{\Delta t} - O_{\Delta t} \quad (28)$$

Where *S* is reach storage, *I* is the upstream inflow and *O* is the downstream discharge. The storage can be described using the Muskingum storage equation (equation 18):

$$S = K[XI + (1-X)O] \quad (18)$$

Combining the continuity equation with the Muskingum storage equation gives the following routing equation (Chow et al., 1988):

$$O_{t+\Delta t} = C_1 * I_{t+\Delta t} + C_2 * I_t + C_3 * O_t \quad (57)$$

The constants C_1, C_2 and C_3 are then expressed as (Chow et al., 1988):

$$C_1 = \frac{\Delta t - 2KX}{2K(1-X)+\Delta t} \quad (58)$$

$$C_2 = \frac{\Delta t + 2KX}{2K(1-X)+\Delta t} \quad (59)$$

$$C_3 = \frac{2K(1-X)-\Delta t}{2K(1-X)+\Delta t} \quad (60)$$

Where *K* and *X* are the model parameters.

3.7 Computer hardware and software

3.7.1 Computer hardware

Below follows a specification of the hardware of the computer that was used for testing the routing routines.

CPU: Intel (R) Core (TM) 2 Duo CPU T9400 @ 2.53GHz
Internal memory (RAM): 4.00 GB

Hard drive: Hitachi SATA Device (5400 rpm)
Graphics card: NVIDIA GeForce 9600M GT (512 MB dedicated)

3.7.2 Computer software

The computer software used to develop and run the routing routines is Mathworks MATLAB 7.12.0.635 (R2011a) and Microsoft Excel 2010. The only toolbox used in MATLAB is the optimization toolbox, which includes a function called “fzero” that is used to solve an equation in the cascade3 code. Other MATLAB functions that were used: xlsread, xlswrite, datenum, datetick.

4. Results & Discussion

4.1 Solution procedure using the cascade3 routing routine

Below in Figure 15 the solution algorithm that is included in the cascade3 routing routine is presented. The full MATLAB code is provided in the appendix along with a routing example. The appendix also includes the MATLAB code for the objective functions. The routing routine basically interpolates the input data over the user specified time step and solves equation 34 repeatedly for the subsequent time steps and phases. The computational time step should not be too big (see chapter 3.1.2) and is therefore checked and adjusted manually outside the cascade3 routing routine.

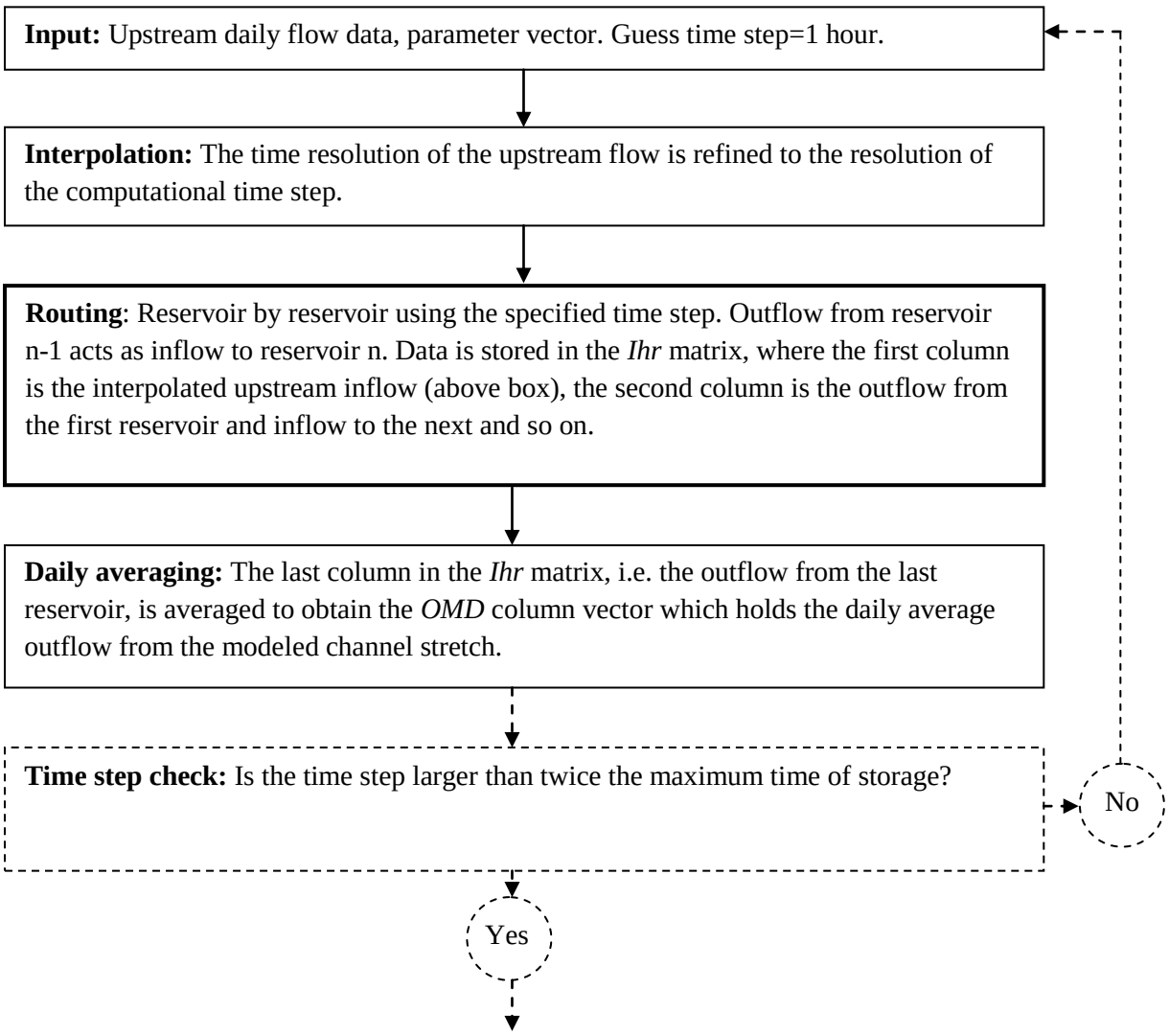

Figure 15: The solution procedure for channel routing using the cascade3 routing routine. The dashed parts are performed outside the cascade3 function.

The input data to the cascade3 routing routine is described in Table 1 below.

Table 1: The input data required in the cascade3 routing routine.

Input	Description
Upstream inflow data	The observed upstream hydrograph
KTS	Model parameter (see chapter 3.1.2, chapter 3.2.1 and chapter 3.3.2)
n	Model parameter (see chapter 3.1.2, chapter 3.2.1 and chapter 3.3.2)
nbrPhases	Model parameter (see chapter 3.1.2, chapter 3.2.1 and chapter 3.3.2)
T	The computational time step (see Figure 15 and chapter 3.1.2)
tIndata	The time resolution of the upstream inflow data

The output data from the cascade3 routing routine is described in Table 2 below.

Table 2: The output data from the cascade3 routing routine.

Output	Description
OMD	The routed outflows at the same timescale as the upstream inflow data
Ihr	The full solution matrix including all phases at the timescale of the computational time step

4.2 Model verification

4.2.1 Rock Island to Wanapum (distance 60 km)

The stretch between Rock Island (RIS) and Wanapum (WAN) is shown on a map in Figure 12. The fit between the cascade3 model and the ARF (Average daily unregulated Routed Flow, see chapter 2.2.2) data from BPA is very good for all flows, as can be seen in Figure 16 and Figure 17 below. This is also confirmed by the objective functions (Table 3). Since there are no local inflows between RIS and WAN the figures show the effects of routing. Some flow attenuation and a small time delay can be seen in the figures, however not close to the time scale of the input data, which is given in days. The errors in this case are so small that they approach round off errors. However, the errors will be discussed more in detail in subsequent chapters. Even if the fit is very good in this reach, conclusions regarding the model performance cannot be made on such a small geographical scale and will therefore be treated in later chapters.

Figure 16 and Figure 17 include not only the resulting ARF values from the cascade3 routing routine and from the BPA streamflow dataset (at WAN), but also the upstream ARF value from BPA (at RIS). This is just to give the reader a reference for comparison and will be used as a reoccurring aid throughout chapter 4.2.

Table 3: Value of objective functions for RIS-WAN, Model verification 1984.

Objective function	Value
r^2	0.999999988
Q_{av} (cfs)	3.86

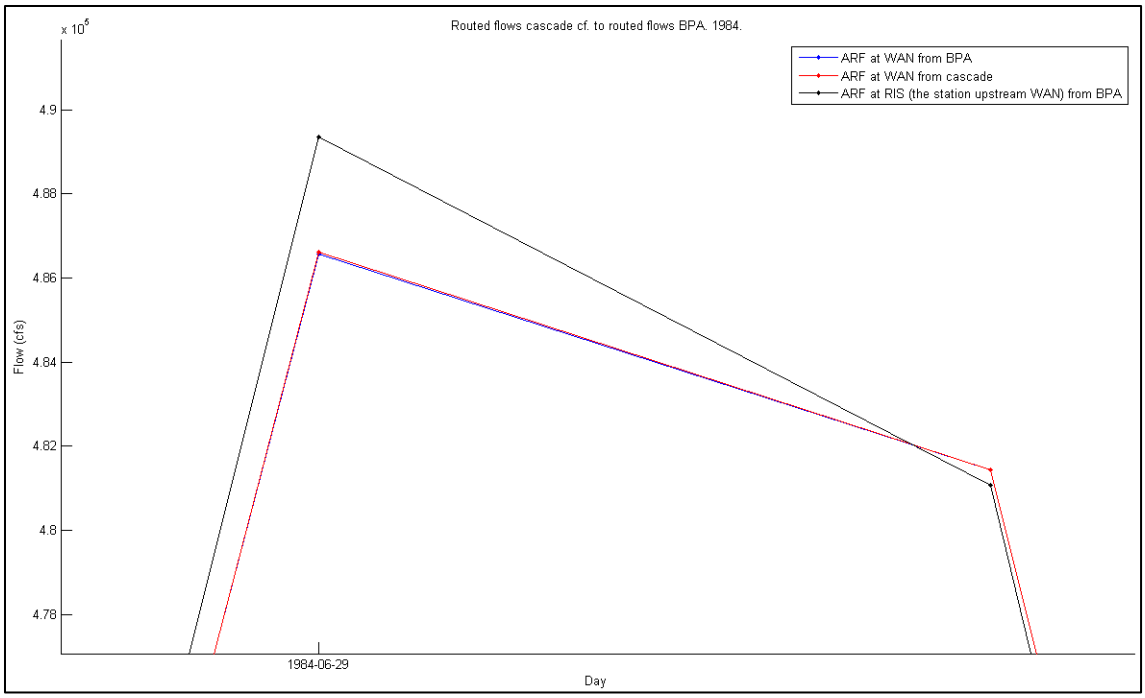

Figure 16: Rock Island ARF (average daily unregulated routed flow) routed to Wanapum. High flow.

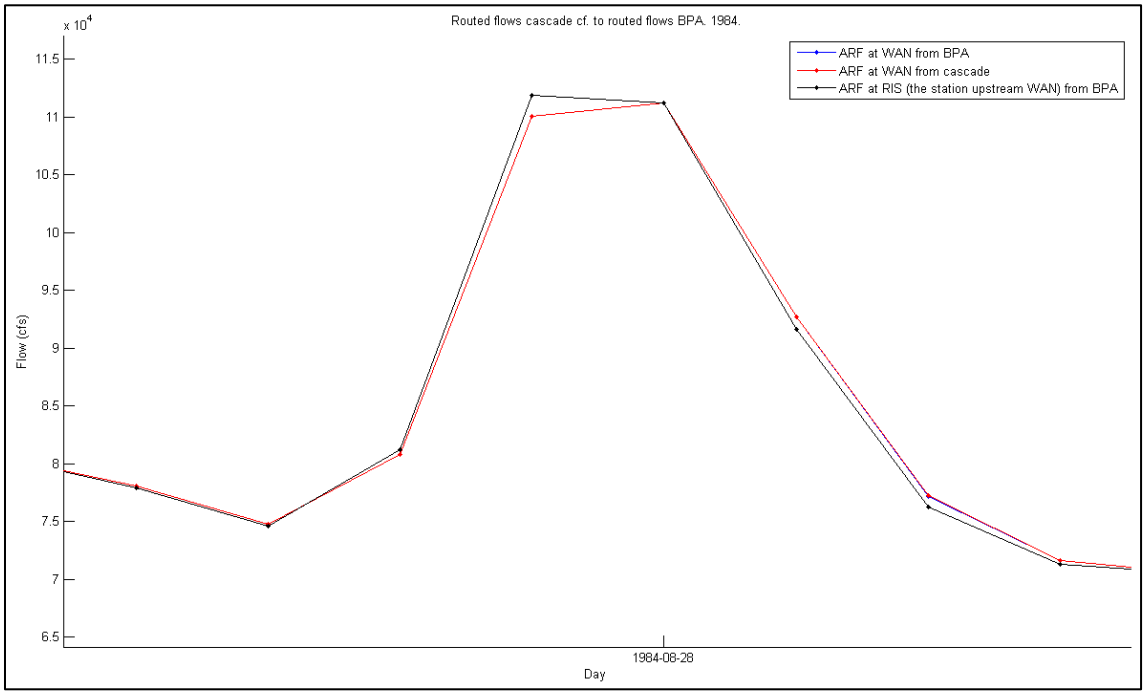

Figure 17: Rock Island ARF routed to Wanapum. Low flow.

4.2.2 Grand Coulee to Priest Rapids (distance 310 km)

The fit between the models for the river reach between Grand Coulee (GCL) and Priest Rapids (PRD) are quite good for both high and low flows, see Figure 18 and Figure 19. With an increasing distance model errors begin to appear, which can be seen in Figure 18, Figure 19 and Figure 20. This is also confirmed by the objective functions and especially in Q_{av} (see Table 4), which increases many folds as compared to the reach between RIS and WAN (Table 3). Furthermore, at this geographical distance sections of poorer fit appear, as can be seen in Figure 20. These errors are probably caused by the interpolation procedure in the cascade3 function, as explained in chapter 3.1.3. Interpolation errors are

first introduced at GCL (when interpolating the daily input data over 24 hours) and reoccur repeatedly through the local inflows over the entire stretch. Interpolation errors will be discussed extensively throughout the chapter.

Figure 18 to Figure 19 do not only show the effects of routing since the local inflows are not negligible and thereby substantially affect the appearance of the graphs. Effects of routing for all river stretches in this chapter will be discussed in chapter 4.3.

Table 4: Value of objective functions for GCL-PRD, Model verification 2001-2006.

Objective function	Value
r^2	0.9999956
Q_{av} (cfs)	133

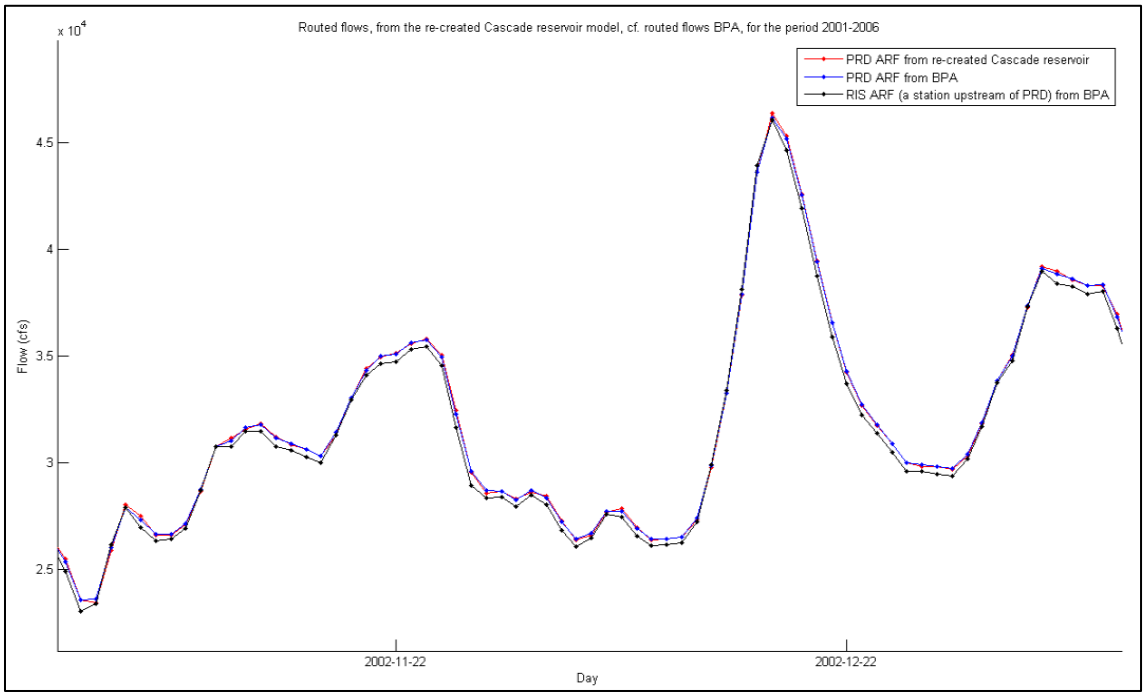

Figure 18: Grand Coulee ARF routed to Priest Rapids. Low Flow.

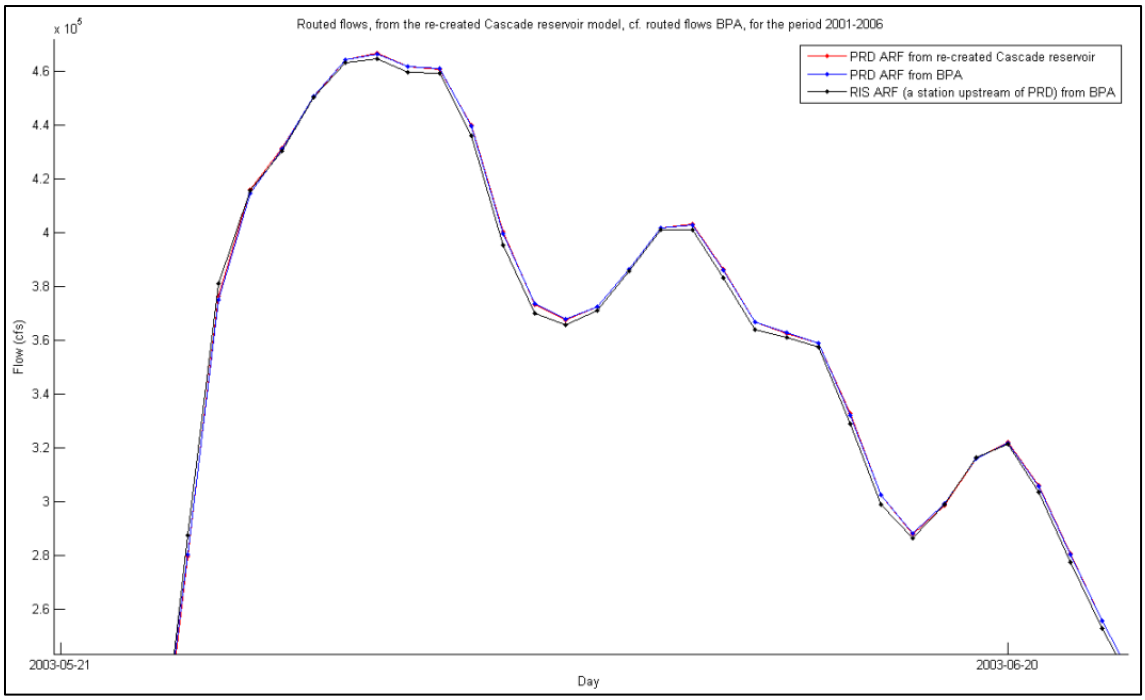

Figure 19: Grand Coulee ARF routed to Priest Rapids. High flow.

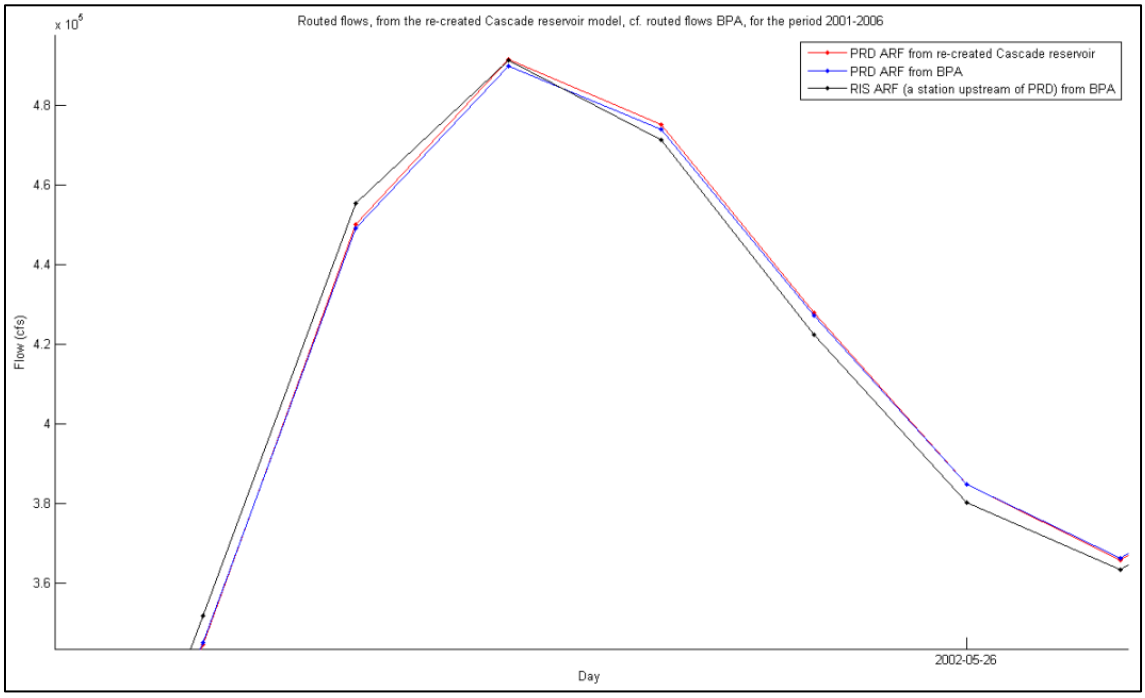

Figure 20: Grand Coulee ARF routed to Priest Rapids. A time period of poorer fit.

4.2.3 Albeni Falls to Grand Coulee (distance 360 km)

The river reach between Albeni Falls (ALF) and Grand Coulee (GCL) is of approximately the same distance as the previous stretch (GCL-PRD). The model errors (see Figure 21, Figure 22 and Figure 23) and the value of the objective functions (Table 5) are similar to those of the previous stretch.

Figure 20 and Figure 23 show that the time period with a poor fit reoccurs at the exact same date in both river reaches (GCL-PRD and ALF-GCL). This will be discussed more in detail in the next chapter.

Table 5: Value of objective functions for ALF-GCL, Model verification 2001-2006.

Objective function	Value
r^2	0.999989
Q_{av} (cfs)	168

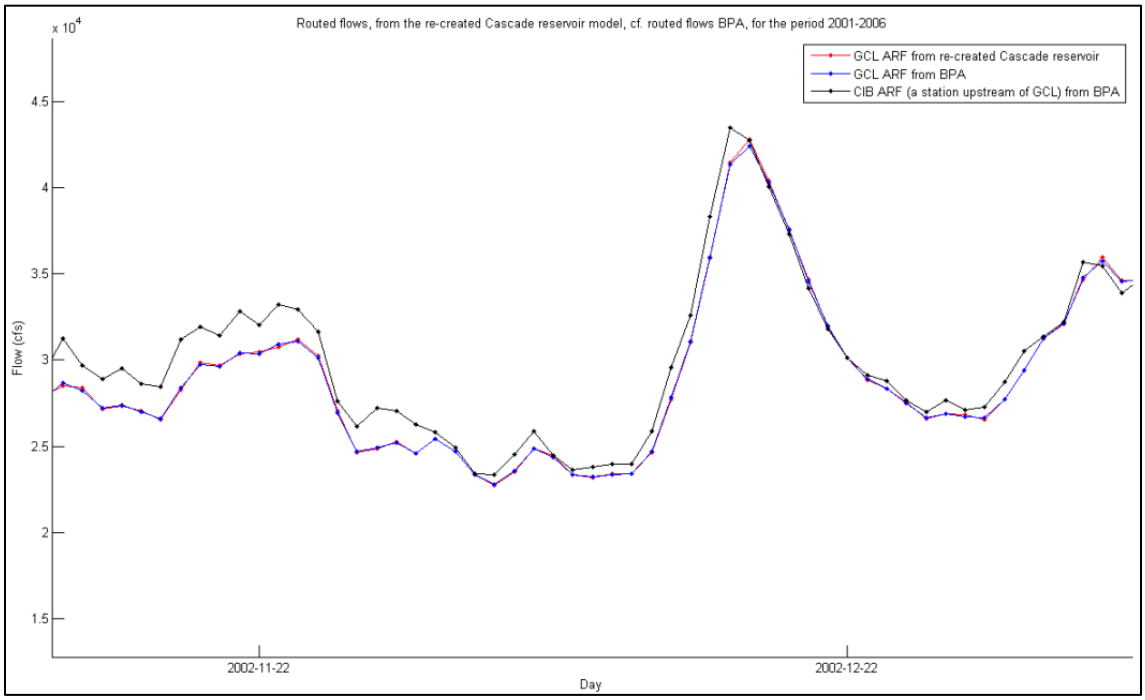

Figure 21: Albeni Falls ARF routed to Grand Coulee. Low flow.

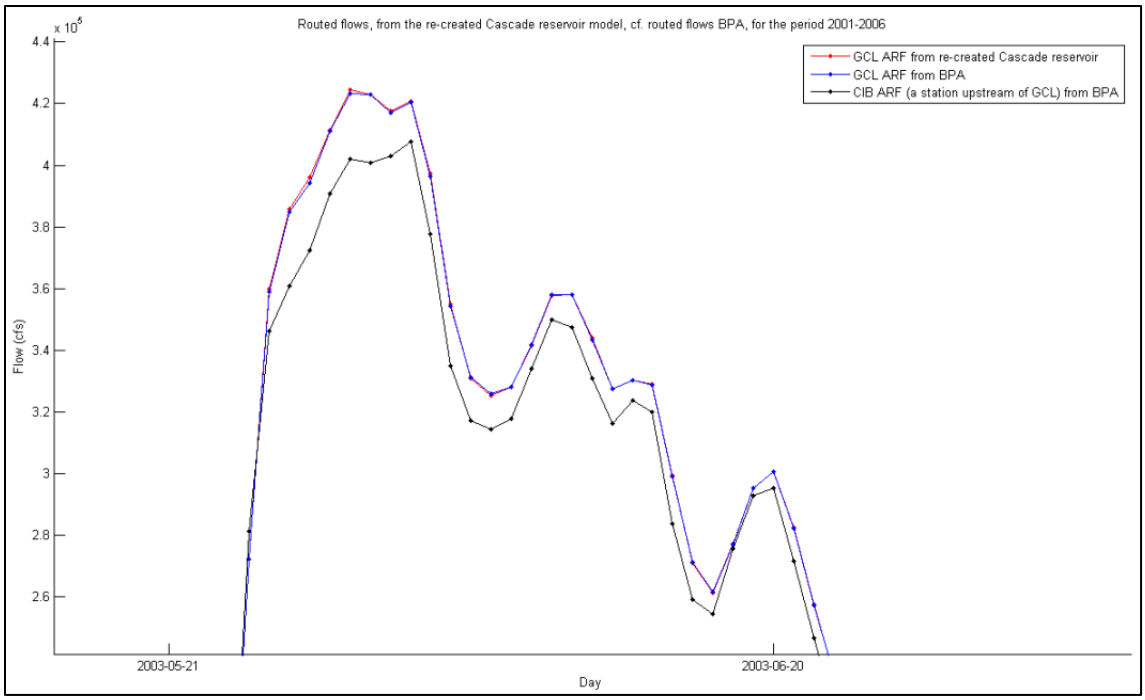

Figure 22: Albeni Falls ARF routed to Grand Coulee. High flow.

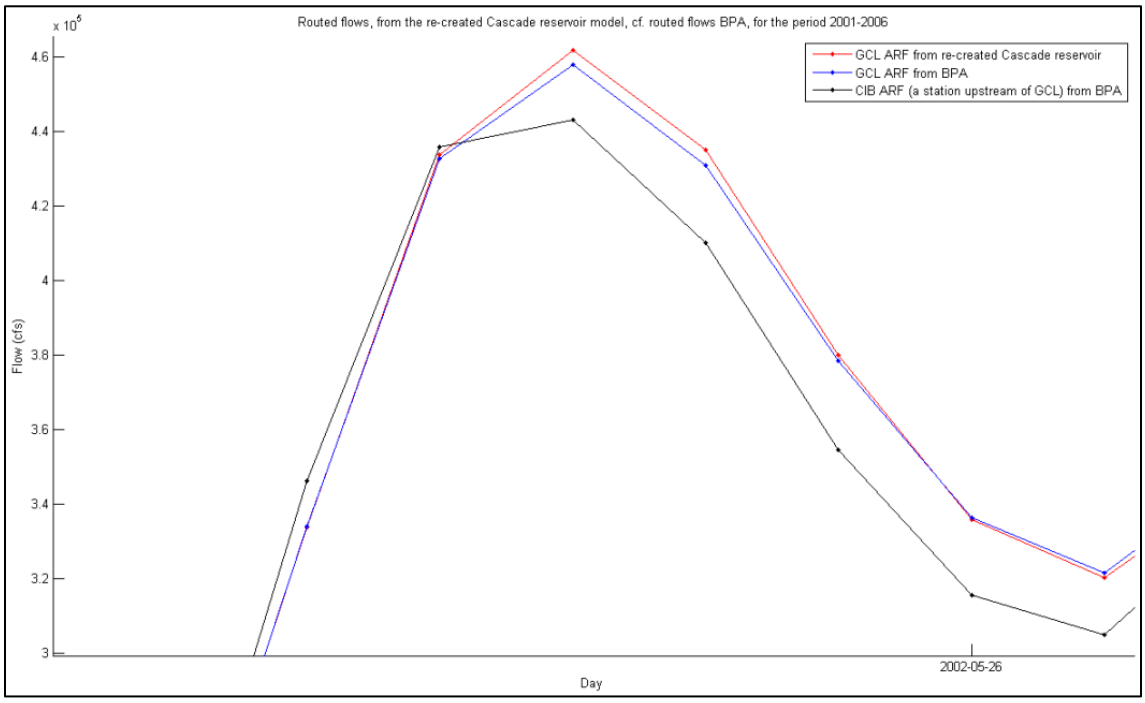

Figure 23: Albeni Falls ARF routed to Grand Coulee. A time period of poorer fit.

4.2.4 Mica to The Dalles (distance 1300 km)

At the largest geographical distance, between Mica (MCD) and The Dalles (TDA), the errors become more apparent, see Figure 24, Figure 25 and Figure 26. Also the values objective functions are clearly impaired as compared to previous river reaches (see Table 6). Apparently, the errors increase as the geographical distance increases. As the geographical distance increases, so does the number of sub reaches, within which local inflows are generated. All these local inflows are interpolated and included in the model output.

The period of poorer fit reappears at the same date as in the previous two reaches (see Figure 26 c.f. Figure 20 and Figure 23). Since the two previous stretches, ALF to GCL and GCL to PRD, are both included in the river stretch between MCD and TDA (see Figure 12), it plausible that it reappears at this stretch. Figure 27 shows the model check for a full year (2002). It appears that the cascade3 routing routine performs well in period of low variation of flow and worse in regions with very sharp variations in the hydrograph. A possible explanation to these kinds of errors is further discussed in chapter 4.3.3.

Table 6: The value of objective functions for MCD-TDA, model verification 2001-2006.

Objective function	Value
r^2	0.9994
Q_{av} (cfs)	1780

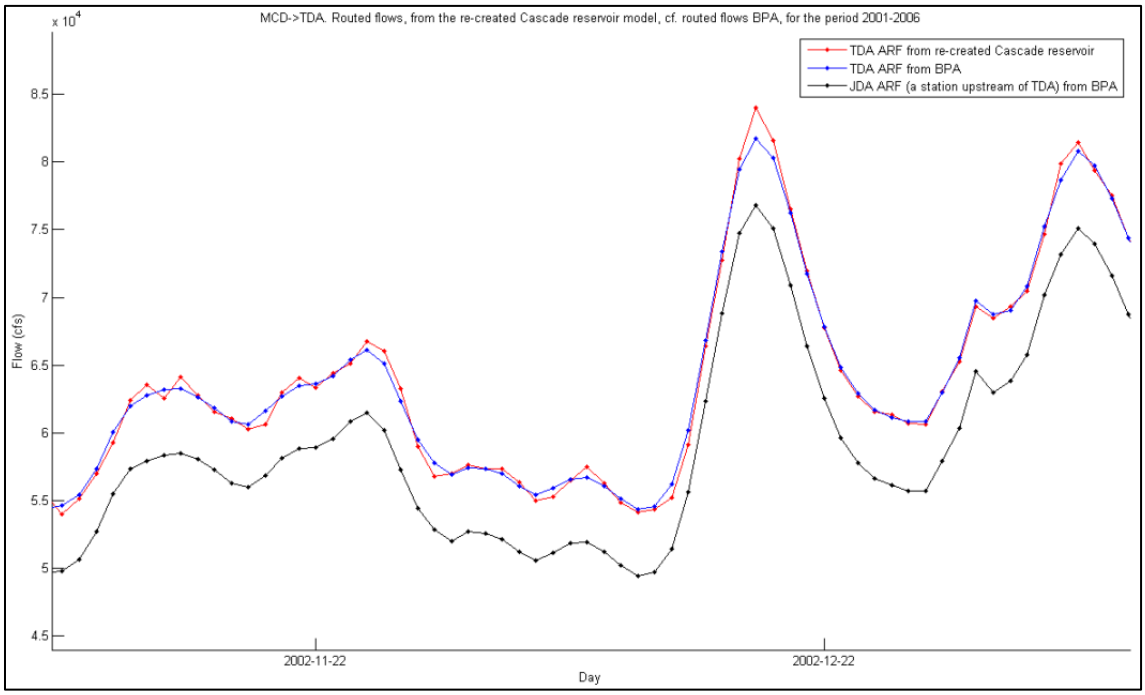

Figure 24: Mica ARF routed to The Dalles. Low flow.

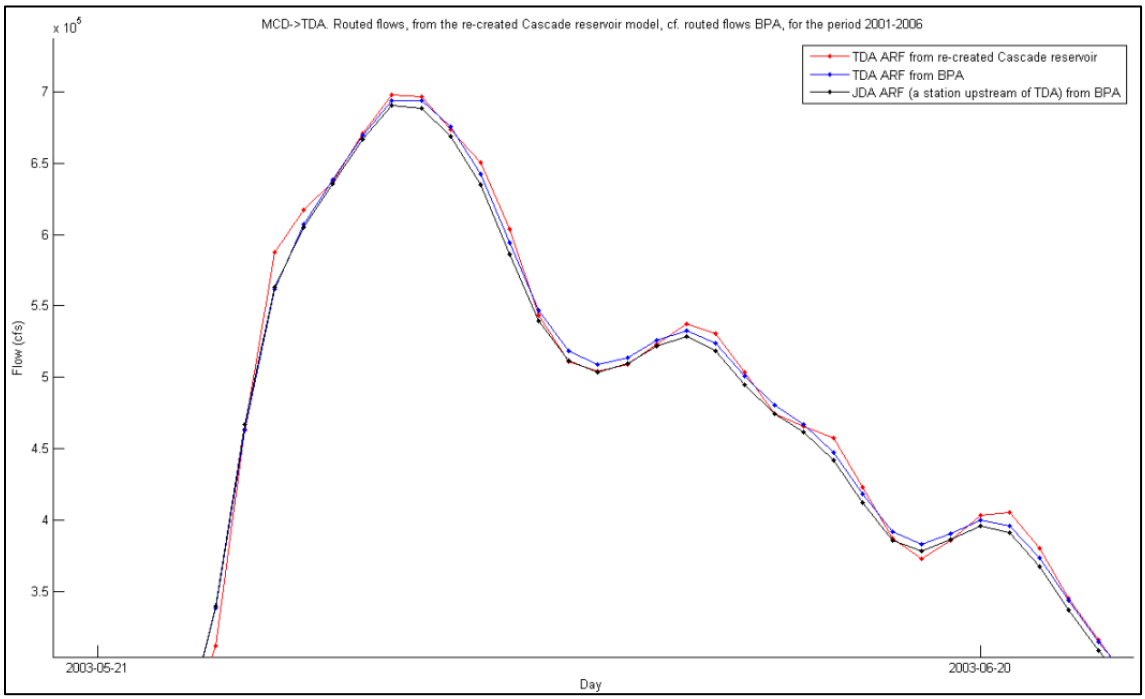

Figure 25: Mica ARF routed to The Dalles. High flow.

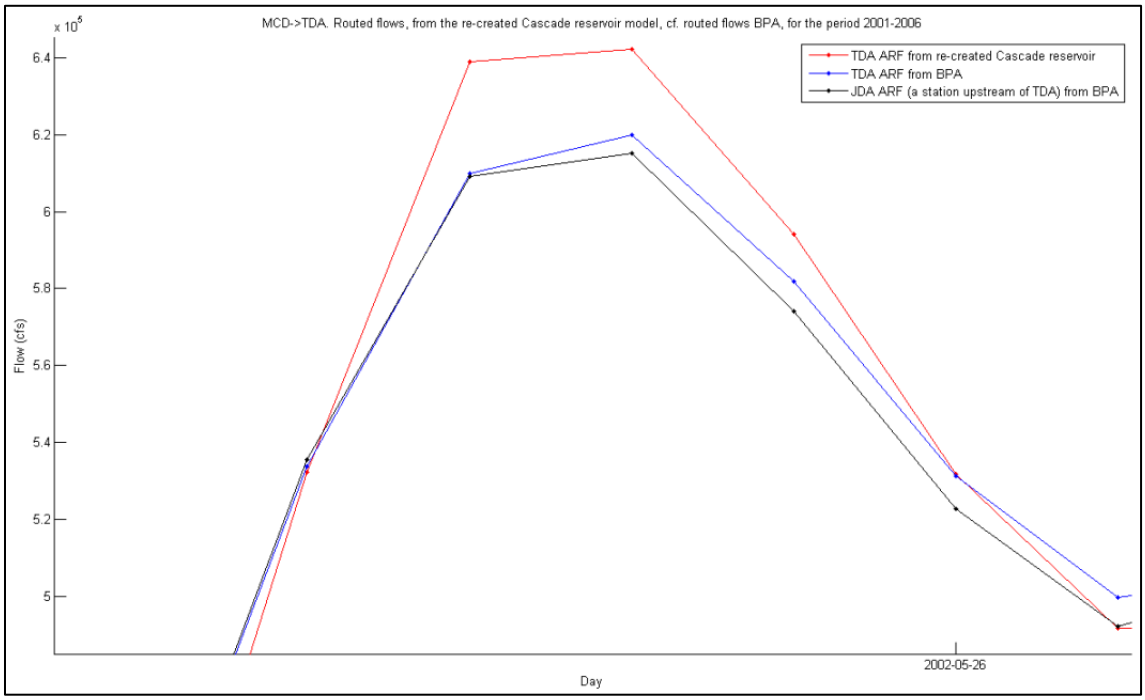

Figure 26: Mica ARF routed to The Dalles. A time period of poorer fit.

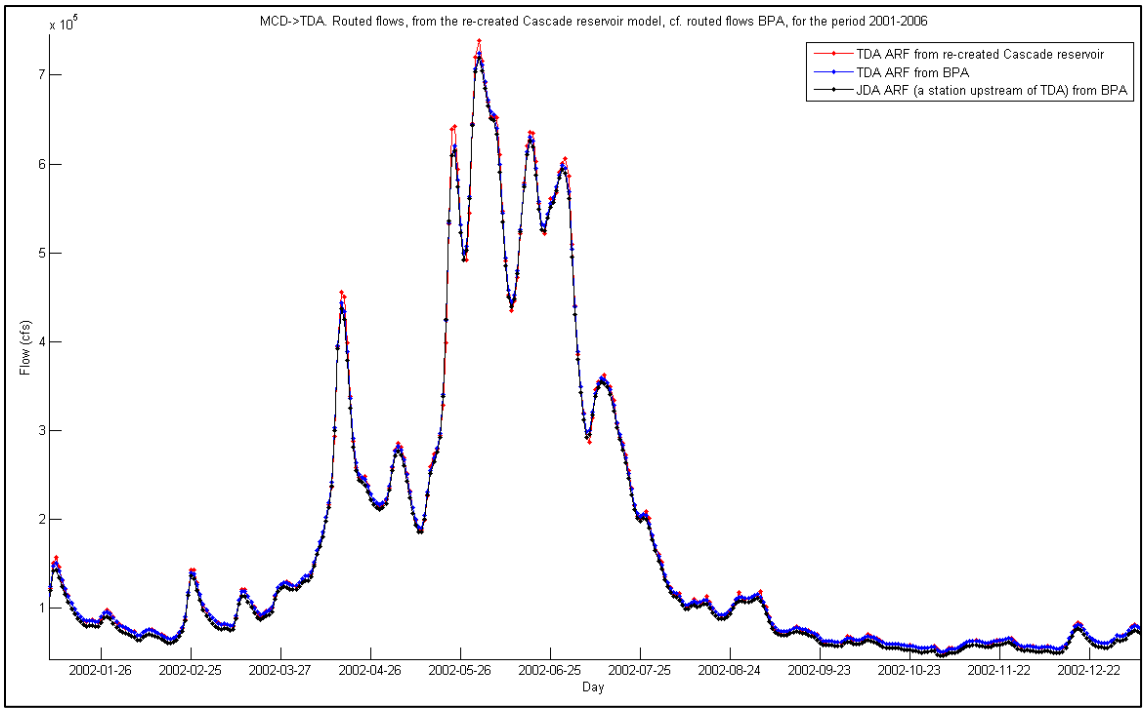

Figure 27: Mica ARF routed to The Dalles. The full year 2002.

4.3 Effects of routing

4.3.1 Grand Coulee to Priest Rapids (distance 310 km)

Figure 28 and Figure 29 show the effects of routing and the local inflows for the stretch Grand Coulee (GCL) to Priest Rapids (PRD). The effects are larger than for the stretch Rock Island (RIS) to Wanapum (WAN) (see Figure 16), but the time lag is still smaller than the time scale of the input data (i.e. days). Notice that the inflow at GCL is larger than the local inflows for the reach. There are no apparent differences in the routing effects for high and low flows.

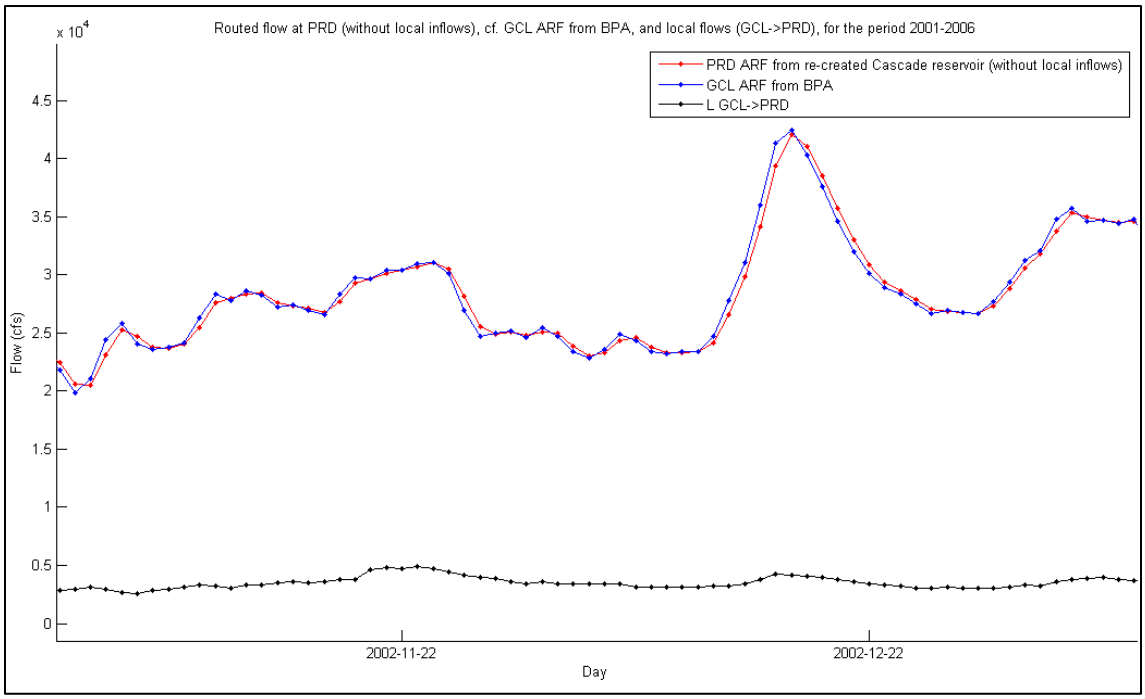

Figure 28: Grand Coulee ARF routed to Priest Rapids without local inflows. Low flow.

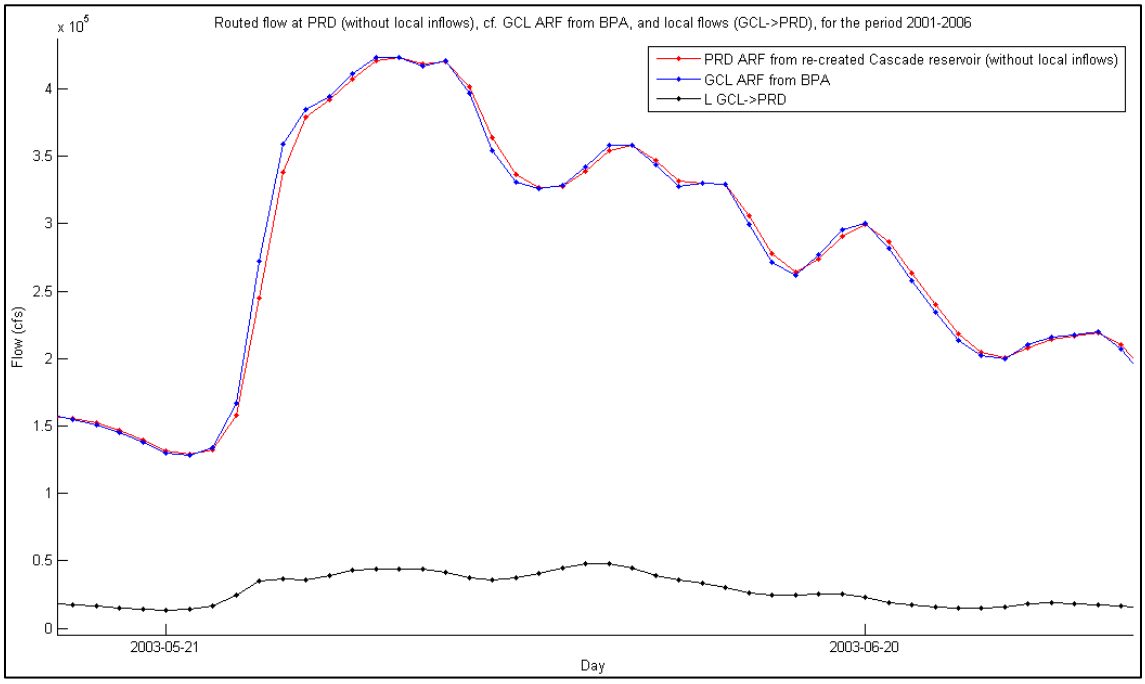

Figure 29: Grand Coulee ARF routed to Priest Rapids without local inflows. High flow.

4.3.2 Albeni Falls to Grand Coulee (distance 360 km)

Figure 30 and Figure 31 shows the effects of routing and the local inflows for the river stretch Albeni Falls (ALF) to Grand Coulee (GCL). Local inflows are consistently higher than the inflow at ALF. The routing causes a time delay of about one day and some flow attenuation. Some small differences in the time lag are observable between the high and low flows (low flows have a larger time lag). The "spikiness" of the inflow hydrograph in Figure 30 is smoothened out by the routing.

Notice that even though the two river stretches GCL to PRD and ALF to GCL are of approximately the same length, the effects of routing differs markedly (see Figure 30 and Figure 31 c.f. Figure 28 and Figure 29). This indicates that the effects of routing do not only depend on the length of the river reach. Other factors that affect the routing are for example, river slope, cross-sectional shape, friction (see for example equation 44). The latter includes a variety of different sub factors such as bottom materials, obstacles, meanderings etc. (French, 1994). The difference in "routing behavior" can also be seen directly in the routing parameters (higher values of the parameters for ALF-GCL) which are listed in Table 20 and
Table 21 in appendix.

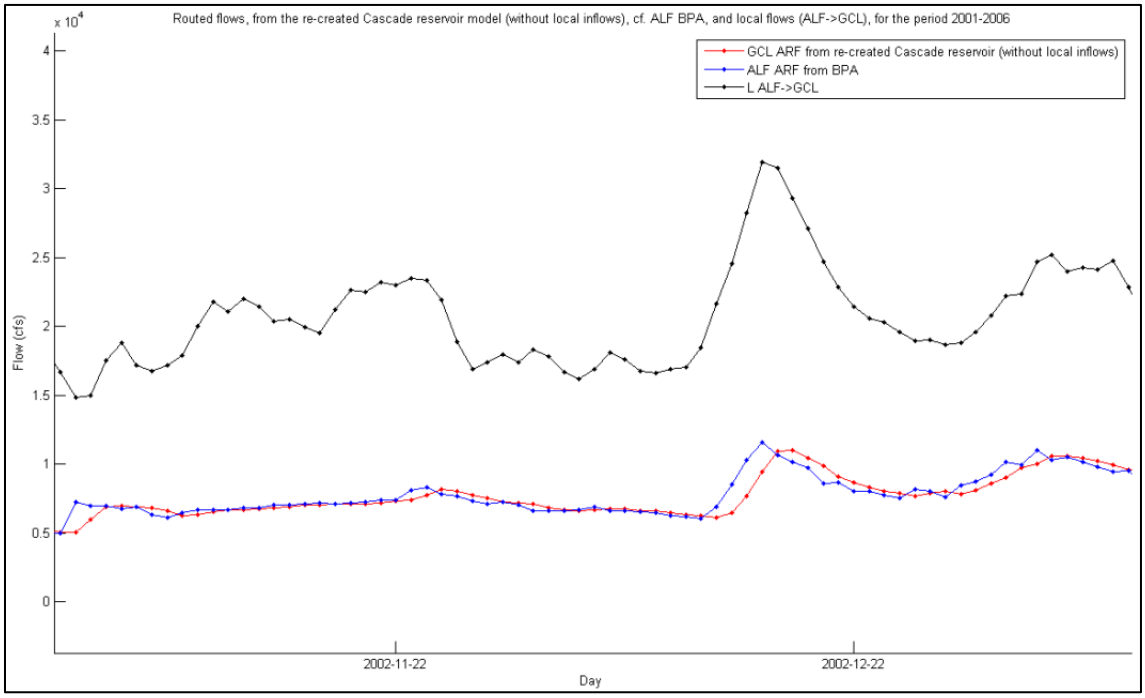

Figure 30: Albeni Falls ARF routed to Grand Coulee without local inflows. Low flow.

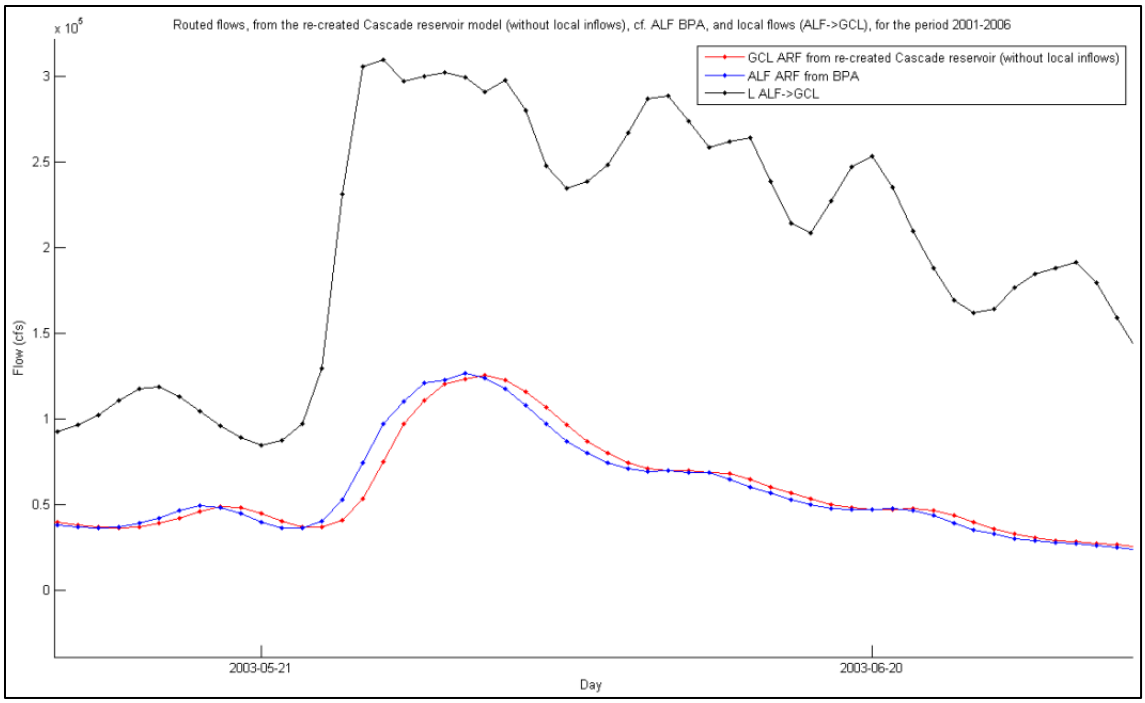

Figure 31: Albeni Falls ARF routed to Grand Coulee without local inflows. High flow.

4.3.3 Mica to The Dalles (distance 1300 km)

The stretch between Mica (MCD) and The Dalles (TDA) is shown on a map in Figure 12. In Figure 32 and Figure 33 below the effects of routing between MCD and TDA can be seen. Since MCD is at the headwaters of Columbia River it is not unreasonable that the local inflows along the stretch are much higher than the upstream inflow. Also there are many larger tributaries that connect to the main river channel along this stretch, for example Snake River. The routing causes a time delay of about 2-3 days (see Figure 32 and Figure 33). The differences in the effects of routing between high and low flows are approximately one day in time delay. This clearly shows the flow dependence of the time of storage and thereby the routing (see for example equation 35).

The attenuation is best seen in Figure 34. It can be seen that some peaks seem to be more dampened than others (compare full and dashed circles in Figure 34). For the sake of reasoning, study equation 34, which is used in the cascade3 routing routine.

$$O_{t+\Delta t} = O_t + \frac{\Delta t(I_m - O_t)}{\left(T_{sm} + \frac{\Delta t}{2}\right)} \quad (34)$$

It basically says that the flow at a certain time step is estimated by weighing the outflow and inflow at a previous time step with the inflow at the current time step. This means that “sharp single peaks” will be more dampened than peaks that persist over longer time. The fact that the shape of the hydrograph largely affects the routing means that depending on which interpolation method the model uses, the outflow hydrograph will be different. This supports the explanation that the errors in the model verification likely are due to differences in interpolation methods between the cascade3 routing routine and the routing routine in the SSARR model used by the BPA.

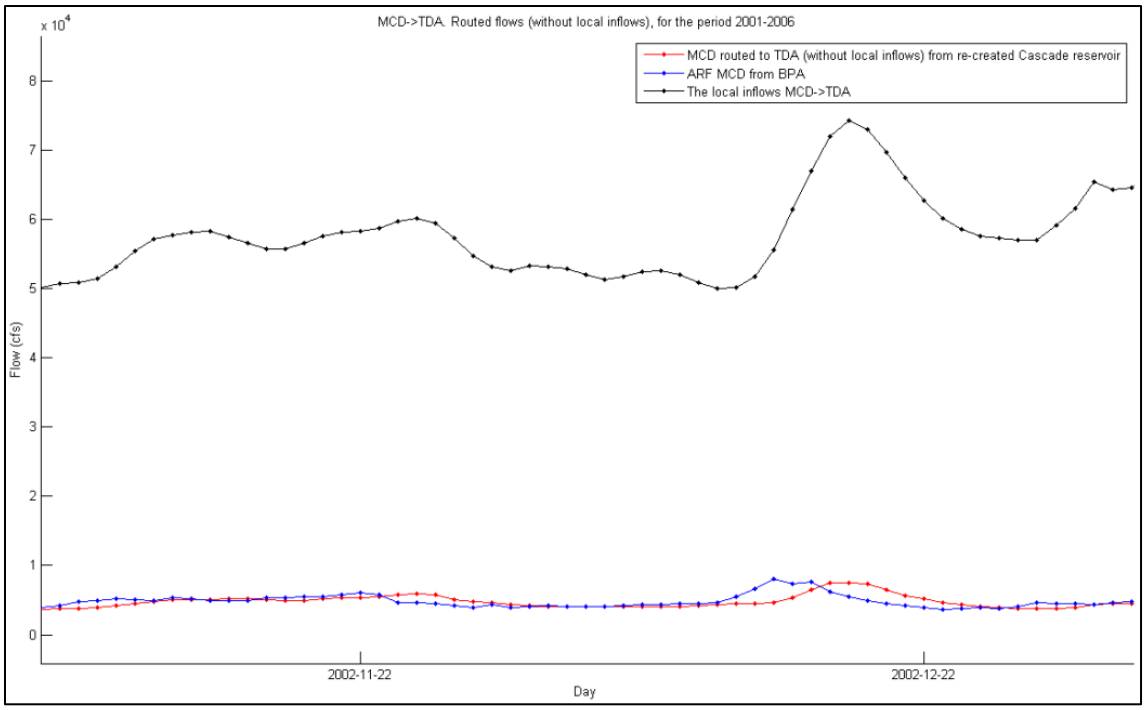

Figure 32: Mica ARF routed to The Dalles without local inflows. Low flow.

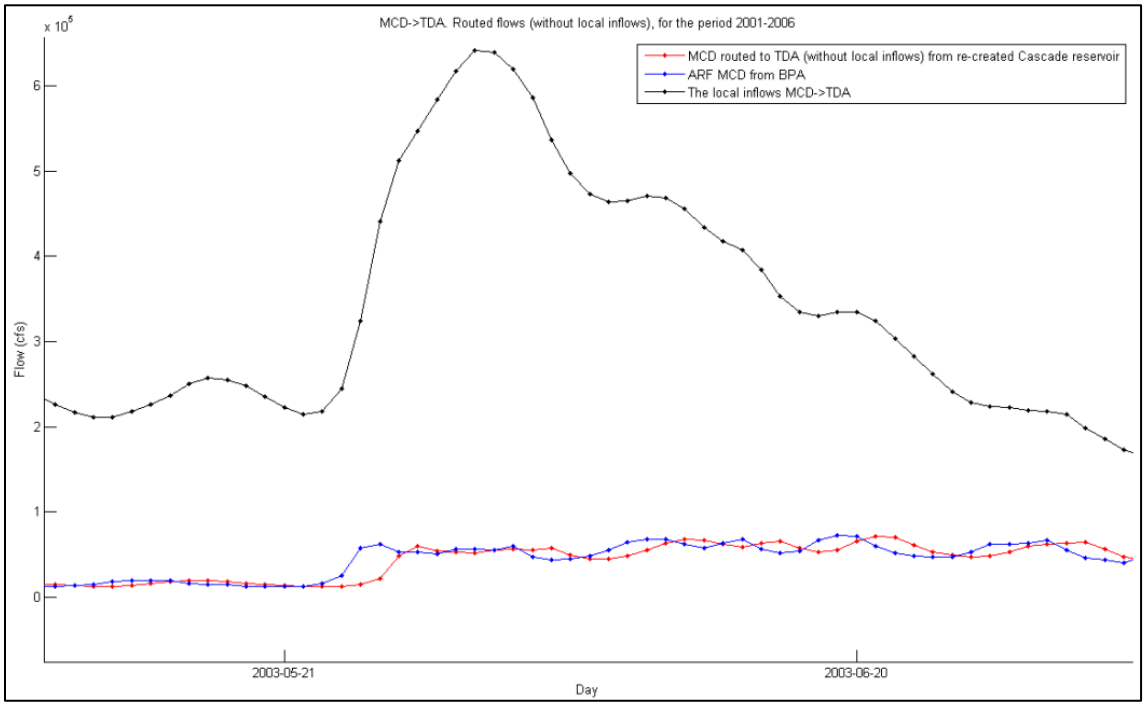

Figure 33: Mica ARF routed to The Dalles without local inflows. High flow.

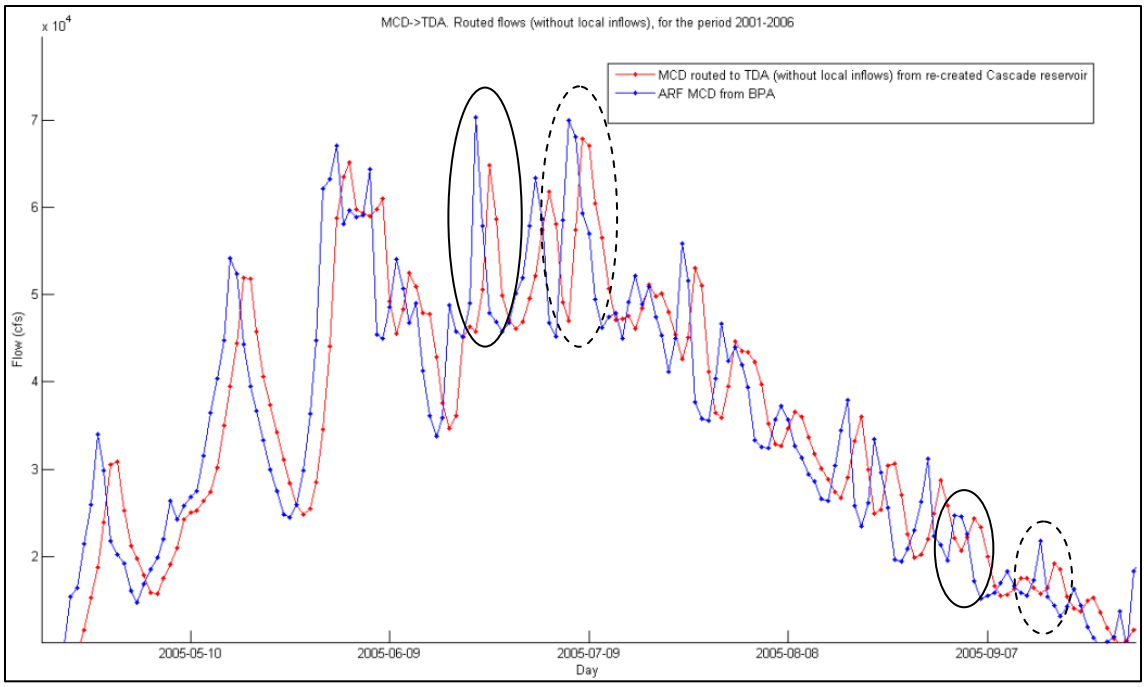

Figure 34: Mica ARF routed to The Dalles without local inflows. A time period that displays visible effects of routing.

4.4 Applying the model in Columbia River – Lumped parameters

4.4.1 Lumping known parameter values

The procedure used in this chapter is described in chapter 3.3.2. Parameter values for all sub reaches can be found in appendix Table 20. The sum of all phases from Mica (MCD) to The Dalles (TDA) is (equation 50):

$$nbrPhases = 43$$

The total time of storage from MCD to TDA is:

$$T_S = 51.2\ h$$

The *KTS* parameter is (equation 52):

$$KTS = 8.65\ h * cfs^{0.2}$$

The *n* parameter is (equation 54):

$$n = 0.2$$

4.4.2 Parameter values and resulting routing effects Mica to The Dalles

Figure 35 and Figure 36 show how well the lumped parameters (see Table 7) mimic the routing effects from reach by reach routing. It is not a perfect fit (see Table 8) but it is a good starting point for calibration, which will be done in chapter 4.7.

Table 7: Lumped parameter values, MCD-TDA.

Parameter	Value
nbrPhases	43
n	0.2
KTS ($\mathrm{h} * \mathrm{cfs}^{0.2}$)	8.65

Table 8: Objective functions for lumped parameter values, MCD-TDA.

Objective function	Value
r^2	0.997
Q_{av} (cfs)	552

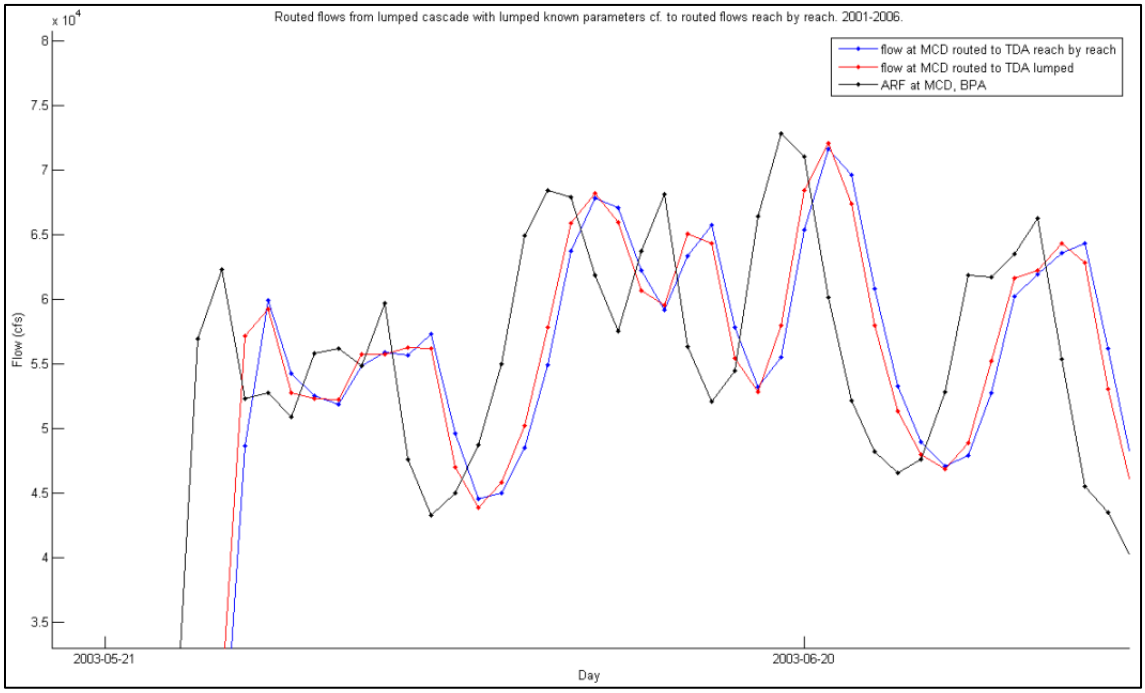

Figure 35: The effects of routing MCD-TDA. Lumped parameter approximation. High flow.

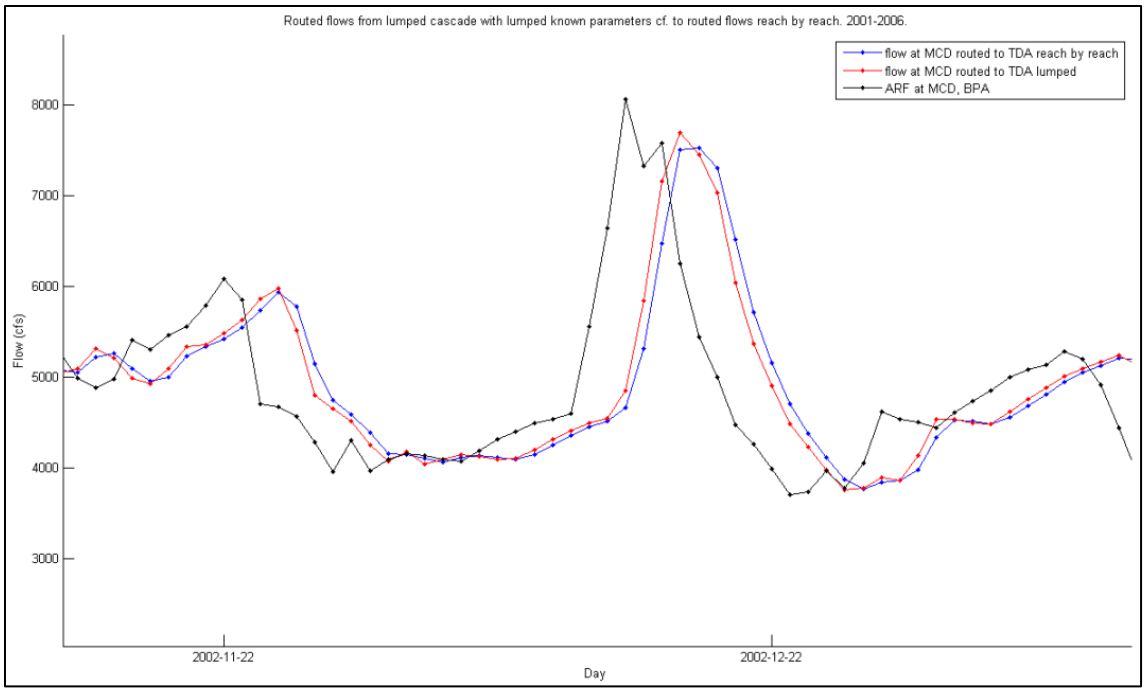

Figure 36: The effects of routing MCD-TDA. Lumped parameter approximation. Low flow.

4.5 Applying the model in the general case

In the following section routing parameters are going to the approximated for the river reach Mica (MCD) to The Dalles (TDA), in Columbia River, as they would have been approximated in the general case when no parameter information is known a priori. This will be done with two different methods, one that can be used when scarce amount of stream data is available and a second one when some additional data is available.

4.5.1 Scarce amount of data

The n parameter

Equation 44 gives the following approximate value of *n*:

$$n = \frac{2}{5} = 0.4$$

The assumptions that are included in this value are:

i. Uniform steady flow in the river channel
ii. Wide channel, which means that the width is much bigger than the depth ($B>>y$).

Although these assumptions in most cases may not be fulfilled, it can still serve as a first rough estimation of the *n* parameter.

The number of phases parameter

If there is almost no data available for the river channel's physical characteristics it is appropriate to use equation 45, which is based on a suggestion from the U.S. Army Corps. Using this equation gives the following number of phases:

$$nbrPhases = \frac{1300}{16} = 81$$

Total time of storage

The total time of storage for a stream reach can be approximated to be equal to the time of travel for the reach (USACE, 1991). The time of storage is estimated with equation 46 and the estimation procedure is described more in detail in section 3.2.1.

The hydrograph at Grand Coulee (GCL) is plotted against the hydrograph at The Dalles (TDA) (distance 620 km) in Figure 37. This was found to be an appropriate stream length, because the time lag between peaks around the average flow was one day, which also was the time resolution of the hydrograph data. The average flow between GCL and TDA is calculated by taking the mean of the mean flow at each station. Figure 38 shows a zoomed view of the area inside of the dashed red circle in Figure 37 with date marks at some of the peaks to show that the peak lag around the average flow in this case is one day. The time of storage is then estimated according to equation 46:

$$T_s = \frac{24}{620000} * 1300000 = 50\ h$$

An obvious problem with this method of estimating the total time of storage occurs when local inflows are large in comparison to the upstream inflow. Then the figure, of the inflow and outflow hydrograph, will not clearly show the lag time of the upstream flow because it will be disturbed by the shape of the local inflow hydrograph. It is therefore important to study and compare hydrographs at different geographical distances and over a long time period when applying this method.

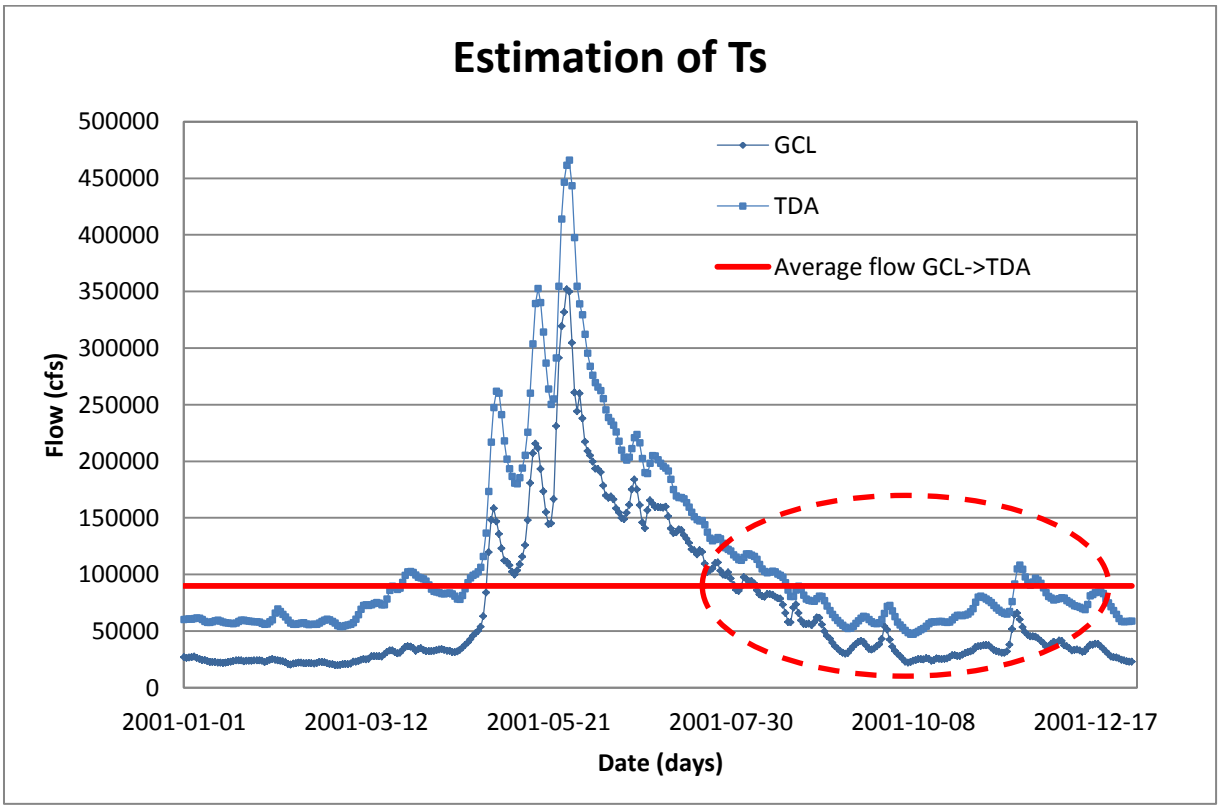

Figure 37: Upstream and downstream hydrographs from the stations Grand Coulee (upstream) and The Dalles (downstream).

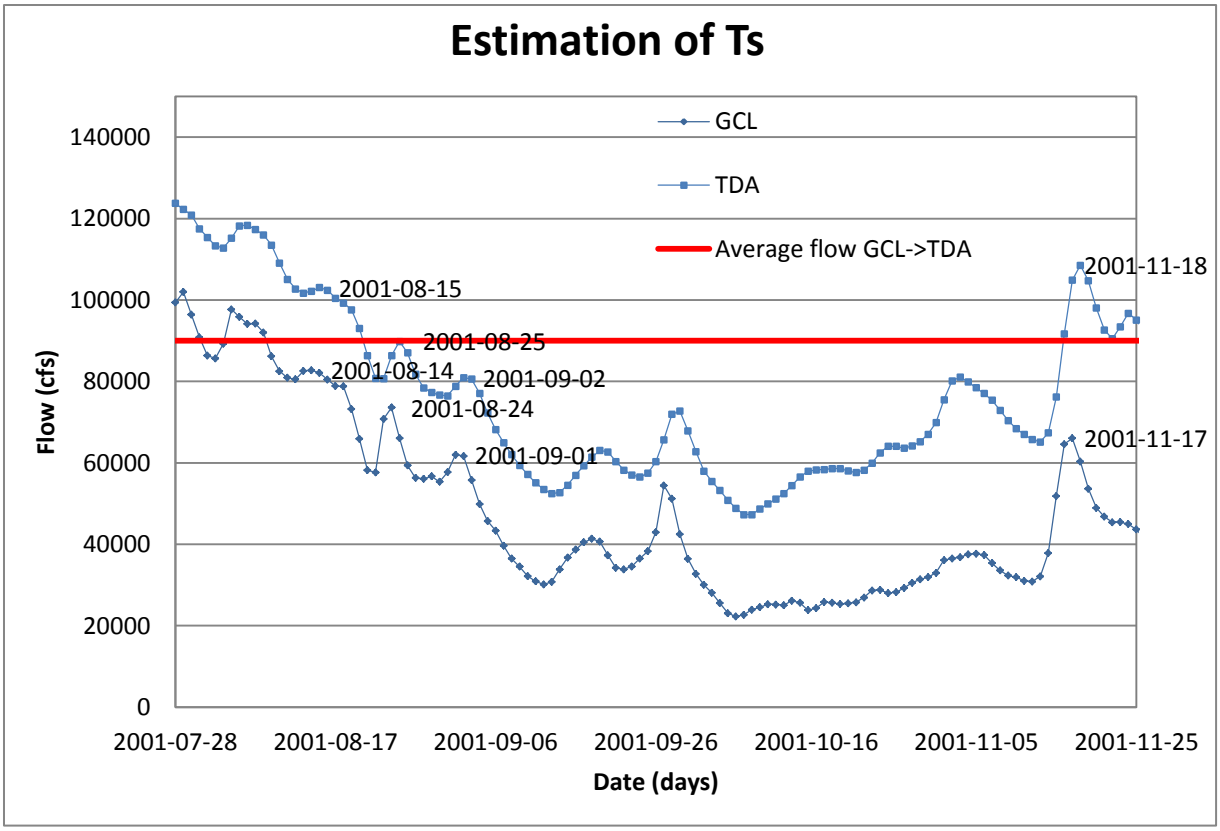

Figure 38: Zoomed view of the area inside the dashed red circle in Figure 37. Upstream and downstream hydrographs from Grand Coulee (upstream) and The Dalles (downstream) with date markings for four individual peak occurrences.

The KTS parameter

When *n*, *nbrPhases*, T_s and the average flow, Q_{mean}, have been estimated it is possible to calculate *KTS* with equation 49, which gives the following value of *KTS*:

$$KTS = \frac{50}{81} * 19000^{0.4} = 32\ (h * cfs^{0.4})$$

Q_{mean} is calculated for the upstream station Mica (2001-2006), because when the routing parameters are calibrated for the reach Mica (MCD) → The Dalles (TDA), streamflow is routed from MCD down to TDA without any addition of local inflows.

The parameters of the scarce data method are summarized in Table 9.

Table 9: Routing parameters for the stream reach Mica – The Dalles using the scarce data method of parameter approximation.

Ts (h)	*nbrPhases*	*n*	Q_{mean} (MCD 2001-2006, cfs)
50	81	0.4	19000

4.5.2 Additional amount of data

The n parameter

The method for estimating *n* when there is additional data is the same as when data is scarce, which gives the following value of *n*:

$n = 0.4$

The nbrPhases parameter

Heatherman (2008) gives two methods for computing the *nbrPhases* parameter when additional data is available (Table 10); equation 37 and equation 39. These two equations yield the following two values of *nbrPhases* and the average of the two:

$$nbrPhases_{eq\,37} = \frac{2 * 4265000 * 0.000194}{30} = 55$$

$$nbrPhases_{eq\,39} = \frac{4265000 * 1.5 * 8.37 * 1700 * 0.000194}{406000} = 43$$

$$nbrPhases_{av} = \frac{43 + 55}{2} = 49$$

This approximation was made with data from the U.S. Geological Survey (USGS) at a station called Vernita (USGS, n.d.), just downstream of Priest Rapids. The data in Table 10 was recorded on the 22nd of May 1949 for the peak discharge, which in the approximation is used as the reference discharge. It is obvious that using values of mean flow velocity, flow depth, top width and flow recorded at peak discharge (and slope) at a point along a reach, does not give a value that is the most representative for that particular reach. Furthermore the data is affected by the flow regulations from that time. But, it gives a value that could be used as a reasonable starting point for calibration.

Table 10: Recorded data at Vernita, just downstream of Priest Rapids (USGS, n.d.).

L_{reach}	S_0	y_0	v_0	T	Q_0
4265000 ft	0.000194	30 ft	8.37 ft/s	1700 ft	406000 ft^3/s

The total time of storage – T_s

When measurements of mean flow velocity are available, equation 48 can be used and T_s becomes:

$$T_s = \frac{4265000}{1.5 * 8.37 * 3600} = 94\ h$$

In this particular case, where the mean velocity from Table 10 is used, the resulting value of T_s will inherit the problems connected to the mean velocity, which was recorded at peak discharge and perhaps not in a sub reach that is representative for the entire river. Thus, the time of storage estimated using the scarce data method will in this case, when the additional data is of poor quality or relevance, provide a better estimate than the additional data method. This is why a method that combines the scarce and the additional data methods is presented in the next section.

The KTS parameter

Equation 49 gives the following value of *KTS*:

$$KTS = \frac{94}{49} * 19000^{0.4} = 99\ (h * cfs^{0.4})$$

The parameters from the additional data method are summarized in Table 11.

Table 11: Routing parameters for the stream reach Mica – The Dalles using the additional data method of parameter approximation.

KTS (h ∗ cfs$^{0.4}$)	*nbrPhases*	*n*	Q_{mean} (MCD 2001-2006, cfs)
99	49	0.4	19000

4.5.3 Combination scarce amount of data and additional data

As mentioned previously, the total time of storage parameter is in this case better estimated using the scarce data method than the additional data method. However, for the *nbrPhases* parameter, using the additional data method is possibly advantageous. A combination of the two methods yields the following *KTS* value:

$$KTS = \frac{50}{49} * 19000^{0.4} = 53\ (h * cfs^{0.4})$$

The parameters from the combined data method are summarized in Table 12.

Table 12: Routing parameters for the stream reach Mica – The Dalles using the combined method of parameter approximation.

KTS (h ∗ cfs$^{0.4}$)	*nbrPhases*	*n*	Q_{mean} (MCD 2001-2006, cfs)
53	49	0.4	19000

4.5.4 Summary of parameter values and resulting routing effects Mica to The Dalles

Figure 39 to Figure 44 show how well the lumped model, with the general parameter approximations, fit with the reach by reach routing. For high flows (see Figure 39 to Figure 41) the additional data method appears to give the best fit. For low flows (see Figure 42 to Figure 44) the scarce and the combined method appear to give the best fits. The time lag, the flow attenuation and the relation between high and low flows are all slightly wrong, which suggests that all parameters need to be adjusted by calibration. Since the lumped known parameters give the best fit this will be the starting point in the sensitivity analysis (chapter 4.6) and the calibration (chapter 4.7).

According to the objective functions (see Table 14) the scarce and the combined methods give the best general fit. However, in this case where are all the parameters for the sub reaches are known, the lumped known parameter approximation gives the overall best fit. As can be seen in Table 13, the *nbrPhases* parameter for the scarce amount of data method is somewhat larger than the rest. This is likely because it is a very rough estimate that does not consider any properties of the catchment. The *KTS* parameter is a direct result of the other parameters and the total time of storage (see equation 49) and therefore also incorporates their variations.

Table 13: Summary of parameter values including the lumped parameters values from chapter 4.4, MCD-TDA.

Parameter	Lumped known parameters	Scarce amount of data	Additional data	Combination of scarce and additional data
nbrPhases	43	81	49	49
n	0.2	0.4	0.4	0.4
KTS (h ∗ cfs^{n})	8.65	32	99	53

Table 14: Objective functions for lumped and general parameter approximations.

Parameter	Lumped known parameters	Scarce amount of data	Additional data	Combination of scarce and additional data
r^2	0.99730	0.99022	0.98593	0.99038
Q_{av} (cfs)	552	860	1400	846

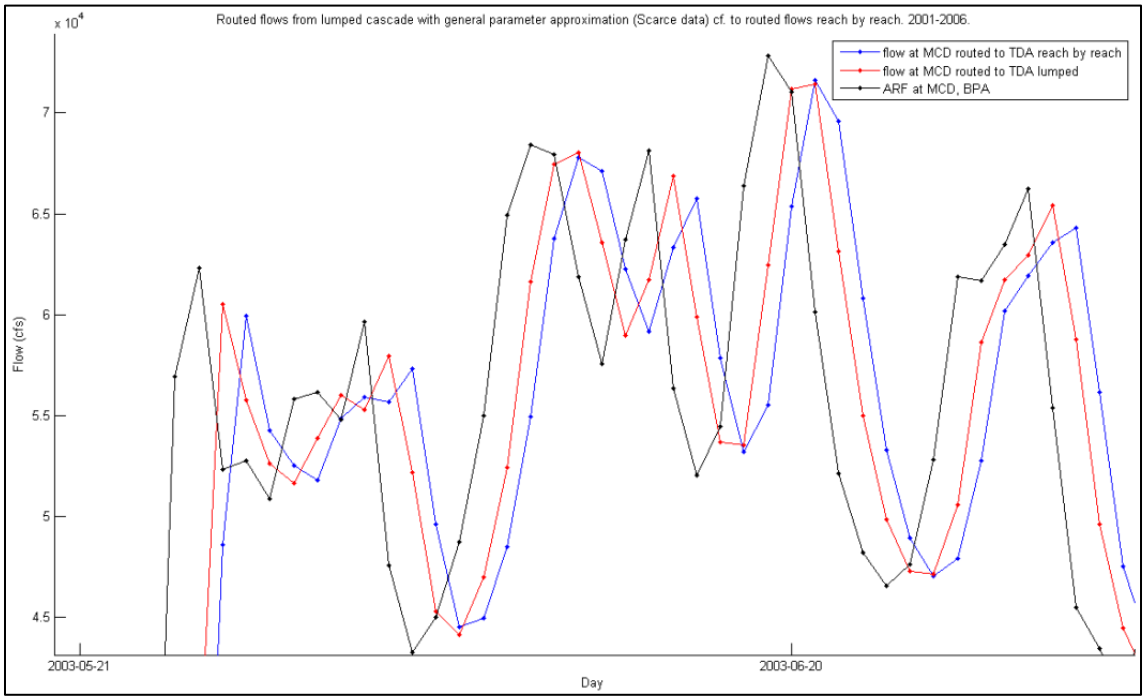

Figure 39: The effects of routing MCD – TDA. General parameter approximation with scarce amount of data. High flow.

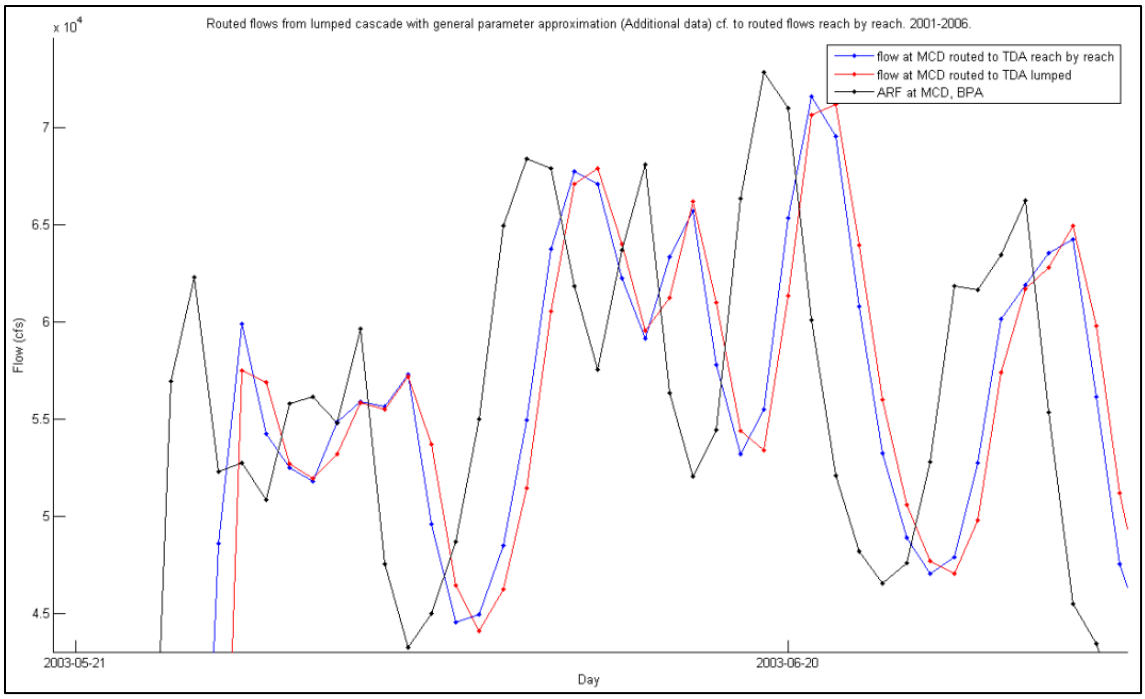

Figure 40: The effects of routing MCD – TDA. General parameter approximation with additional amount of data. High flow.

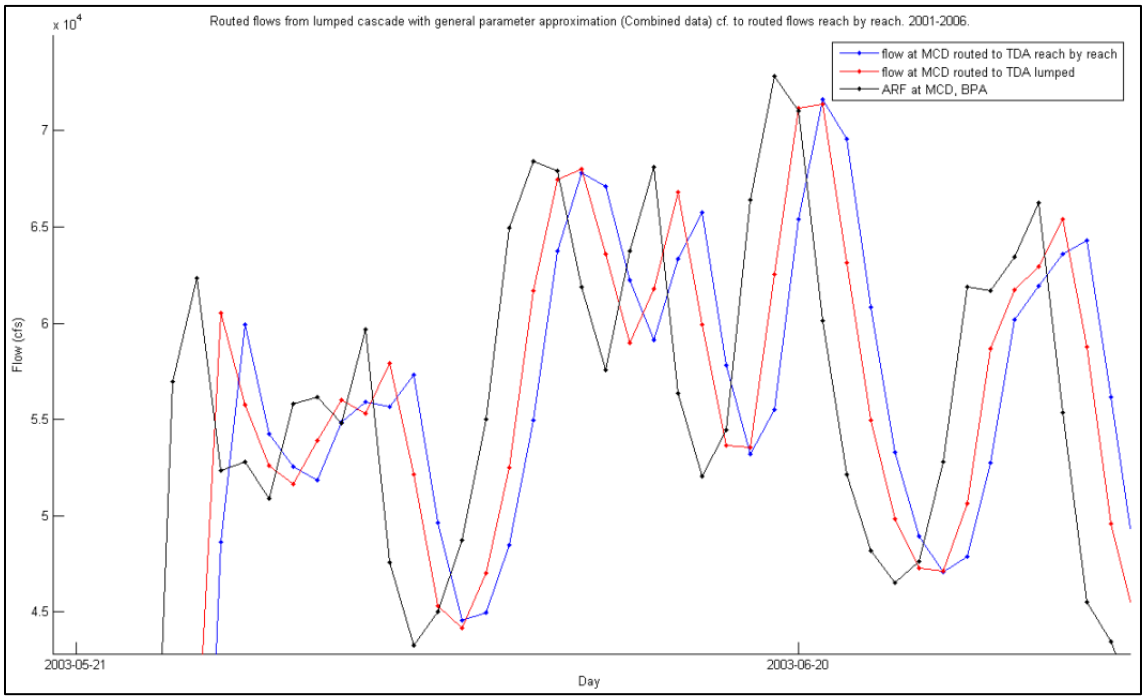

Figure 41: The effects of routing MCD – TDA. General parameter approximation with combined amount of data. High flow.

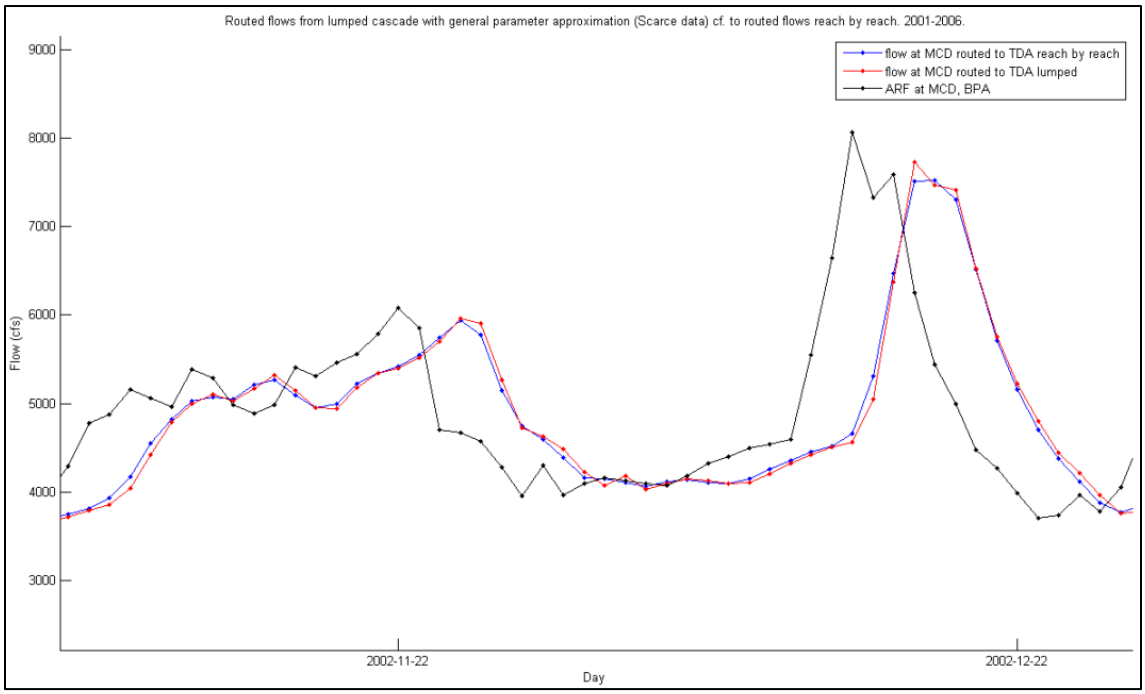

Figure 42: The effects of routing MCD – TDA. General parameter approximation with scarce amount of data. Low flow.

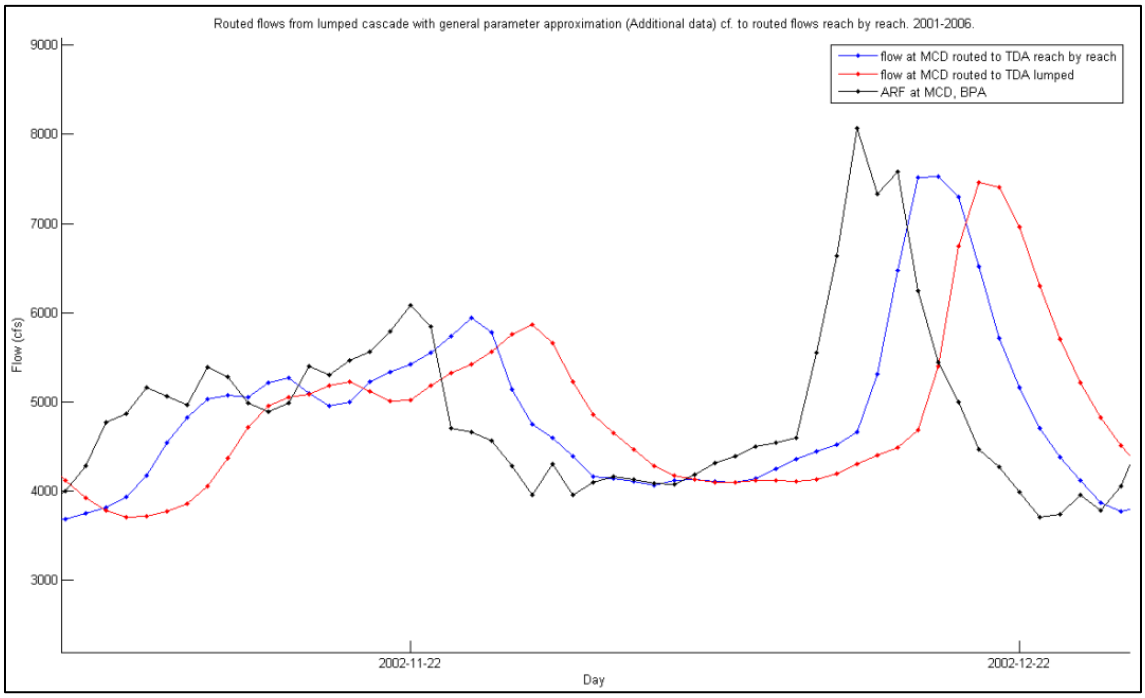

Figure 43: The effects of routing MCD – TDA. General parameter approximation with additional amount of data. Low flow.

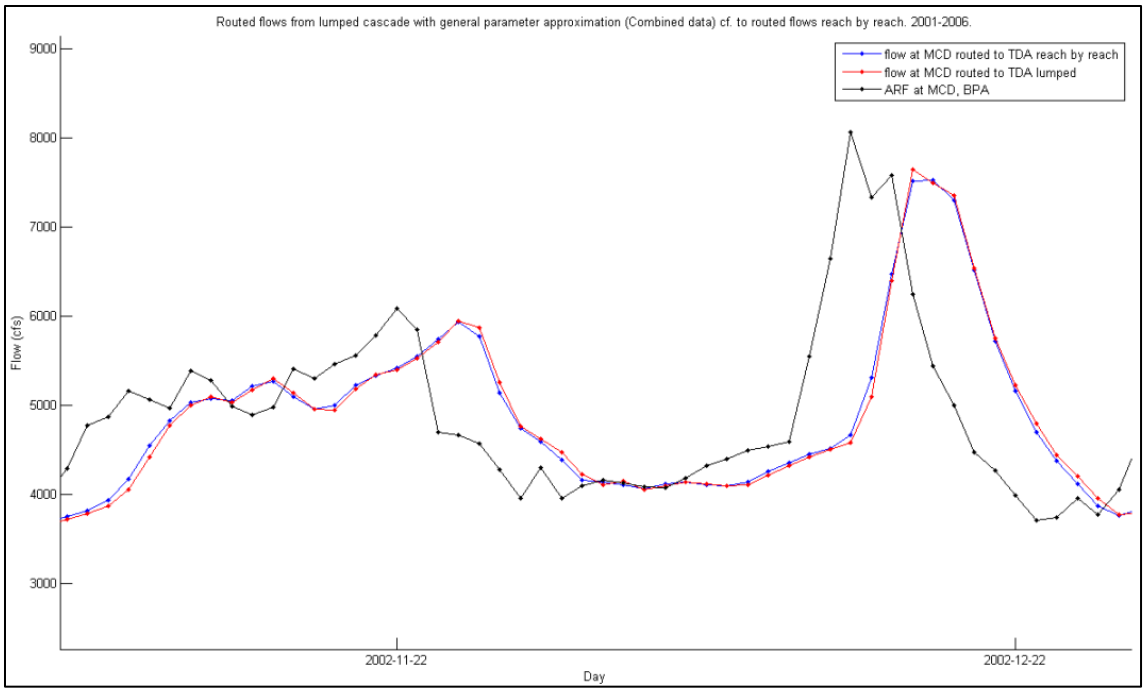

Figure 44: The effects of routing MCD – TDA. General parameter approximation with combined amount of data. Low flow.

4.6 Sensitivity analysis

The start values in this case are chosen to be the resulting values of the lumping of known parameters (see chapter 4.4.1). These values give the best fit (see Table 14) compared to the reach-by-reach routing and are therefore chosen as start values in the sensitivity analysis.

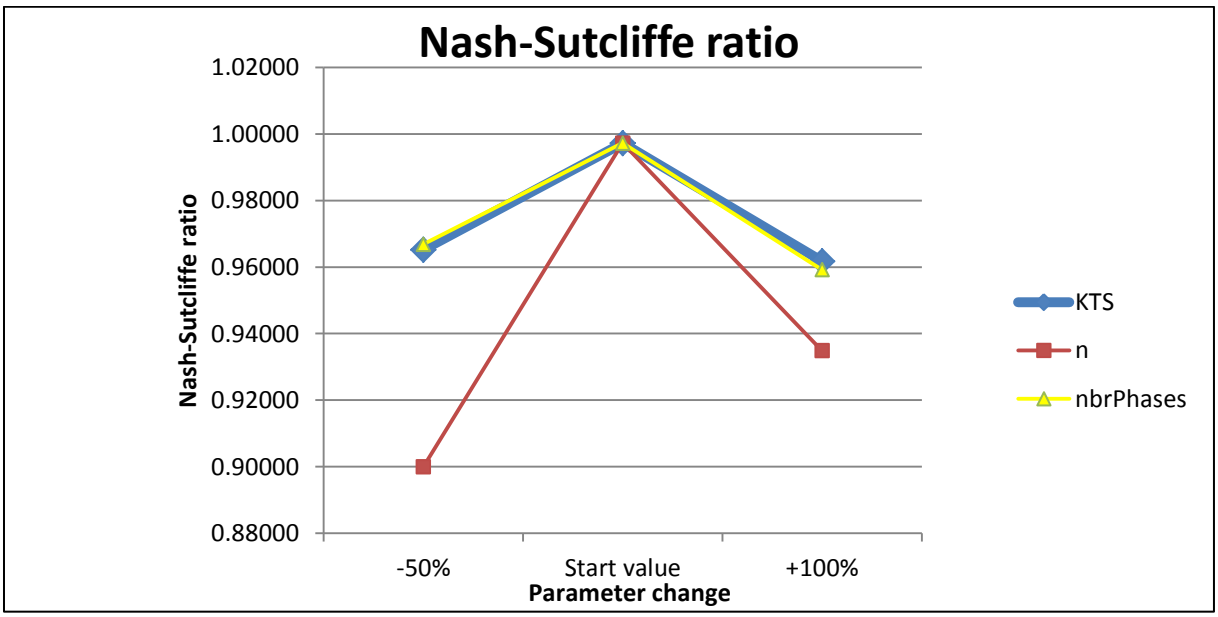

Figure 45: The result of the sensitivity analysis, Nash-Sutcliffe ratio.

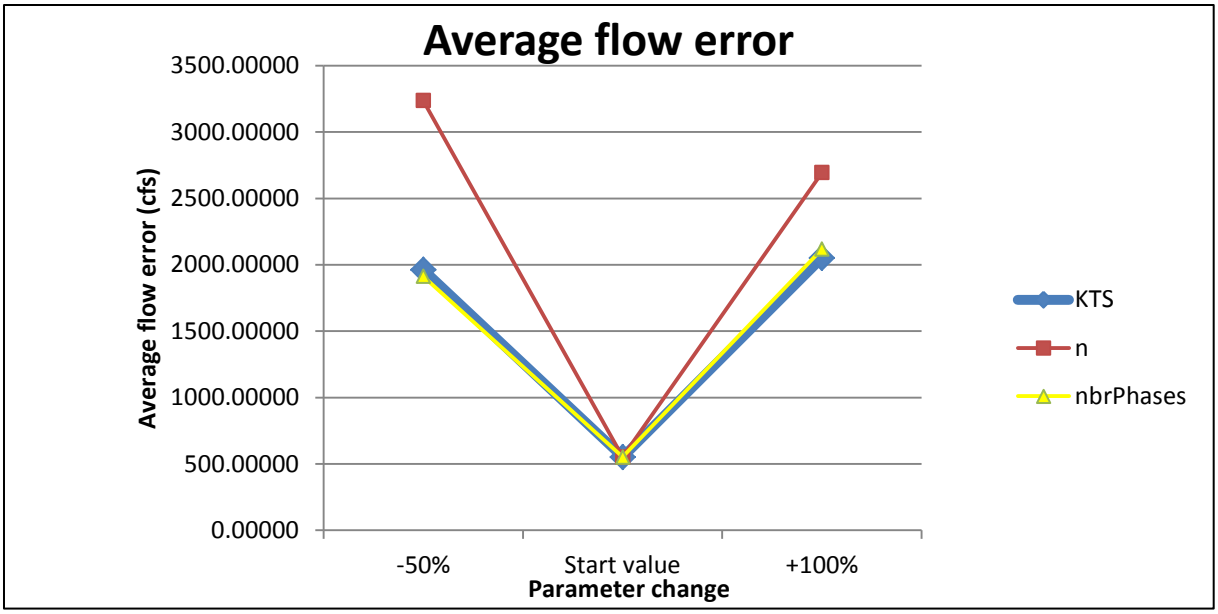

Figure 46: The result of the sensitivity analysis, the average flow error.

The result of the sensitivity analysis is presented in Figure 45 and Figure 46. The lumped known parameters are used as start values. Each parameter is then decreased by 50% and increased by 100% and the resulting values of the objective functions are presented. The following remarks can be made:

- ✓ The *n* parameter is the most sensitive parameter.
- ✓ The *KTS* and *nbrPhases* parameters are almost equally sensitive.
- ✓ The start values produce the best objective function results.

The fact that the *n* parameter is more sensitive to change than the other two is obvious since it exponentially affects the total time of storage. The reason why *KTS* and *nbrPhases* are almost equally sensitive is because they both linearly affect the total time of storage. They are not equally sensitive because they affect attenuation differently. Notice that the start values produce the best results of the objective functions. This means that to calibrate these parameters, changes smaller than the ones made in the sensitivity analysis should be done.

The following steps are suggested when performing the calibration:

1. If the time lag is too large, decrease *KTS*, and vice versa, until the timing around the mean flow is correct.
2. The "tilt" of timing between high and low flows can be altered using the *n* parameter. If high flows have too large time lag, and low flows have too low time lag, increase *n*.
3. The attenuation is altered by changing *nbrPhases* and *KTS* simultaneously. To increase flow attenuation without affecting the timing, the *nbrPhases* should be decreased and the *KTS* increased by the same factor, and vice versa.

These three steps are repeated until the values of the objective functions and the resulting hydrograph reach an acceptable result.

4.7 Calibrating the model

To calibrate the model parameters for the entire Mica – The Dalles stretch, the lumped model parameters from chapter 4.4 are used as start values. The calibration procedure used is the one presented in chapter 4.6 above. Figure 47 and Figure 48 show an almost perfect fit, compared to the

reach-by-reach routing, after calibration. The values of the objective functions in Table 16 show a great improvement in the general fit as well.

The calibration procedure suggested in chapter 4.6 obviously works well. Mainly because it provides a method with which one can manipulate individual routing effects. For example if, during calibration, the timing around the mean flow is good, it is possible keep the total time of storage constant while changing the attenuation (*KTS* and *nbrPhases*). This is possible since both the *nbrPhases* and *KTS* parameter linearly affect the total time of storage (see for example equation 49).

Table 15: Parameter values before and after calibration.

Parameter	Starting values	Values after calibration
nbrPhases	43	28
n	0.2	0.2
KTS (h*cfs$^{0.2}$)	8.65	15.8

Table 16: Values of the objective functions before and after the calibration.

Objective function	Starting values	Values after calibration
r^2	0.997	0.9999996
Q_{av} (cfs)	552	6.17

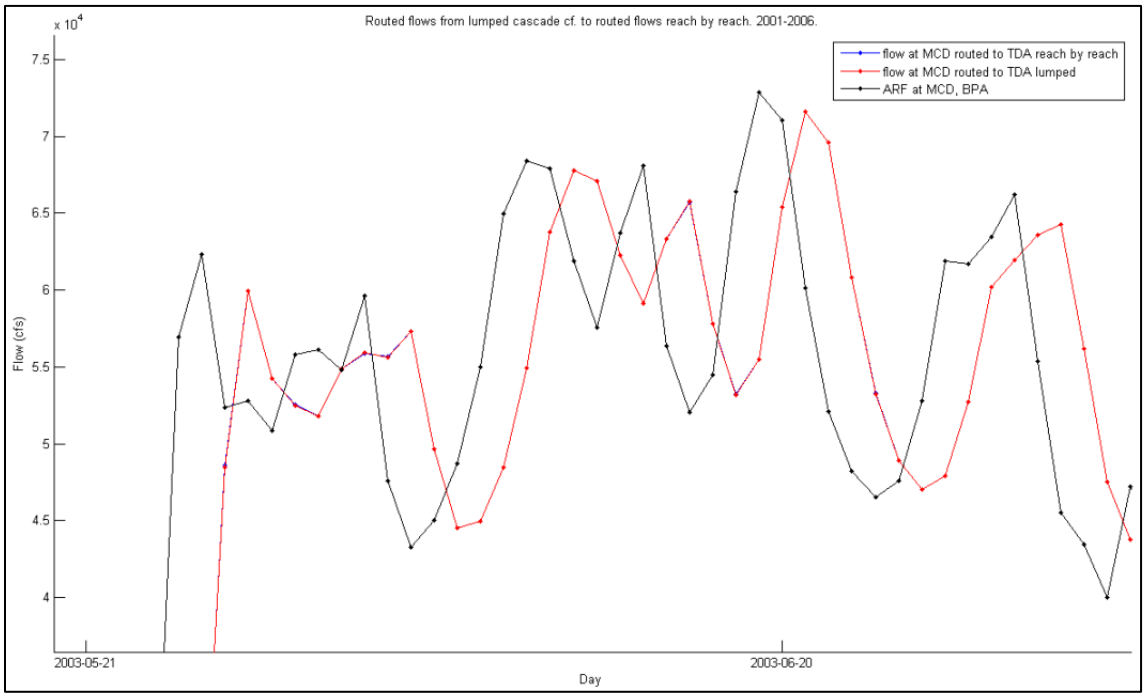

Figure 47: The effects of routing MCD – TDA. Lumped parameter approximation after calibration. High flow.

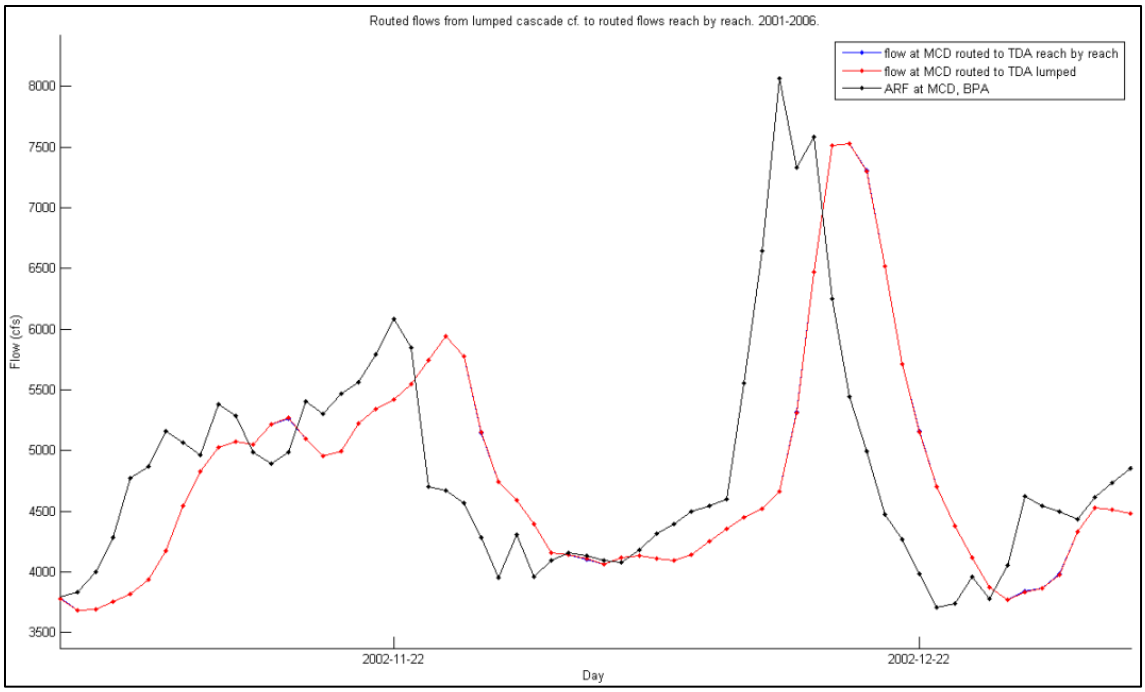

Figure 48: The effects of routing MCD – TDA. Lumped parameter approximation after calibration. Low flow.

4.8 The importance of routing in hydrological models

To get an idea of the importance of routing, three different cases (see Figure 14) with an increasing level of routing of local inflows are presented below and compared with the full reach-by-reach routed ARF flows from the cascade3 routing routine. This is further explained in the following sections.

4.8.1 No sub reaches

Figure 49 and Figure 50 show how well the flow hydrograph, if there is no routing of the local inflows, fits the ARF data provided by the cascade3 routing routine. The timing of both high and low flows is wrong; sometimes the time lag even differs by two days.

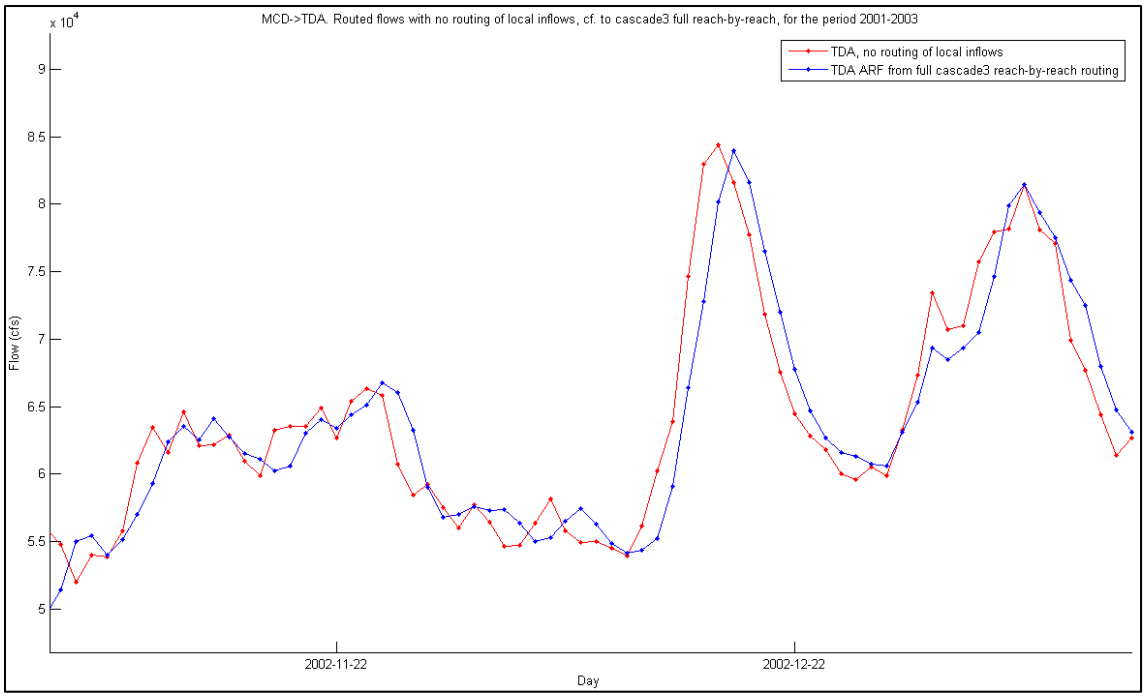

Figure 49: MCD routed to TDA, no routing of local inflows. Low flow.

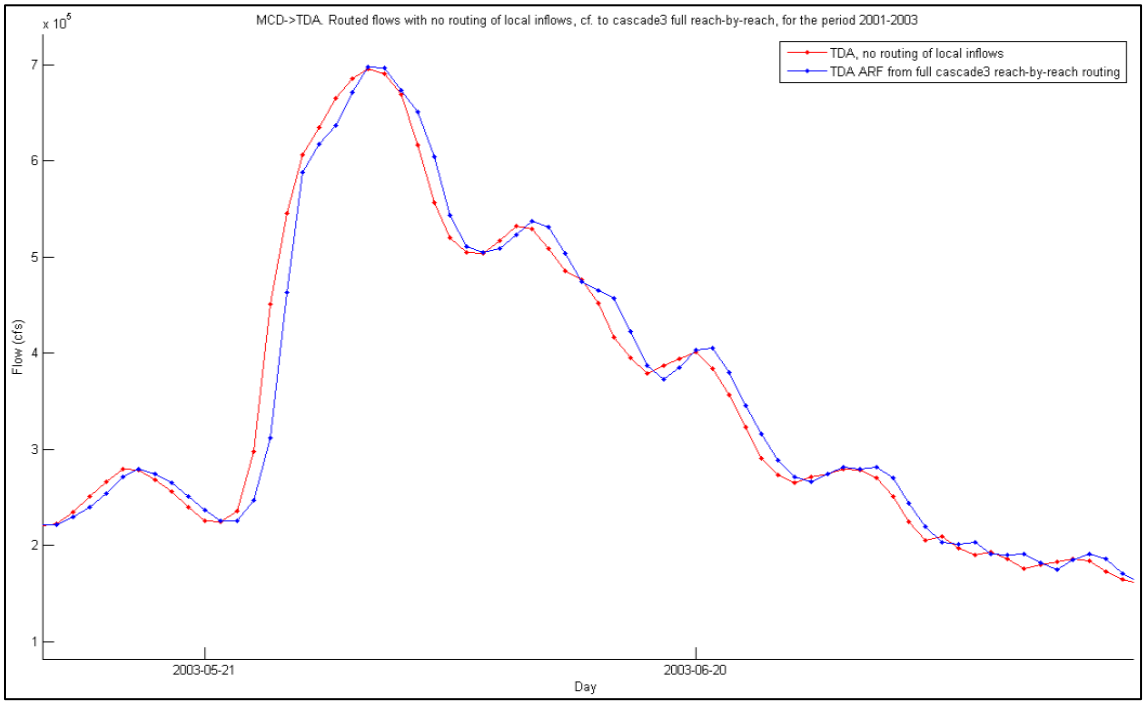

Figure 50: MCD routed to TDA, no routing of local inflows. High flow.

4.8.2 Two sub reaches

In this case Columbia River is divided into two parts of roughly the same length, where the accumulated local inflows for the first part is added in the middle (and then routed to the most downstream station), while the accumulated local inflows for the second part is added at the most downstream station. Figure 51 and Figure 52 show how well the flow hydrograph, when the division of the stream described above is used, fits the ARF data provided by the cascade3 routing routine. The

timing and the attenuation of both high and low flows has clearly improved as compared to the case of no routing of the local inflows.

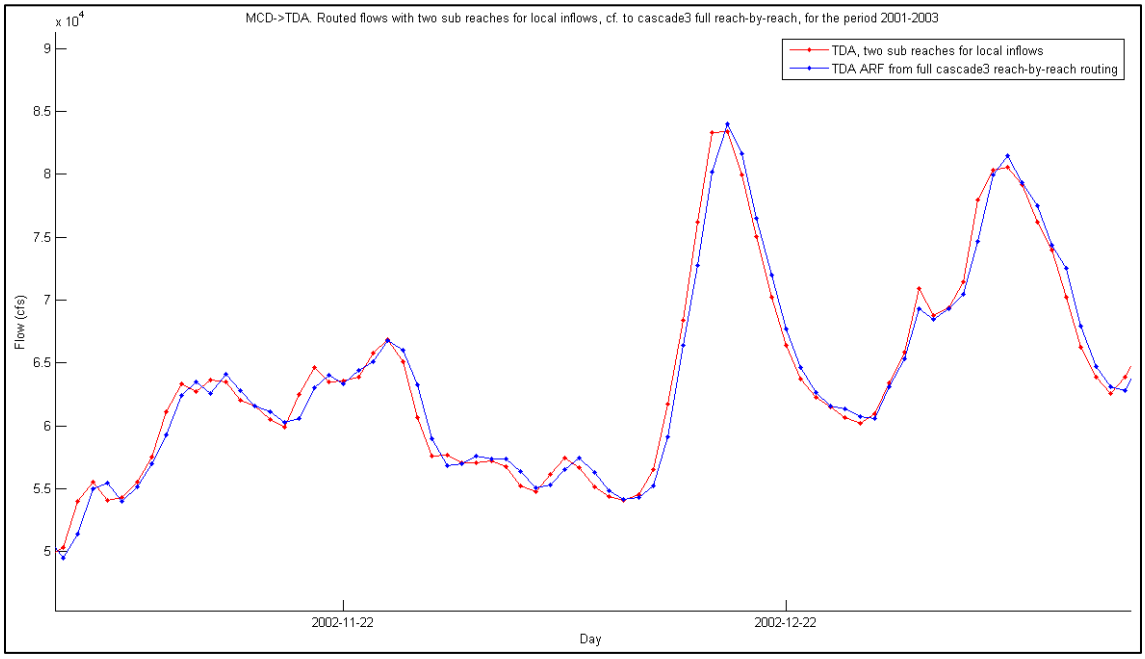

Figure 51: MCD routed to TDA, two sub reaches with local inflows. Low flow.

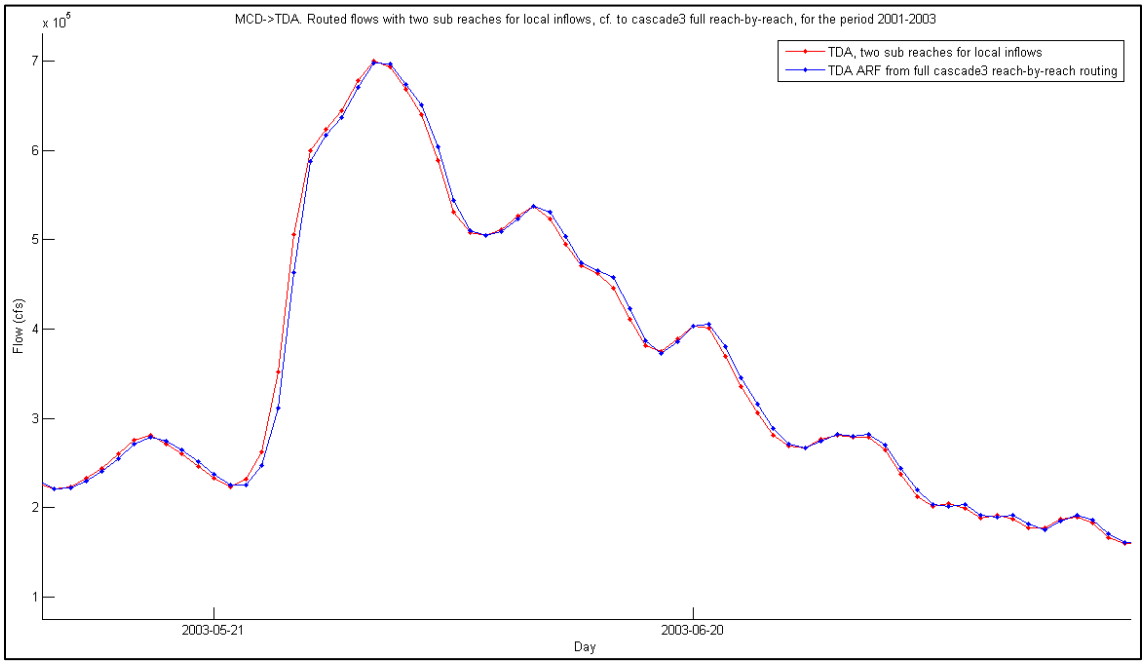

Figure 52: MCD routed to TDA, two sub reaches with local inflows. High flow.

4.8.3 Four sub reaches

The division in this case is as in the preceding case with two sub reaches, but this time it is further divided into four sub reaches. Figure 53 and Figure 54 show how well the flow hydrograph, when the division of the stream described above is used, fits the ARF data provided by the cascade3 routing routine. The timing and the attenuation of both high and low flows has further improved compared to the previous case and the shape and timing of the hydrograph approaches the full reach-by-reach hydrograph.

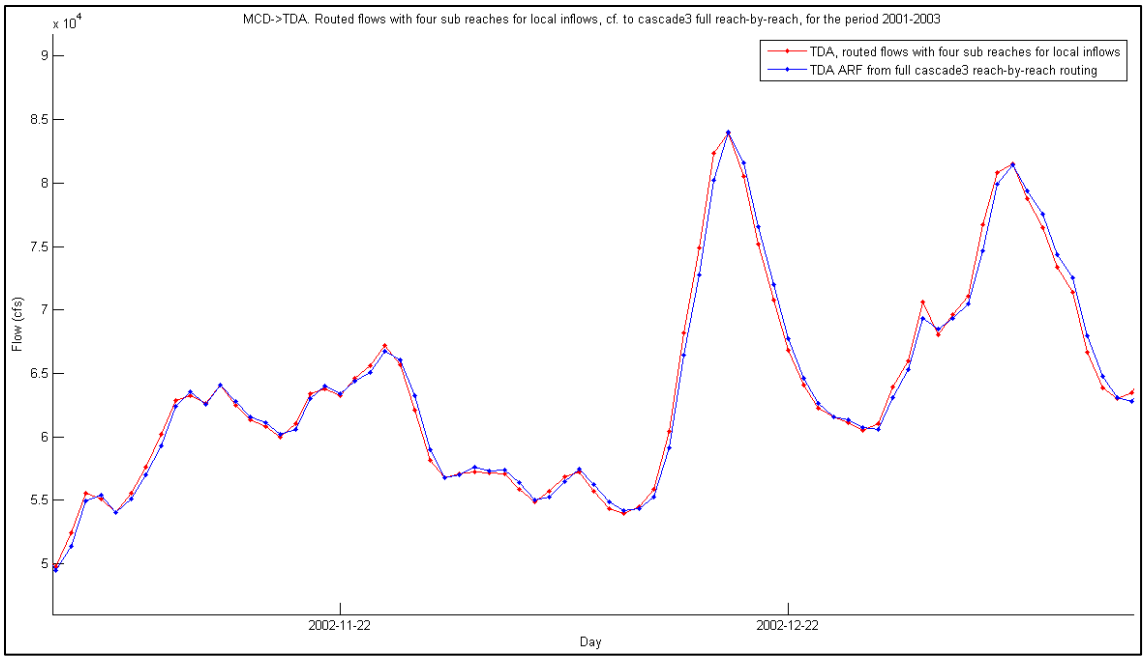

Figure 53: MCD routed to TDA, four sub reaches with local inflows. Low flow.

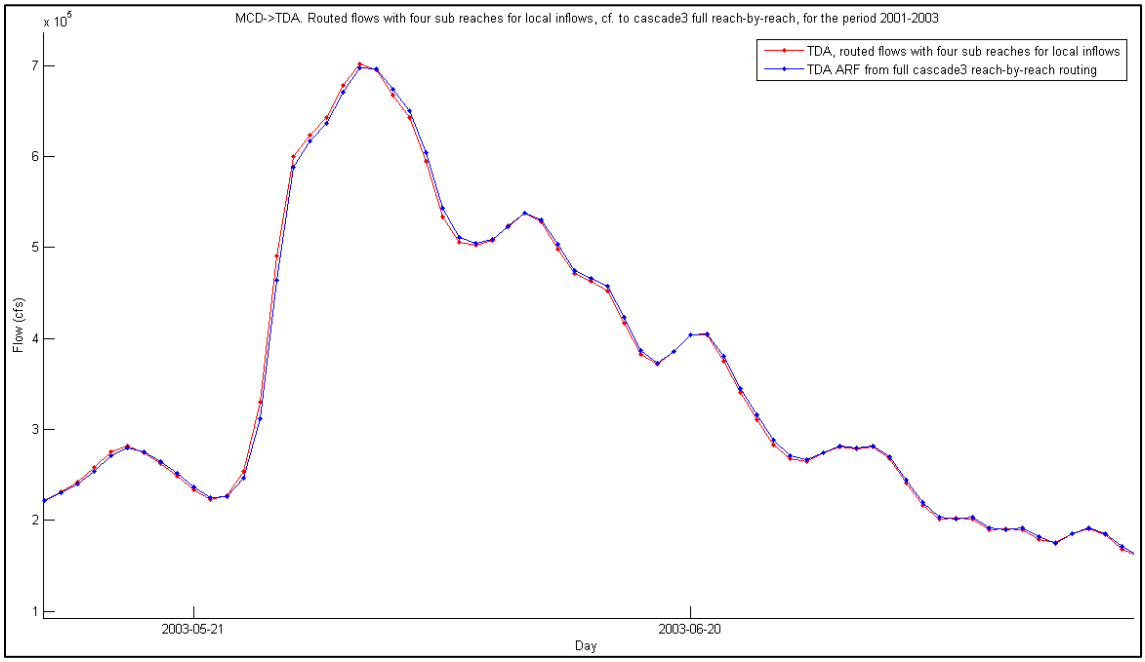

Figure 54: MCD routed to TDA, four sub reaches with local inflows. High flow.

4.8.4 Summary of the results of the objective functions

Table 17 shows a summary of the results above. The resulting values of the objective functions improve as the number of divisions increase. Depending on what requirements of precision that the full hydrological model has, the number of divisions can be decided upon accordingly. This decision will be a compromise between simplicity and precision.

The crudest division (no sub reaches) gives a time delay of one or two days (see Figure 49 and Figure 50), which can be compared to the effects of routing (see Figure 32 and Figure 33) between Mica and The Dalles that have a time delay of two to three days. This suggests that not only channel specific

properties (friction, slope, cross-sectional shape) affect the routing, but also the topology of the river, i.e. how and where tributaries and local inflows are connected to the main river channel.

Table 17: Summary of the results of the objective functions.

Objective functions	No sub reaches	Two sub reaches	Four sub reaches
r^2	0.987	0.998	0.9993
Q_{av} (cfs)	7530	2970	1760

4.9 Comparison with Muskingum routing

The MATLAB code of the Muskingum routing routine is presented in appendix.

To calibrate the Muskingum model parameters for the entire stretch from Mica (MCD) to The Dalles (TDA) (distance 1300 km), starting values are required for both *K* (h) and *X* (-). *K* is chosen as the value of total time of storage (see Table 18), same as in chapter 4.4.1. The *X* parameter is chosen based on Chow et al. (1988), who say that the mean value of *X* in natural streams is around 0.2.

Figure 55 and Figure 56 compare the routing effects of the calibrated Muskingum routing with the cascade3 reach-by-reach routing. The figures show differences in routing effects between the two methods, both in time lag and flow attenuation. Some peaks are more attenuated by the Muskingum routing than the cascade3 routing, while other peaks are less attenuated. The lag time appears to be better matched between the two models for high flows than for low flows. This difference in routing between high and low flows is because the cascade3 routing is flow dependent, while the Muskingum routing is not.

The values of the calibrated model parameters can be seen in Table 18. *K* does not change significantly before and after the calibration, which indicates that the total time of storage is approximately the same as travel time, *K*. Chow et al. (1988) and the U.S. Army Corps (1994) states that the range of *X* is somewhere in between 0 and 0.5. Furthermore, Chow (1988) states that *X* for natural streams usually is between 0 and 0.3. The calibrated value of *X* is 0.38, which is within acceptable range of *X* according to the literature cited above.

Even though the two routing methods are different, they produce similar routing effects according to the values of the objective functions in Table 19. Part of the reason why they are similar is that the effects of routing are small. Furthermore, similarities between the methods can be seen in their principles. If *X* in the Muskingum equation is set to zero then equation 18 reduces to the linear storage equation 16. Additionally, if *n* is set to zero and the number of phases is set to one, then the cascade3 routing routine also reduces to the linear storage equation 16.

Table 18: Muskingum parameter values before and after calibration.

Parameter	Start values	Values after calibration
K (h)	51.2	63
X (-)	0.2	0.38

Table 19: Values of the objective functions before and after calibration.

Objective functions	Start values	Values after calibration
r^2	0.991	0.994
Q_{av} (cfs)	1040	819

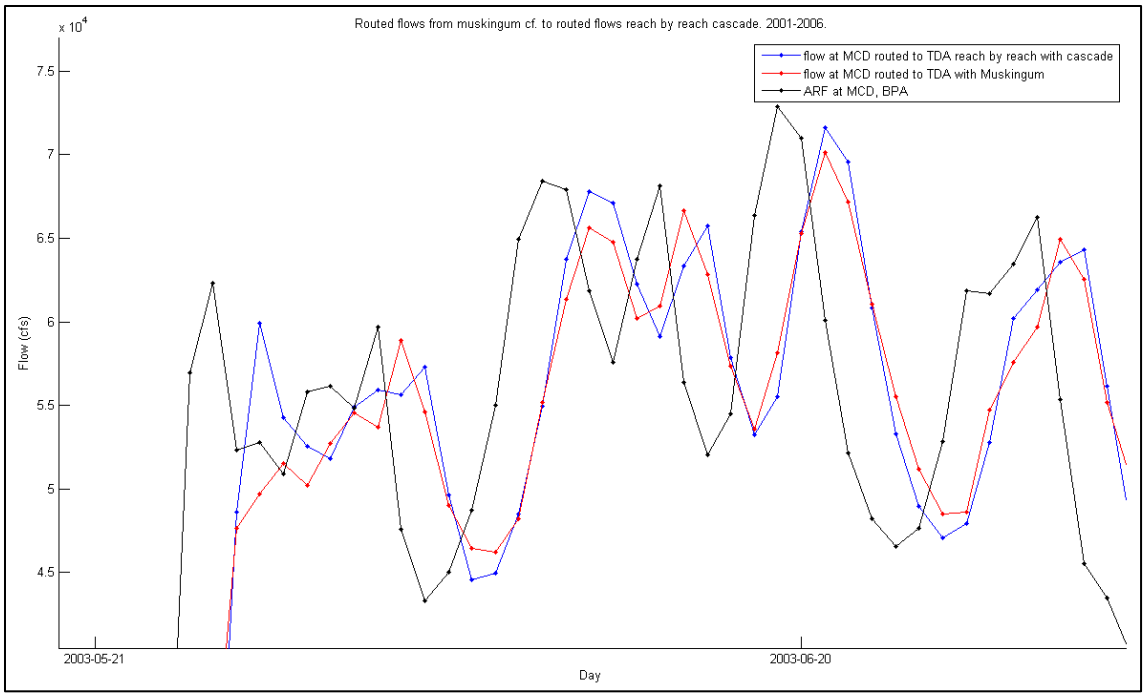

Figure 55: The effects of routing, MCD – TDA, using both the cascade3 (reach-by-reach) routine and the Muskingum method, high flow.

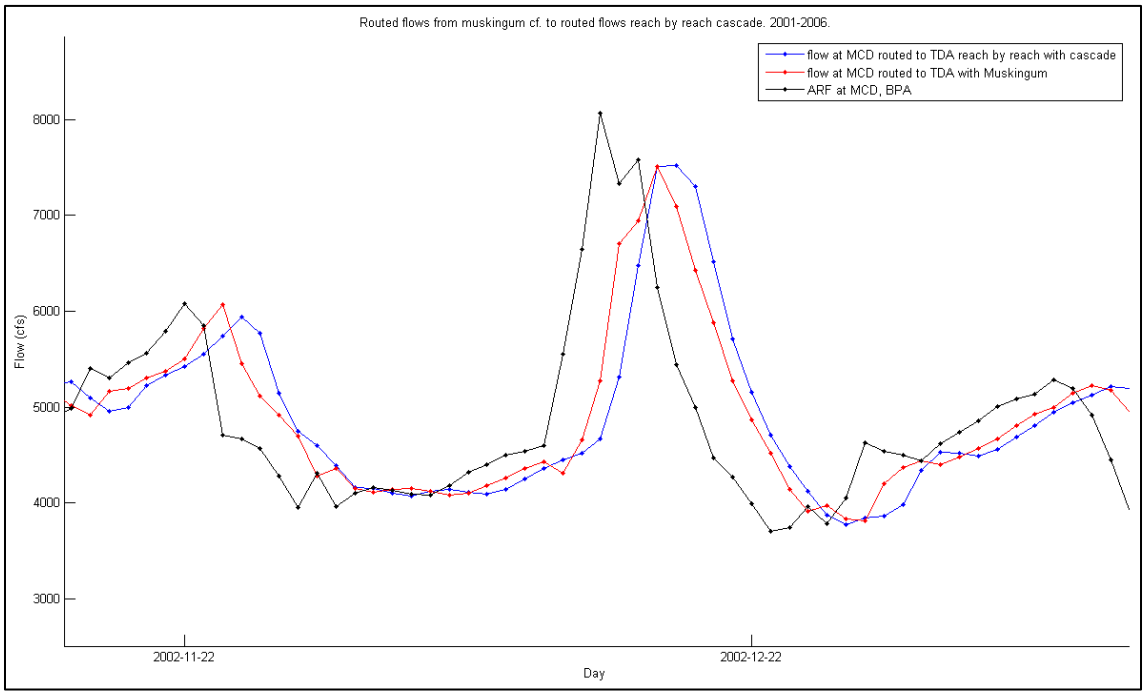

Figure 56: The effects of routing, MCD – TDA, using both the cascade3 (reach-by-reach) routine and the Muskingum method, low flow.

4.10 Issues with the Bonneville Power Administration dataset

The model verification for the shortest geographical distance (see chapter 4.2.1), which is Rock Island (RIS) to Wanapum (WAN), was performed using the Bonneville Power Association (BPA) streamflow data from 1984, as opposed to other stretches where the BPA data was taken from the

years 2001-2006. This was due to problems with the WAN ARF (Average daily unregulated Routed Flow) from the last ten years. Figure 57 and Figure 58 shows the ARF data provided by BPA plotted at RIS, WAN and Priest Rapids (PRD), which are three subsequent stations in Columbia River. The figures also include the WAN ARF data provided by the cascade3 routing routine. Both figures show that WAN has the highest flow, even though it is situated in between RIS and PRD and local inflows between RIS and WAN is said to be negligible. The hydrograph at WAN is, over these years, in the authors' opinion, therefore unrealistic.

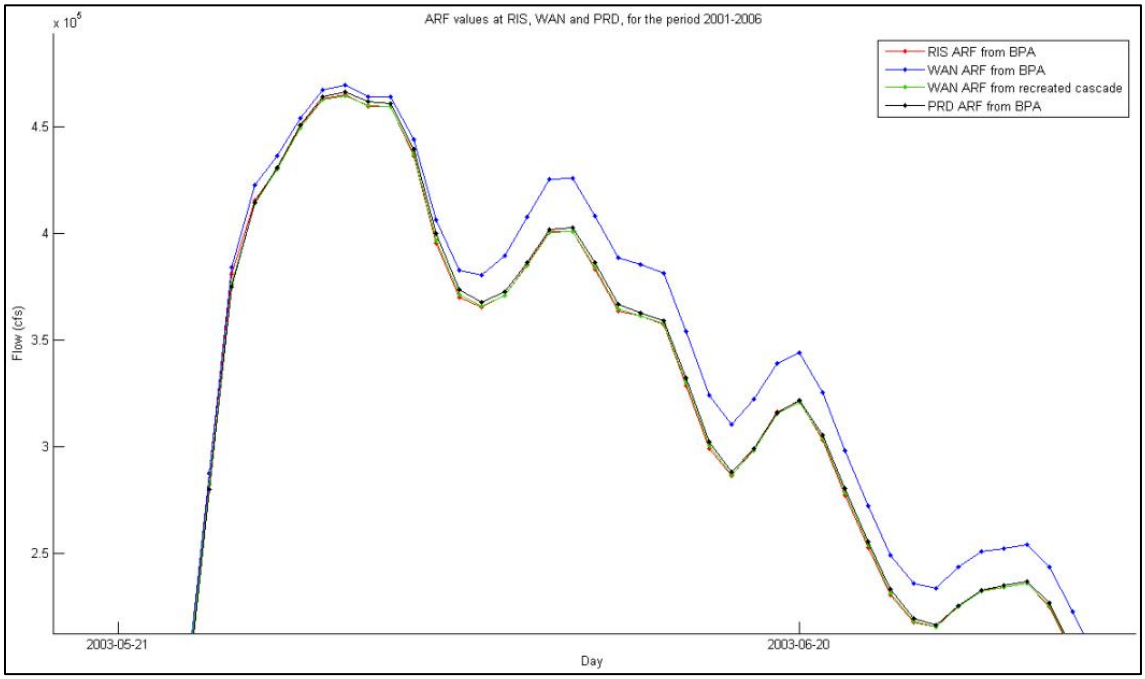

Figure 57: ARF data at RIS, WAN and PRD. High flow.

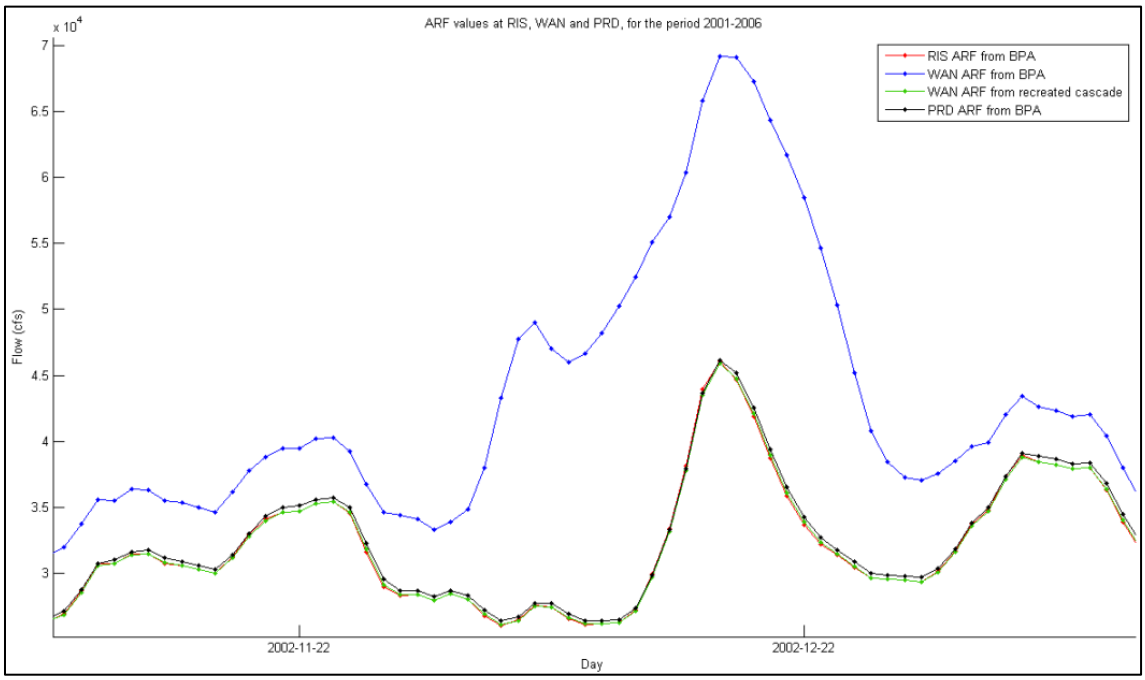

Figure 58: ARF data at RIS, WAN and PRD. Low flow.

Since the BPA dataset comprises 80 years of data from a large number of different dams and gaging stations, it will inevitably contain data errors. In order to adjust these errors several different techniques have been used by the BPA. Two major correction techniques are described and discussed below.

A major problem with the data is that the dam storages (S) often are determined from elevation/storage tables. The elevation is affected by for example wind setup, which induces severe errors in the storage volumes. Since the dam inflows (A) are estimated using the outflow data (H) and the storage data (S) according to equation 24, the errors in the storage volumes are also inherited in the dam inflows, which sometimes causes negative inflows. To correct this, an arbitrary volume was added to the storage on the affected day and then subtracted from another day the same month, in order to preserve the overall monthly storage change volumes. This method is somewhat arbitrary and may not provide a logical correction. Furthermore, even if the inflow values are positive they may still include errors which were not adjusted for.

Another problem that concerns the local inflow data (L) is that it most of the time contains erratic (irregular) spikes or negative values. To correct this, a method called indexing is used, which smooths out the hydrograph so that it has a more reasonable hydrologic shape. Indexing involves calculating the monthly average local inflow and the monthly average local flow at an adjacent index station. The ratio of the local inflow average and the index average flow is then calculated. This ratio is then multiplied with the daily index flows to get the hydrograph of the local inflow. As for the correction of the storage volumes described in the previous section, the data is only corrected when there are negative or irregular values. Even if the local inflows appear to be reasonable it could still contain errors. Furthermore, the success of the indexing method depends on the quality of the adjacent station data and also on how close the index station is.

Even if the correction methods are somewhat arbitrary, they still help to produce a reasonable dataset. With such an extensive amount of data and the complexity of hydrology, it is a very difficult task to handle.

4.11 Suggestions for further studies of the cascade3 routing routine

To further evaluate the cascade3 routing routine and the importance of including routing in Thomson Reuters Point Carbon's proprietary hydrological HBV-type energy model, it is necessary to implement the routing routine into the model and calibrate the routing routine and the model simultaneously. This would give the ultimate answer to whether it is relevant to include streamflow routing in Thomson Reuters Point Carbon's proprietary hydrological HBV-type energy model.

5. Conclusion

The Bonneville Power Administration (BPA) dataset is extensive and includes data from a great number of stations throughout the Columbia River catchment (with an area larger than Sweden's) over 80 years. The data has been revised and corrected repeatedly since 1970. Some of the correction methods are somewhat arbitrary but produce reasonable data given the complex circumstances.

A routing routine (the cascade3 routing routine) based on the "cascade of reservoir" routing technique, similar to the one used in the SSARR model, was developed. The routine was verified by using the parameters and the average daily unregulated routed flow (ARF) data provided by the BPA. For short distances (60 km) the routing routine gave very similar results to the routing in SSARR, whilst for longer distances (1300 km) periods of poorer fit appeared. These are likely to be caused by the differences in the interpolation methods between the routing routine in SSARR and the cascade3 routing routine.

A methodology for parameter estimation, in Columbia River and in the general case, was developed. For the general case where the parameters are unknown, two alternative parameters estimation methods were presented, one method that can be used with a scarce amount of data and a second one for when additional data is available. Which of the methods that provides the best estimates largely depends on the quality and appropriateness of the additional data.

The reasonableness of the routing produced by the cascade3 routing routine was evaluated using the Muskingum method. The Muskingum method was calibrated to fit the effects of routing of the cascade3 routing routine, and the calibrated Muskingum parameters were evaluated. The X parameter was within reasonable range of the values for natural streams and the K parameter was close to the total time of storage, which confirms the assumption that total time of storage is approximately the same as the travel time.

The overall effects of routing in the Columbia River catchment are relatively small. The effects of routing between Mica (MCD) and The Dalles (TDA) (distance 1300 km) are apparent with time lags around 2-3 days and with noticeable flow attenuation. Most of the water in the Columbia River enters as tributaries or local inflows along the flow path, which reduces the effects of routing at TDA. To get a clear answer to whether it is favorable to include streamflow routing in a hydrological rainfall runoff model, it is necessary to implement the routing routine into the model and calibrate them simultaneously, which is suggested for future studies.

6. References

Amenu, G.G., Killingtveit, Å., 2001. Real-time inflow forecasting for GilgelGibe reservoir, Ethiopia. In: B. Honningsvåg, et al., ed. 2001. Hydropower in the New Millenium. Lisse: A.A.Balkema.

Bergström, S., 1976. Development And Application of a Conceptual Runoff Modell for Scandinavian Catchments. Phd thesis. Lund: Institutionen för Teknisk Vattenresurslära, LTH, Lunds universitet.

Bonneville Power Administration United States Army Corps of Engineers, United States Bureau of Reclamation, 2011. 2010 Level Modified Streamflow 1928-2008. Bonneville Power Administration, Portland, OR.

Chadwick, A., Morfett, J., Borthwick, M., 2004. Hydraulics in civil and environmental engineering. 4th ed. Abington: Spon Press.

Chaudhry, M.H., 2007. Open-Channel Flow. 2nd ed. New York: Springer.

Chow, V.T., 1959. Open-Channel Hydraulics. New York: McGraw-Hill.

Chow, V. T., Maidment, D. R., Mays, L. W., 1988. Applied hydrology. New York: McGraw-Hill Book Company.

French, R. H., 1994. Open-Channel Hydraulics. Singapore: McGraw-Hill Book Co.

Gordon, N.D., McMahon, T.A., Finlayson, B.L., Gippel, C.J., Nathan, R.J., 2004. Stream Hydrology – An introduction for Ecologists. 2nd ed. Chichester: John Wiley & Sons Ltd.

Google Earth, version 6.1.0.5001. (2011-10-17). Columbia River, 47°57'25.00"N, 118°58'50.93"W, 721. [Accessed 2011-12-22].

Hasan, E., Elshamy, M., 2011. Application of Hydrologial Models for Climate Sensitivity Estimation of the Atbara Sub-basin. In: A.M. Melesse, ed. 2011. Nile Rive Basin – Hydrology, Climate and Water Use. New York: Springer.

Heatherman, 2008. Flood Routing on Small Streams: A Review of Muskingum-Cunge, Cascading Reservoirs, and Full Dynamic Solutions. University of Kansas.

Henderson, F. M., 1966. Open Channel Flow. New York: MacMillan Publishing CO., inc.

Lindström, G., Johansson, B., Persson, M., Gardelin, M., Bergström, S., 1997. Development and test of the distributed HBV-96 hydrological model. Journal of Hydrology, 201(1997), pp. 272-288.

Nash, J.E., 1957. The form of the instantaneous unit hydrograph. International Association of Science and Hydrology, 45(3) pp. 114-121.

Nash, J.E., Sutcliffe, J.V, 1970. River flow forecasting through conceptual models. Journal of Hydrology 10(1970), pp. 282-290.

Perumal, M., 1992. The cause of negative initial outflow with the Muskingum method. Hydrological Sicence, 37(4) pp. 391-401.

Rantz, S.E., 1982. Measurement and Computation of Streamflow: Volume 2. Computation of Discharge. Geological Survey Water-Supply Paper 2175. Washington: United States Government Printing Office.

Rice C. E., Larson C. L., 1972. Methods for routing hydrographs through open channels. WRRC, Bulletin 51.

Singh, V.P., Frevert, D.K, 2005. Watershed Models [online], pp. 245-272. United States: CRC Press. Available at: http://www.dhigroup.com/upload/dhisoftwarearchive/papersanddocs/waterresources/MSHE_Book_Chapter/MIKE_SHE_Chp10_in_VPSinghDKFrevert.pdf [Accessed 2012-01-18]

SMHI, n.d.a HBV-modellen 1972.[online] (updated 2011-09-16) Available at: http://www.smhi.se/kunskapsbanken/hbv-modellen-1.17857 [Accessed 2012-01-18]

SMHI, n.d.b The HBV model. [online] (updated 2006-05-03) Available at: http://www.smhi.se/sgn0106/if/hydrologi/hbv.htm [Accessed 2011-11-25]

Strelkoff, T. 1980. Comparative analysis of flood routing methods (Research Document 24). U.S. Army Corps of Engineers, Hydrologic Engineering Center, Davis, California.

Subramanya, E., 2008. Engineering hydrology. 3rd ed. New Dehli: Tata McGraw-Hill Publishing Company Limited.

Tingsanchali T., 1986. Flood Simulation in the Tidal Delta of the Mekong River by the SSARR Model. Water International, 11(3), pp. 117-126.

USACE, 1991. SSARR: Model Streamflow Synthesis and Reservoir Regulation Model. North Pacific Division, US Army Corps of Engineers, Portland, OR. Available online at: http://www.nwd-wc.usace.army.mil/report/ssarr.htm [Accessed 2011-11-25]

USACE, 1994. Engineering and Design: Flood-Runoff Analysis. US Army Corps of Engineers, Washington DC. Ch. 9.

USACE, 2000. Hydrologic Modeling System HEC-HMS, Technical reference manual.

USACE, n.d.. [online] (updated 2003-11-21) Available at: http://www.nwd-wc.usace.army.mil/report/colmap.htm [Accessed 2012-01-22]

U.S. Environmental Protection Agency, n.d. Columbia River Basin. [online] (updated 2012-01-18) Available at: http://yosemite.epa.gov/r10/ecocomm.nsf/Columbia/Columbia

USGS, n.d.. Columbia River at Vernita, Wash. [online] (updated 2011-09-22) Available at: http://il.water.usgs.gov/proj/nvalues/db_barnes/sites/12464500.shtml [Accessed 2012-01-12].

Ward, R.C., Robinson, M., 2000. Principles of Hydrology. London: McGraw-Hill Publishing Company.

7. Appendix A. Routing specifics

Table 20: The full stepwise routing from Mica to the Dalles. Based on BPA (2011).

Stretch		Parameters		
		KTS	n	nbrPhases
MCD->RVC	RVC_ARF=(MCD_ARF routed to RVC)+RVC_L	5.0	0.2	3.0
RVC->ARD	ARD_ARF=(RVC_ARF routed to ARD)+ARD_L	10.0	0.2	2.0
ARD->MUC	MUC_ARF=((ARD_ARF+BRD_ARF) routed to MUC)+MUC_L	10.0	0.2	4.0
MUC->CIB	CIB_ARF=(MUC_ARF routed to CIB)+WAT_ARF+LLK_ARF	10.0	0.2	2.0
CIB->GCL	GCL_ARF=(CIB_ARF routed to GCL)+GCL_L	30.0	0.2	2.0
GCL->CHJ	CHJ_ARF=(GCL_ARF routed to CHJ)+CHJ_L	6.0	0.2	2.0
CHJ->WEL	WEL_ARF=(CHJ_ARF routed to WEL)+WEL_L	5.0	0.2	2.0
WEL->RRH	RRH_ARF=(WEL_ARF routed to RRH)+RRH_L+CHL_A	8.0	0.2	2.0
RRH->RIS	RIS_ARF=(RRH_ARF routed to RIS)+RIS_L	5.0	0.2	2.0
RIS->WAN	WAN_ARF=(RIS routed to WAN)	7.0	0.2	2.0
WAN->PRD	PRD_ARF=(WAN routed to PRD)+PRD_L	5.0	0.2	2.0
PRD /IHR->CP	CP_ARF=(PRD routed to CP)+IHR_ARF	25.0	0.2	5.0
YAK->CP	CP_ARF=CP_ARF+(YAK routed to CP)	6.3	0.1	2.0
CP->MCN	MCN_ARF=(CP routed to MCN)+MCN_L	15.0	0.2	3.0
MCN->JDA	JDA_ARF=(MCN routed to JDA)+JDA_L	5.0	0.2	5.0
JDA->TDA	TDA_ARF=(JDA routed to TDA)+TDA_L	7.0	0.2	3.0

Table 21. The full stepwise routing from Albeni Falls to Grand Coulee.

Stretch		Parameters			
		KTS	n	nbrPhases	Total T_s
ALF->BOX	BOX_ARF=(ALF_ARF routed to BOX)+BOX_L	30	0.2	4.0	16.6
BOX->BDY	BDY_ARF=(BOX_ARF routed to BDY)+BDY_L	10	0.2	4.0	5.5
BDY->SEV	SEV_ARF=BDY_ARF+SEV_L	No routing in this reach			
SEV->WAT	WAT_ARF=SEV_ARF+WAT_S	No routing in this reach			
MUC->CIB WAT->CIB	CIB_ARF=(MUC_ARF routed to CIB)+WAT_ARF+LLK_ARF	10	0.2	2.0	2.8
CIB->GCL	GCL_ARF=(CIB_ARF routed to GCL)+GCL_L	30	0.2	2.0	6.8

8. Appendix B. MATLAB code

The MATLAB code of the cascade3 routing routine

```
function [OMD Ihr]=cascade3(P,ID)
%-------------------------------------------------------------------------
%SYFTE
%   Beräkna routat dagligt utflöde från en flodsträcka med givna
%   kalibreringsparametrar
%
%INPUT:
%       P=[KTS n nbrPhases t tIndata]   Kalibrerade parametrar.
%       ID:                             Dagliga inflöden i kolonnmatris
%
%OUTPUT:
%       OMD:        Dagliga routade utflöden i kolonnmatris, medel av de 24
%                   senast passerade timmarna.
%
%       Ihr:        Lösningsmatrisen med timdata.
%-------------------------------------------------------------------------
%Senast modifierad: Alexander och Victor 2011-12-16.
%Skriven av Victor Pelin & Alexander Påhlsson 2011-11-03.
%-------------------------------------------------------------------------

%Kalibrerade parametrar och koefficienter från INPUT
KTS=P(1,1);
n=P(1,2);
nbrPhases=P(1,3);
t=P(1,4);
tIndata=P(1,5);

%Definition av matriser
%Resultatmatrisen: Inflöden respektive utflöden till alla reservoarer.
Ih=zeros(length(ID)*round(tIndata/t),nbrPhases+1);
ODM=zeros(length(ID),1); %Dagliga routade medelflöden.

%Tim-inflöde interpoleras som konstant värdet under den aktuella dagen
r=0; %Räknaren nollställs
for i=1:length(ID)
    for k=1:round(tIndata/t)
        r=r+1;
        Ih(r,1)=ID(i);
    end
end

%Utflöde från respektive reservoar läggs i nya kolumner i Ih-matrisen och
%fungerar som inflöde till nästa reservoar
for i=1:nbrPhases
    %Inflödet (för timme 1) till reservoar 2/3/... gissas vara inflöde till
    %reservoar 1/2 (bara ett schablon-värde för att kunna börja räkna)
    Ih(1,i+1)=Ih(1,i);
    for k=1:length(Ih)-1
        Im=(Ih(k,i)+Ih(k+1,i))/2; %Medelvärde på inflödet under timme k
        %Lös ut utflödet Q vid slutet av timmen -från reservoar 1- och sätt
        %in som inflöde till reservoar 2 under nästa tidssteg osv:
        Ih(k+1,i+1)=fzero(@(Q) (Ih(k,i+1)+t*(Im-Ih(k,i+1))/((KTS/((Ih...
            (k,i+1)+Q)/2)^n)+t/2)-Q),Im);
    end
end
```

```
%Dagliga medelvärden av utflöde (ODM) beräknas som baklänges interpolering.
r=0; %Räknaren nollställs.
for i=1:length(ID)
    %Summera flödena under 24 h dela med 24. Medel gäller för kommande dag.
    for k=1:round(tIndata/t)
        r=r+1;
        ODM(i)=ODM(i)+Ih(r,nbrPhases+1)/round(tIndata/t);
    end
end

OMD=ODM;        %Slutligen läggs data i OUTPUT-matriserna.
Ihr=Ih;
end
%-------------------------------C'est ca---------------------------------
```

The MATLAB code of the r^2 routine

```
function rsquare=rSquare(Dobs,Dmod)
%-------------------------------------------------------------------------
%SYFTE
%   Beräkna R^2-värdet mellan observerad data och modellerad data
%
%INPUT:
%       Dobs:       Observerad data (kolonnmatris)
%       Dmod:       Modellerad data (kolonnmatris)
%
%OUTPUT:
%       rsquare:    Värdet på R^2
%-------------------------------------------------------------------------
%Last modified: Victor Pelin 2011-11-04
%Skriven av Alexander Påhlsson och Victor Pelin 2011-11-04.
%-------------------------------------------------------------------------
y_mean=0;
for i=1:length(Dobs(:,1))
    y_mean=y_mean+Dobs(i,1)/length(Dobs(:,1));
end

SS_tot=0;
SS_err=0;
for i=1:length(Dobs(:,1))
    SS_tot=SS_tot+(Dobs(i,1)-y_mean)^2;
    SS_err=SS_err+(Dobs(i,1)-Dmod(i,1))^2;
end

rsquare=1-SS_err/SS_tot;
%---------------------------------C'est ca---------------------------------
```

The MATLAB code of the Q_{av} routine

```
function qav=qAverage(Dobs,Dmod)
%-------------------------------------------------------------------------
%SYFTE
%   Beräkna medel för absolutbeloppen av skillnaderna mellan uppmätta och
%   simulerade flöden
%
%INPUT:
%       Dobs:       Observerad data (kolonnmatris)
%       Dmod:       Modellerad data (kolonnmatris)
%
%OUTPUT:
%       qav:        Värdet qav
%-------------------------------------------------------------------------
%Senast modifierad: Victor Pelin och Alexander Påhlsson 2011-12-08
%Skriven av Alexander Påhlsson och Victor Pelin 2011-12-08.
%-------------------------------------------------------------------------

Q_av_abs=0;

for i=1:length(Dobs)
    Q_av_abs=Q_av_abs+abs(Dmod(i,1)-Dobs(i,1));
end

Q_av_abs=Q_av_abs/length(Dmod);

qav=Q_av_abs;

end

%--------------------------------C'est ca---------------------------------
```

The MATLAB code for a routing example

```
clear
'------------------------------------------------------------------------'
format long
%Reading daily inflows at RIS
ID=xlsread('RIS5ARF_daily.xls','B20274:B20639');
%Reading daily outflows at WAN
OD=xlsread('WAN5ARF_daily.xls','B20274:B20639');
%Reading the date strings (for plotting)
[noll dates]=xlsread('WAN5ARF_daily.xls','A20274:A20639');

%Calibrated parameters (Appendix F: BPA, 2011)
KTS=7;
n=0.2;
nbrPhases=2;
t=1;              %Computational time step (hours)
tIndata=24;       %Time scale of input data (hours)
P=[KTS n nbrPhases t tIndata];

[OMD Ihr]=cascade3(P,ID); %Time to route with cascade3

%Drawing graphs
figure(1) %Daily data
hold on
time=datenum(dates);
plot(time,OD,'b.-')
plot(time,OMD,'g.-')
plot(time,ID,'k.-')
set(gca,'XTick',724642:10:725007)
datetick('x', 29, 'keepticks')
xlabel('Day')
ylabel('Flow (cfs)')
title('Routed flows from cascade cf. to routed flows from BPA. 1984.')
legend('ARF at WAN from BPA','ARF at WAN from cascade',...
            'ARF at RIS (upstream) from BPA')
hold off

figure(2) %Data at the computational time step scale
hold on
plot(Ihr(:,1),'b.-')
plot(Ihr(:,nbrPhases+1),'r.-')
xlabel('Computational time step')
ylabel('Flow (cfs)')
title('Routed flows at WAN from cascade cf. to inflow at RIS. 1984.');
legend('ARF at RIS, from BPA. Constant interpolation of inflow'...
            ,'ARF at WAN from cascade')
hold off

%Controlling the computational time step
Tmax=KTS./(max(Ihr)).^n;
if Tmax<t/2
    'Tidssteget t är för stort, prova ett mindre'
else
    'Tidssteget t är tillräckligt litet'
end

%Objective functions: The R^2 value and the average deviation.
R2_WAN=rSquare(OD,OMD)
qAv=qAverage(OD,OMD)
'------------------------------------------------------------------------'
```

The MATLAB code of the Muskingum routing routine

```
function [OMD Ihr]=muskingum(P,ID)
%-------------------------------------------------------------------------
%SYFTE
%   Beräkna routat dagligt utflöde från en flodsträcka med givna
%   kalibreringsparametrar
%
%INPUT:
%       P=[K X t tIndata]   Kalibrerade parametrar. Tidssteget  i timmar.
%
%       ID:                 Dagliga inflöden i kolonnmatris
%
%OUTPUT:
%       OMD:        Dagliga routade utflöden, medelvärden med tidsteget
%                   tIndata.
%
%       Ihr:        Lösningsmatrisen med data i tidsteget t.
%-------------------------------------------------------------------------
%Senast modifierad: Alexander och Victor 2012-01-30.
%Skriven av Victor Pelin & Alexander Påhlsson 2012-01-30.
%-------------------------------------------------------------------------

%Kalibrerade parametrar och koefficienter från INPUT
K=P(1,1);
X=P(1,2);
t=P(1,3);
tIndata=P(1,4);

%Definition av matriser
%Resultatmatrisen: Inflöden respektive utflöden till alla reservoarer.
Ih=zeros(length(ID)*round(tIndata/t),1);
ODM=zeros(length(ID),1); %Dagliga routade medelflöden.

%Tim-inflöde interpoleras som konstant värdet under den aktuella dagen
r=0; %Räknaren nollställs
for i=1:length(ID)
    for k=1:round(tIndata/t)
        r=r+1;
        Ih(r,1)=ID(i);
    end
end

%Utflöde från respektive reservoar läggs i nya kolumner i Ih-matrisen och
%fungerar som inflöde till nästa reservoar

%Inflödet (för timme 1) till reservoar 2/3/... gissas vara inflöde till
%reservoar 1/2 (bara ett schablon-värde för att kunna börja räkna)
Ih(1,2)=Ih(1,1);

%Konstanterna C1, C2 och C3 beräknas från parametrarna.
C1=(t-2*K*X)/(2*K*(1-X)+t);
C2=(t+2*K*X)/(2*K*(1-X)+t);
C3=(2*K*(1-X)-t)/(2*K*(1-X)+t);

%Lösningsrutinen:
for k=1:length(Ih)-1
    Ih(k+1,2)= C1*Ih(k+1,1)+C2*Ih(k,1)+C3*Ih(k,2);
end
```

```
%Dagliga medelvärden av utflöde (ODM) beräknas som baklänges interpolering.
r=0; %Räknaren nollställs.
for i=1:length(ID)
    %Summera flödena under 24 h dela med 24. Medel gäller för kommande dag.
    for k=1:round(tIndata/t)
        r=r+1;
        ODM(i)=ODM(i)+Ih(r,2)/round(tIndata/t);
    end
end

OMD=ODM;        %Slutligen läggs data i OUTPUT-matriserna.
Ihr=Ih;
end
%-------------------------------C'est ca------------------------------
```